Electronic Supplementary Information

Near Infrared Two-Photon-Excited and -Emissive Dyes Based on a Strapped Excited-State Intramolecular Proton-Transfer (ESIPT) Scaffold

Naoya Suzuki,[†] Kayo Suda,[‡] Daisuke Yokogawa,[,†,‡] Hirotaka Kitoh-Nishioka,[†] Stephan Irle,[†,‡] Akihiro Ando,[§]*
Luis M.G. Abegão,[§,¶] Kenji Kamada,[,§] Aiko Fukazawa,[†] and Shigehiro Yamaguchi[*,†,‡]*

[†]Department of Chemistry, Graduate School of Science and Integrated Research Consortium on Chemical Sciences (IRCCS), Nagoya University
[‡]Institute of Transformative Bio-Molecules (WPI-ITbM), Nagoya University, Furo, Chikusa, Nagoya, 464-8602, Japan
[§]IFMRI, National Institute of Advanced Industrial Science and Technology (AIST), 1-8-31 Midorigaoka, Ikeda, Osaka, 563-8577, Japan,
[¶]Departamento de Física, Universidade Federal de Sergipe, 49100-000 São Cristovão, SE, Brazil

Contents

1. Experimental Detail

General. Melting points (mp) or decomposition temperatures were determined with a Yanaco MP-S3 instrument (MP-S3). ^{1}H, ^{13}C{^{1}H}, and ^{11}B{^{1}H} NMR spectra were recorded with a JEOL AL-400 or AL-600 spectrometer in C_6D_6, THF-d_8, and CD_2Cl_2 (400 MHz for ^{1}H, 100 MHz for ^{13}C, 128 MHz for ^{11}B, and 162 MHz for ^{31}P). The chemical shifts in ^{1}H NMR spectra are reported in δ ppm using the residual proton of $CHCl_3$ (7.26 ppm) in $CDCl_3$, C_6H_6 (7.16 ppm) in C_6D_6, and THF (3.58 ppm) in THF-d_8 as internal standards. The chemical shifts in ^{13}C NMR spectra are reported using the solvent signals of $CDCl_3$ (77.16 ppm), C_6D_6 (128.06 ppm), THF-d_8 (67.21 ppm), and CD_2Cl_2 (53.84 ppm) as internal standards, respectively. The chemical shifts in ^{11}B NMR and ^{31}P NMR spectra are reported using $BF_3{\cdot}OEt_2$ (0.00 ppm) and H_3PO_4 (0.00 ppm) as an external standard, respectively. Mass spectra were measured with a Bruker micrOTOF Focus spectrometer with the APCI ionization method, Thermo Fisher Scientific Exactive spectrometer with the ESI ionization method, and JMS-T100GCV (JEOL) with the EI method. Thin layer chromatography (TLC) was performed on plates coated with 0.25 mm thickness of silica gel $60F_{254}$ (Merck). Column chromatography was performed using PSQ100B or PSQ60B (Fuji Silysia Chemicals). Recycling preparative HPLC was performed using LC-918 (Japan Analytical Industry) equipped with silica gel column (Wakosil-II 5-Prep, Wako). Recycling preparative gel permeation chromatography (GPC) was performed using LC-Forte/R (YMC TECHNOS CORPORATION) equipped with polystyrene gel columns (YMC-GPC T2000 and YMC-GPC T4000, YMC TECHNOS CORPORATION). Anhydrous solvents were purchased from Kanto Chemicals and further purified by Glass Contour Solvent Systems. Compounds **1**,[1] **8**,[1] **25**,[1] 5-bromo-2-iodo-1,3-dimethylbenzene,[2] and 4-(3-thienyl)butane-1-ol[3] were prepared according to the literatures.

Scheme S1. Synthesis of **2**.

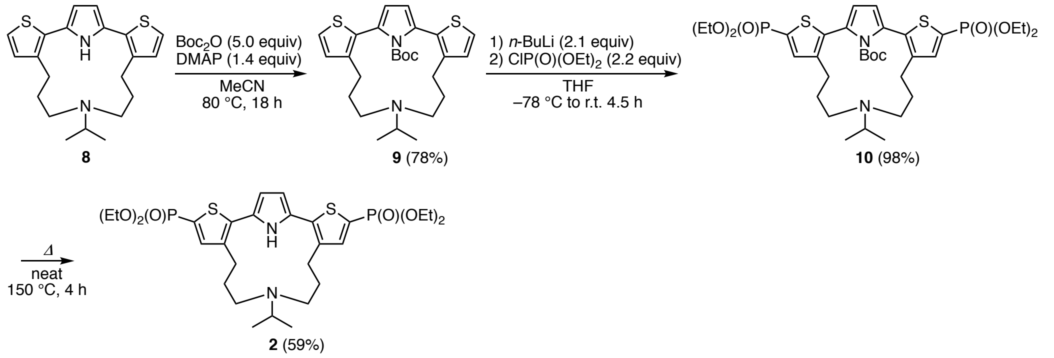

Compound 9. To a solution of **8** (96.2 mg, 0.260 mmol) in acetonitrile (1.0 mL) was added di-*tert*-butyl dicarbonate (0.287 g, 1.31 mmol) and *N*,*N*-dimethyl-4-aminopyridine (43.1 mg, 0.352 mmol). The mixture was stirred at 80 °C for 18 h. After addition of ethyl acetate (2 mL) and water (5 mL), the organic layer was separated, and the aqueous layer was extracted with ethyl acetate (5 mL × 3). The combined organic layer was washed with brine, dried over anhydrous Na_2SO_4, filtered, and concentrated under reduced pressure. The crude product was subjected to silica gel column chromatography (ethyl acetate; $R_f = 0.20$) to afford 95.2 mg (0.202 mmol, 78%) of **9** as a colorless crystal: mp 142.5–142.8 °C; ^{1}H NMR (400 MHz, C_6D_6) δ 6.89 (d, J = 5.2 Hz, 2H), 6.75 (d, J = 5.2 Hz, 2H), 6.22 (s, 2H), 2.64–2.74 (m, 3H), 2.53–2.62 (m, 2H), 2.16–2.28 (m, 4H), 1.43–1.61 (m, 4H), 1.06 (s, 9H), 0.88 (d, J = 6.4 Hz, 6H); ^{13}C{^{1}H} NMR (100 MHz, C_6D_6) δ 148.9, 142.8,

129.8, 129.5, 128.8, 123.9, 115.9, 82.8, 53.0, 51.8, 30.7, 28.3, 27.2, 18.5; HRMS (ESI) Calcd. for $C_{26}H_{35}N_2O_2S_2^+$: 471.2134 ([*M*+H]$^+$). Obsd. 471.2129.

Compound 10. To a solution of **9** (0.149 g, 0.317 mmol) in anhydrous THF (1.0 mL) was added a hexane solution of *n*-BuLi (1.62 M, 0.415 mL, 0.672 mmol), and the mixture was stirred for 2 h at –78 °C under a nitrogen atmosphere. Then, diethyl chlorophosphate (0.100 mL, 0.692 mmol) was added to the solution, and the resulting mixture was stirred at –78 °C for 0.5 h. The mixture was allowed to warm to ambient temperature and stirred for another 2 h. After quenching with water (2 mL), the organic layer was separated, and the aqueous layer was extracted with ethyl acetate (5 mL × 3). The combined organic layer was washed with brine, dried over anhydrous Na_2SO_4, filtered, and concentrated under reduced pressure. The crude product was subjected to silica gel column chromatography (100/1 ethyl acetate/Et_3N; R_f = 0.60) to afford 0.230 g (3.09 mmol, 98%) of **10** as a white solid: mp. 148.5 °C (dec.); ^1H NMR (400 MHz, C_6D_6) δ 7.66 (d, J_{HP} = 8.4 Hz, 2H), 6.10 (s, 2H), 3.96–4.14 (m, 8H), 2.57–2.68 (m, 3H), 2.37–2.47 (m, 2H), 2.07–2.18 (m, 4H), 1.28–1.44 (m, 4H), 1.08 (t, J = 7.2 Hz, 12H), 1.03 (s, 9H), 0.85 (d, J = 6.8 Hz, 6H); $^{13}C\{^1H\}$ NMR (100 MHz, THF-d_8) δ 148.7, 144.2 (d, J_{CP} = 15.7 Hz), 138.8 (d, J_{CP} = 10.7 Hz), 137.8 (d, J_{CP} = 6.6 Hz), 128.6 (d, J_{CP} = 2.5 Hz), 127.7 (d, J_{CP} = 208 Hz), 116.7, 84.4, 62.5 (d, J_{CP} = 5.0 Hz), 53.7, 52.1, 31.0, 28.3, 27.3, 18.5, 16.5 (d, J_{CP} = 5.7 Hz); $^{31}P\{^1H\}$ NMR (100 MHz, C_6D_6) δ 12.4; HRMS (APCI) Calcd. for $C_{34}H_{53}N_2O_8P_2S_2^+$: 743.2713 ([*M*+H]$^+$). Obsd. 743.2739.

Compound 2. Compound **10** (0.120 g, 0.162 mmol) was heated neat for 4 h at 150 °C under a nitrogen atmosphere. After addition of an ethyl acetate (5 mL) and water (5 mL), the organic layer was separated, and the aqueous layer was extracted with ethyl acetate (5 mL × 3). The combined organic layer was washed with brine, dried over anhydrous Na_2SO_4, filtered, and concentrated under reduced pressure. The crude product was subjected to silica gel column chromatography (300/100/1 ethyl acetate/hexane/Et_3N; R_f = 0.21) and further purified by HPLC (300/100/1 ethyl acetate/hexane/Et_3N) to afford 61.0 mg (94.9 μmol, 59%) of **2** as a colorless oil: ^1H NMR (400 MHz, C_6D_6) δ 13.2 (br s, 1H), 7.68 (d, J_{HP} = 8.8 Hz, 2H), 6.57 (d, J = 2.8 Hz, 2H), 3.96–4.12 (m, 8H), 2.48–2.58 (m, 5H), 1.92 (t, J = 5.6 Hz, 4H), 1.42–1.50 (m, 4H), 1.06 (t, J = 7.2 Hz, 12H), 0.29 (d, J = 6.4 Hz, 6H); $^{13}C\{^1H\}$ NMR (100 MHz, C_6D_6) δ 140.1 (d, J_{CP} = 11.5 Hz), 139.5 (d, J_{CP} = 6.6 Hz), 136.6 (d, J_{CP} = 15.7 Hz), 127.5 (d, J_{CP} = 3.3 Hz), 126.4 (d, J_{CP} = 208 Hz), 111.8, 62.3 (d, J_{CP} = 4.9 Hz), 47.9, 45.9, 26.9, 25.6, 16.4 (d, J_{CP} = 5.8 Hz), 15.2; $^{31}P\{^1H\}$ NMR (100 MHz, C_6D_6) δ 12.3; HRMS (APCI) Calcd. for $C_{29}H_{44}N_2O_6P_2S_2$: 642.2116 ([*M*]$^+$). Obsd. 642.2133.

Scheme S2. Synthesis of **3**.

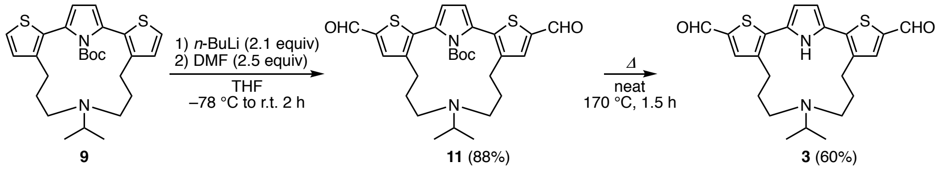

Compound 11. To a solution of **9** (0.195 g, 0.413 mmol) in anhydrous THF (1.0 mL) was added a hexane solution of *n*-BuLi (1.62 M, 0.530 mL, 0.857 mmol), and the mixture was stirred for 1 h at –78 °C under a

nitrogen atmosphere. Then, *N*,*N*-dimethylformamide (80.0 μL, 1.03 mmol) was added to the solution and the resulting mixture was stirred at –78 °C for 0.5 h. The mixture was allowed to warm to ambient temperature and stirred for 0.5 h. After addition of water (2.0 mL) and ethyl acetate (2.0 mL), the organic layer was separated, and the aqueous layer was extracted with ethyl acetate (2 mL × 3). The combined organic layer was washed with brine, dried over anhydrous Na_2SO_4, filtered, and concentrated under reduced pressure. The crude product was recrystallized from toluene to afford 0.192 g (0.449 mmol, 88%) of **11** as a yellow crystal: mp. 152.3 °C (dec.); ^{1}H NMR (400 MHz, C_6D_6) δ 9.61 (s, 2H), 6.96 (s, 2H), 6.00 (s, 2H), 2.61–2.70 (m, 3H), 2.29–2.38 (m, 2H), 2.13–2.26 (m, 4H), 1.23–1.40 (m, 4H), 0.93 (s, 9H), 0.90 (d, *J* = 6.4 Hz, 6H); ^{13}C{^{1}H} NMR (100 MHz, C_6D_6) δ 182.0, 148.2, 144.0, 142.2, 139.4, 137.4, 128.6, 116.9, 84.2, 53.3, 51.9, 30.5, 28.2, 27.0, 18.5; HRMS (ESI) Calcd. for $C_{28}H_{35}N_2O_4S_2^+$: 527.2033 ([*M*+H]$^+$). Obsd. 527.2030.

Compound 3. Compound **11** (51.1 mg, 97.0 μmol) was heated neat for 1.5 h at 170 °C under a nitrogen atmosphere. The crude product was subjected to silica gel column chromatography (ethyl acetate; R_f = 0.58) to afford 25.0 mg (58.6 μmol, 60%) of **3** as a brown crystal: mp. 214.8 °C (dec.); ^{1}H NMR (400 MHz, C_6D_6) δ 13.1 (br s, 1H), 9.61 (s, 2H), 6.86 (s, 2H), 6.50 (d, *J* = 2.0 Hz, 2H), 2.50 (sept, *J* = 6.6 Hz, 1H), 2.47 (t, *J* = 6.0 Hz, 4H), 1.98 (t, *J* = 5.6 Hz, 4H), 1.42–1.52 (m, 4H), 0.28 (d, *J* = 6.6 Hz, 6H); ^{13}C{^{1}H} NMR (100 MHz, C_6D_6) δ 181.4, 141.1, 140.7, 138.1, 136.6, 128.5, 113.3, 48.1, 45.8, 27.1, 25.5, 15.1; HRMS (APCI) Calcd. for $C_{23}H_{26}N_2O_2S_2$: 426.1436 ([*M*]$^+$). Obsd. 426.1447.

Scheme S3. Synthesis of **4**.

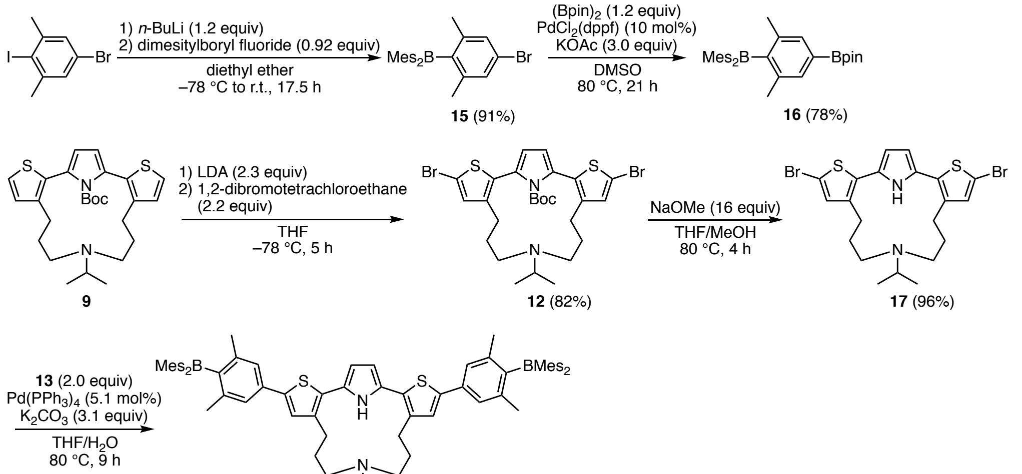

Compound 15. To a solution of 5-bromo-2-iodo-1,3-dimethylbenzene (3.40 g, 10.9 mmol) in anhydrous diethyl ether (44 mL) was added a hexane solution of *n*-BuLi (1.6 M, 6.8 mL, 11 mmol), and the mixture was stirred for 3 h at –78 °C under an argon atmosphere. Then, a diethyl ether solution (10 mL) of dimesitylboryl fluoride (2.86 g, 9.99 mmol) prepared at 0 °C was added to the solution. The mixture was allowed to warm to ambient temperature and stirred for 17.5 h. After addition of water, the organic layer was separated, and the aqueous layer was extracted with dichloromethane. The combined organic layer was dried over anhydrous $MgSO_4$, filtered, and concentrated under reduced pressure. The crude product was subjected to silica gel chromatography (hexane; R_f = 0.43) to afford 3.94 g (9.11 mmol, 91%) of **15** as a white powder: mp.

206.4-207.0 °C; ^{1}H NMR (400 MHz, $CDCl_3$) δ 7.08 (s, 2H), 6.34 (s, 4H), 2.26 (s, 6H), 1.97 (s, 6H), 1.97 (s, 6H), 1.96 (s, 6H); $^{13}C\{^1H\}$ NMR (100 MHz, $CDCl_3$) δ 146.2, 143.7, 142.6, 140.8, 140.6, 139.7, 130.5, 128.9, 128.9, 123.5, 23.0, 23.0, 22.8, 21.4; $^{11}B\{^1H\}$ NMR (128 MHz, $CDCl_3$) δ 75.9; HRMS (EI) Calcd. for $C_{26}H_{30}BBr^+$: 432.1624 ([*M*]$^+$). Obsd. 432.1624.

Compound 16. A solution of **15** (1.00 g, 2.31 mmol), bis(pinacolate)diboron (0.705 g, 2.78 mmol), $PdCl_2$(dppf) (170 mg, 0.232 mmol), and potassium acetate (0.684 g, 6.97 mmol) in degased dimethylsulfoxide (20 mL) was stirred for 21 h at 80 °C under a nitrogen atmosphere. The mixture was cooled to ambient temperature and water was added. The organic layer was separated, and the aqueous layer was extracted with ethyl acetate. The combined organic layer was washed with brine, dried with anhydrous $MgSO_4$, filtered, and concentrated under reduced pressure. The crude product was subjected to silica gel column chromatography (1/1 hexane/dichloromethane; R_f = 0.58) to afford 0.868 g (1.81 mmol, 78%) of **15** as a white solid; mp. 186.8-187.4 °C; ^{1}H NMR (400 MHz, $CDCl_3$) δ 7.33 (s, 2H), 6.73 (s, 2H), 6.72 (s, 2H), 2.26 (s, 6H), 2.02 (s, 2H), 1.98 (s, 6H), 1.94 (s, 6H), 1.35 (s, 12H); $^{13}C\{^1H\}$ NMR (100 MHz, $CDCl_3$) δ 150.9, 143.9, 140.8, 140.8, 139.5, 139.4, 133.8, 128.7, 128.7, 83.8, 25.1, 25.0, 23.0, 25.0, 23.0, 22.9, 22.8, 21.4. One signal for the carbon atom bound to the boron atom was not observed due to the quadrupolar relaxation; $^{11}B\{^1H\}$ NMR (128 MHz, $CDCl_3$) δ 76.3, 30.5; HRMS (ESI) Calcd. for $C_{32}H_{42}B_2NaO_2^+$: 503.3263 ([*M*+Na]$^+$). Obsd. 503.3262.

Compound 12. To a solution of *i*Pr_2NH (1.05 mL, 0.758 g, 7.49 mmol) in anhydrous THF (4.35 mL) was added a hexane solution of *n*-BuLi (1.62 M, 4.66 mL, 7.55 mmol), and the mixture was stirred for 1 h at –78 °C under a nitrogen atmosphere. The LDA solution (1.10 mL) thus prepared was added dropwise to a solution of **9** (0.171 g, 0.363 mmol) in anhydrous THF (1.0 mL) at –78 °C under a nitrogen atmosphere. Then, a THF solution (2.0 mL) of 1,2-dibromotetrachloroethane (0.257 g, 0.789 mmol) was added to the solution and the resulting mixture was stirred at –78 °C for 5 h. The mixture was allowed to warm to ambient temperature and quenched with water (2 mL). The organic layer was separated, and the aqueous layer was extracted with ethyl acetate (5 mL × 3). The combined organic layer was washed with brine, dried over anhydrous Na_2SO_4, filtered, and concentrated under reduced pressure. The crude product was subjected to silica gel column chromatography (ethyl acetate; R_f = 0.35) to afford 0.187 g (0.297 mmol, 82%) of **12** as a colorless solid: mp. 122.5-123.2 °C; ^{1}H NMR (400 MHz, C_6D_6) δ 6.67 (s, 2H), 6.06 (s, 2H), 2.61 (sept, *J* = 6.4 Hz, 1H), 2.30–2.48 (m, 4H), 2.10–2.14 (m, 4H), 1.26–1.44 (m, 4H), 1.04 (s, 9H), 0.84 (d, *J* = 6.4 Hz, 6H); $^{13}C\{^1H\}$ NMR (100 MHz, C_6D_6) δ 148.4, 143.6, 132.4, 131.1, 127.7, 116.5, 110.6, 83.6, 53.0, 51.6, 30.4, 28.1, 27.2, 18.4; HRMS (ESI) Calcd. for $C_{26}H_{33}Br_2N_2O_2S_2^+$: 627.0345 ([*M*+H]$^+$). Obsd. 627.0338.

Compound 17. A solution of **12** (0.129 g, 0.205 mmol) and sodium methoxide (0.182 g, 3.36 mmol) in a mixture of THF (1.0 mL) and methanol (1.0 mL) was stirred for 4 h at 80 °C. The reaction mixture was allowed to cool to ambient temperature and quenched with water (5 mL). The organic layer was separated, and the aqueous layer was extracted with ethyl acetate (5 mL × 3). The combined organic layer was washed with brine, dried over anhydrous Na_2SO_4, filtered, and concentrated under reduced pressure. The crude mixture was subjected to silica gel column chromatography (ethyl acetate, R_f = 0.93) to afford 0.104 g (0.198

mmol, 96%) of **17** as a pale yellow powder: mp. 184.3-185.1 °C; ^{1}H NMR (400 MHz, C_6D_6) δ 12.9 (br s, 1H), 6.57 (s, 2H), 6.41 (d, J = 2.4 Hz, 2H), 2.59 (sept, J = 6.8 Hz, 1H), 2.46 (t, J = 6.0 Hz, 4H), 1.96 (t, J = 5.6 Hz, 4H), 1.37–1.46 (m, 4H), 0.32 (d, J = 6.8 Hz, 6H); ^{13}C{^{1}H} NMR (100 MHz, C_6D_6) δ 136.0, 133.6, 132.5, 126.5, 110.7, 109.7, 47.7, 45.8, 26.7, 25.7, 15.1; HRMS (APCI) Calcd. for $C_{21}H_{25}Br_2N_2S_2^+$: 526.9820 ([M+H]$^+$). Obsd. 526.9841.

Compound 4. A solution of **16** (97.6 mg, 0.203 mmol), **17** (52.5 mg, 99.4 μmol), potassium carbonate (42.3 mg, 0.306 mmol), and $Pd(PPh_3)_4$ (5.82 mg, 5.04 μmol) in a mixture of degassed THF (0.50 mL) and water (0.50 mL) was stirred for 9 h at 80 °C under a nitrogen atmosphere. After cooling the reaction mixture to ambient temperature, the organic layer was separated, and the aqueous layer was extracted with ethyl acetate (5 mL × 3). The combined organic layer was washed with brine, dried over with Na_2SO_4, filtered and concentrated under reduced pressure. The crude product was subjected to silica gel column chromatography (3/1 hexane/dichloromethane, R_f = 0.20) and further purified by HPLC (toluene) to afford 65.3 mg (60.7 μmol, 61%) of **4** as an orange powder: mp. 248.2 °C (dec.); ^{1}H NMR (400 MHz, THF-d_8) δ 13.0 (br s, 1H), 7.32 (s, 2H), 7.23 (s, 4H), 6.76 (s, 8H), 6.31 (d, J = 2.0 Hz, 2H), 3.00 (sept, J = 5.6 Hz, 1H), 2.93 (t, J = 6.0 Hz, 4H), 2.58 (t, J = 5.4 Hz, 4H), 2.08 (m, 4H), 2.05 (s, 12H), 2.03 (s, 12H), 1.99 (s, 12H), 0.71 (d, J = 5.6 Hz, 6H); ^{13}C{^{1}H} NMR (100 MHz, THF-d_8) δ 147.1, 144.7, 141.8, 141.3, 141.1, 141.0, 140.0, 137.0, 135.9, 131.6, 129.3, 129.3, 128.1, 126.6, 124.9, 110.2, 48.7, 46.7, 27.8, 26.4, 23.1, 23.1, 23.0, 21.2, 15.6; ^{11}B{^{1}H} NMR (128 MHz, THF-d_8) δ 79.5; HRMS (ESI) Calcd. 1073.6189 for: $C_{73}H_{83}B_2N_2S_2$ ([M–H]$^-$). Obsd. 1073.6192.

Scheme S4. Synthesis of **5**.

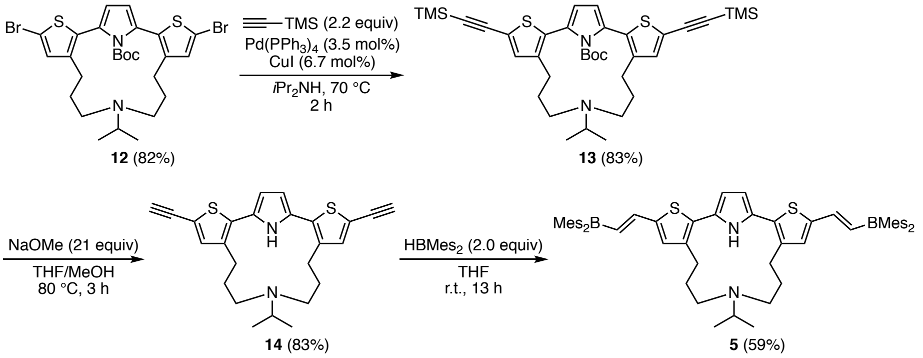

Compound 13. To a solution of **12** (99.2 mg, 0.159 mmol), $Pd(PPh_3)_4$ (6.51 mg, 5.63 μmol), and CuI (2.04 mg, 10.7 μmol) in degassed anhydrous iPr$_2$NH (1.0 mL) was added trimethylsilylacetylene (50.0 μL, 0.354 mmol), and the mixture was stirred for 2 h at 70 °C under a nitrogen atmosphere. The mixture was cooled to ambient temperature and quenched with water (2 mL). After addition of ethyl acetate (2 mL), the organic layer was separated, and the aqueous layer was extracted with ethyl acetate (5 mL × 3). The combined organic layer was washed with brine, dried over anhydrous Na_2SO_4, filtered, and concentrated under reduced pressure. The crude product was subjected to silica gel column chromatography (1/1 ethyl acetate/hexane; R_f = 0.43) to afford 0.116 g (0.175 mmol, 83%) of **13** as a pale yellow solid: mp. 81.5–82.2 °C; ^{1}H NMR (400 MHz, C_6D_6) δ 7.06 (s, 2H), 6.04 (s, 2H), 2.50–2.63 (m, 3H), 2.31–2.40 (m, 2H), 2.05–2.16 (m, 4H), 1.26–1.45 (m, 4H), 1.02 (s, 9H), 0.82 (d, J = 6.4 Hz, 6H), 0.21 (s, 18H); ^{13}C{^{1}H} NMR (100 MHz, C_6D_6) δ 148.4,

142.8, 135.3, 131.8, 128.0, 121.8, 116.5, 99.0, 98.9, 83.6, 53.0, 51.6, 30.5, 28.1, 27.2, 18.4, 0.01; HRMS (ESI) Calcd. for $C_{36}H_{51}N_2O_2S_2Si_2^+$: 663.2945 ([*M*+H]$^+$). Obsd. 663.2922.

Compound 14. To a solution of **13** (0.197 g, 0.297 mmol) in THF (1.0 mL) was added a methanol suspension (1.0 mL) of sodium methoxide (0.340 g, 6.30 mmol), and the mixture was stirred for 3 h at 80 °C. The mixture was cooled to ambient temperature and quenched with water (4 mL). After addition of ethyl acetate (4.0 mL), the organic layer was separated, and the aqueous layer was extracted with ethyl acetate (5 mL × 3). The combined organic layer was washed with brine, dried over anhydrous Na_2SO_4, filtered, and concentrated under reduced pressure. The crude product was subjected to silica gel column chromatography (ethyl acetate; R_f = 0.83) to afford 0.104 g (0.247 mmol, 83%) of **14** as a yellow solid: mp. 52.0 °C (dec.); ^{1}H NMR (400 MHz, C_6D_6) δ 12.9 (br, 1H), 6.90 (s, 2H), 6.46 (d, *J* = 2.4 Hz, 2H), 2.98 (s, 2H), 2.55 (sept, *J* = 6.6 Hz, 1H), 2.44–2.49 (m, 4H), 1.95 (t, *J* = 5.8 Hz, 4H), 1.39–1.47 (m, 4H), 0.31 (d, *J* = 6.6 Hz); ^{13}C{^{1}H} NMR (100 MHz, C_6D_6) δ 136.0, 135.4, 133.9, 127.1, 119.6, 111.4, 82.4, 77.6, 47.9, 45.9, 26.9, 25.5, 15.2; HRMS (APCI) Calcd. for $C_{25}H_{27}N_2S_2^+$: 419.1610 ([*M*+H]$^+$). Obsd. 419.1616.

Compound 5. To a solution of **14** (0.119 g, 0.285 mmol) in anhydrous THF (1.0 mL) was added an anhydrous THF suspension (8.5 mL) of dimesitylborane (0.143 g, 0.570 mmol), and the mixture was stirred for 13 h under a nitrogen atmosphere in the dark. After all volatiles were removed under reduced pressure, the crude product was washed with ether (10 mL) to afford 0.155 g (0.169 mmol, 59%) of **5** as an orange powder: mp. 158.2 °C (dec.); ^{1}H NMR (400 MHz, C_6D_6) δ 13.2 (br, 1H), 7.43 (d, *J* = 17 Hz, 2H), 7.29 (d, *J* = 17 Hz, 2H), 6.85 (s, 8H), 6.66 (d, *J* = 2.0 Hz, 2H), 6.32 (s, 2H), 2.62 (sept, *J* = 6.6 Hz, 1H), 2.48–2.57 (m, 4H), 2.35 (s, 24H), 2.22 (s, 12H), 1.96–2.06 (m, 4H), 1.46–1.57 (m, 4H), 0.29 (d, *J* = 6.6 Hz, 6H); ^{13}C{^{1}H} NMR (100 MHz, THF-d_8) δ 146.3, 142.9, 141.6, 140.9, 138.6, 137.5, 136.9, 135.3, 135.0, 128.8, 128.8, 111.8, 48.6, 46.5, 27.6, 26.2, 23.4, 21.1, 15.5; ^{11}B{^{1}H} NMR (128 MHz, THF-d_8) δ 70.7; HRMS (ESI) Calcd. for $C_{61}H_{71}B_2N_2S_2$: 917.5250 ([*M*–H]$^-$). Obsd. 917.5239.

Scheme S5. Synthesis of **6**.

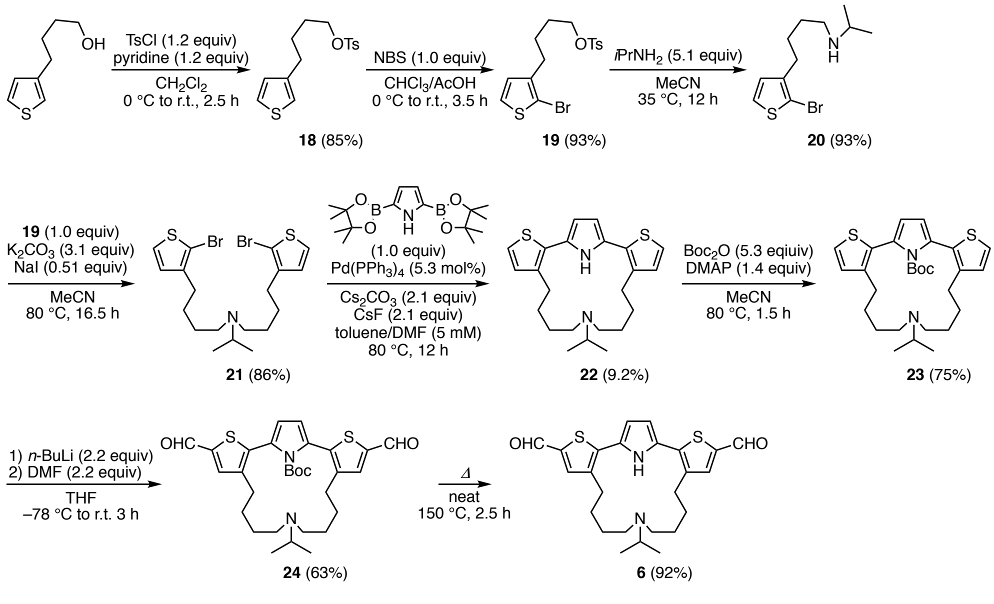

4-(3-Thienyl)butyl *p*-tolylsulfonate (18). To a solution of 4-(3-thienyl)butane-1-ol (0.508 g, 3.25 mmol) in dichloromethane (3.0 mL) was added pyridine (0.310 mL, 0.304 mg, 3.85 mmol) and *p*-toluenesulfonyl chloride (0.735 g, 3.85 mmol) at 0 °C. The mixture was stirred for 2.5 h at ambient temperature and water (5 mL) was added. The organic layer was separated, and the aqueous layer was extracted with ethyl acetate (5 mL × 3). The combined organic layer was washed with brine, dried over anhydrous Na_2SO_4, filtered, and concentrated under reduced pressure. The crude product was subjected to silica gel column chromatography (5/1 hexane/ethyl acetate; $R_f = 0.44$) to afford 0.858 g (2.76 mmol, 85%) of **18** as a colorless oil: ^{1}H NMR (400 MHz, C_6D_6) δ 7.75 (d, J = 8.2 Hz, 2H), 6.88 (dd, J = 3.0, 4.9 Hz, 1H), 6.68 (d, J = 8.2 Hz, 2H), 6.57 (dd, J = 0.8, 4.9 Hz, 1H), 6.46–6.50 (m, 1H), 3.76 (t, J = 6.0 Hz, 2H), 2.16 (t, J = 7.0 Hz, 2H), 1.82 (s, 3H), 1.16–1.30 (m, 4H); ^{13}C{^{1}H} NMR (100 MHz, C_6D_6) δ 144.2, 142.1, 134.6, 129.8, 128.2, 128.2, 125.5, 120.4, 70.1, 29.5, 28.5, 26.4, 21.2; HRMS (APCI) Calcd. for $C_{15}H_{18}O_3S_2$: 310.0697 ([*M*]$^+$). Obsd. 310.0707.

4-(2-Bromo-3-thienyl)butyl *p*-tolylsulfonate (19). To a solution of **18** (9.37 g, 30.2 mmol) in chloroform (30 mL) and acetic acid (30 mL) was added *N*-bromosuccinimide (5.37 g, 30.3 mmol) portionwise at 0 °C over 17 min under a nitrogen atmosphere, and the mixture was stirred for 3.5 h. After addition of a 10 M KOH aqueous solution (50 mL), the organic layer was separated, and the aqueous layer was extracted with chloroform (30 mL × 3). The combined organic layer was washed with brine, dried over anhydrous Na_2SO_4, filtered, and concentrated under reduced pressure. The crude mixture was subjected to silica gel column chromatography (10/1 hexane/ethyl acetate; $R_f = 0.25$) to afford 10.9 g (28.0 mmol, 93%) of **19** as a colorless oil: ^{1}H NMR (400 MHz, C_6D_6) δ 7.74 (d, J = 8.0 Hz, 1H), 6.69 (d, J = 8.0 Hz, 1H), 6.58 (d, J = 5.6 Hz, 1H), 6.27 (d, J = 5.6 Hz, 1H), 3.73 (t, J = 6.0 Hz, 2H), 2.18 (t, J = 7.2 Hz, 2H), 1.83 (s, 3H), 1.15–1.28 (m, 4H); ^{13}C{^{1}H} NMR (100 MHz, C_6D_6) δ 144.2, 141.2, 134.5, 129.8, 128.2, 128.2, 125.7, 109.4, 70.0, 28.6, 28.4, 25.6, 21.2; HRMS (APCI) Calcd. for $C_{15}H_{18}BrO_3S_2^+$: 388.9875 ([*M*+H]$^+$). Obsd. 388.9873.

[4-(2-Bromo-3-thienyl)butyl](2-propyl)amine (20). To a solution of **19** (0.744 g, 1.92 mmol) in acetonitrile (2.0 mL) was added 2-propylamine (0.830 mL, 0.568 g, 9.62 mmol). The mixture was stirred at 35 °C for 28 h, and all volatiles were removed under reduced pressure. After addition of 1 M NaOH aqueous solution (4 mL) and ethyl acetate (4 mL), the organic layer was separated, and the aqueous layer was extracted with ethyl acetate (4 mL × 3). The combined organic layer was washed with 1 M NaOH aqueous solution (4 mL) and brine, dried over anhydrous Na_2SO_4, and concentrated under reduced pressure to afford 0.491 g (1.78 mmol, 93%) of **20** as a pale yellow oil: ^{1}H NMR (400 MHz, C_6D_6) δ 6.63 (d, J = 5.6 Hz, 1H), 6.45 (d, J = 5.6 Hz, 1H), 2.60 (sept, J = 6.2 Hz, 1H), 2.45 (t, J = 7.6 Hz, 2H), 2.42 (t, J = 6.8 Hz, 2H), 1.50 (quint, J = 7.5 Hz, 2H), 1.32 (quint, J = 7.3 Hz, 2H), 0.96 (d, J = 6.2 Hz, 6H); ^{13}C{^{1}H} NMR (100 MHz, C_6D_6) δ 142.1, 128.4, 125.5, 109.2, 49.0, 47.4, 30.5, 29.6, 27.9, 23.4; HRMS(APCI) Calcd. for $C_{11}H_{19}BrNS^+$: 276.0416 ([*M*+H]$^+$). Obsd. 276.0428.

Bis[4-(2-bromo-3-thienyl)butyl](2-propyl)amine (21). To a solution of **19** (4.54 g, 11.7 mmol) in acetonitrile (12 mL) was added **20** (3.24 g, 11.7 mmol), potassium carbonate (4.94g, 35.7 mmol), and sodium iodide (0.902 g, 6.02 mmol), and the mixture was stirred at 80 °C for 16.5 h. After addition of water (10 mL) and ethyl acetate (10 mL) the organic layer was separated, and the aqueous layer was extracted with ethyl acetate (10 mL × 3). The combined organic layer was washed with brine (5 mL), dried over anhydrous Na_2SO_4, filtered, and concentrated under reduced pressure. After hexane (40 mL) was added, the precipitates were removed by filtration, and the filtrate was concentrated under reduced pressure. The crude mixture was subjected to silica gel column chromatography (200/1 hexane/Et_3N; $R_f = 0.13$) to afford 4.95 g (10.0 mmol, 86%) of **21** as a colorless oil: ^1H NMR (400 MHz, C_6D_6) δ 6.64 (d, J = 5.6 Hz, 2H), 6.49 (d, J = 5.6 Hz, 2H), 2.77 (sept, J = 6.6 Hz, 1H), 2.49 (t, J = 7.6 Hz, 4H), 2.22 (t, J = 7.0 Hz, 4H), 1.53 (quint, J = 7.6 Hz, 4H), 1.35 (quint, J = 7.3 Hz, 4H), 0.88 (d, J = 6.6 Hz, 6H); $^{13}C\{^1H\}$ NMR (100 MHz, C_6D_6) δ 142.2, 128.4, 125.6, 109.2, 50.1, 49.6, 29.7, 29.0, 27.8, 18.1; HRMS (APCI) Calcd. for $C_{19}H_{28}Br_2NS_2^+$: 492.0024 ([M+H]$^+$). Obsd. 492.0000.

Compound 22. To a solution of $Pd(PPh_3)_4$ (0.123 g, 0.106 mmol), Cs_2CO_3 (1.36 g, 4.17 mmol), CsF (0.631 g, 4.15 mmol), and 2,5-bis(4,4,5,5-tetramethyl-1,3,2-dioxaborolan-2-yl)pyrrole (0.637 g, 2.00 mmol) in degassed toluene (266 mL) and DMF (133 mL) was added **21** (0.984 g, 2.00 mmol) at 80 °C under an argon atmosphere. The mixture was stirred at 80 °C for 12 h. All volatiles were removed under reduced pressure, and water (5 mL) and ethyl acetate (10 mL) were added. The organic layer was separated, and the aqueous layer was extracted with ethyl acetate (5 mL × 3). The combined organic layer was washed with brine (5 mL), dried over anhydrous Na_2SO_4, filtered, and concentrated under reduced pressure. The mixture was subjected to silica gel column chromatography (ethyl acetate; $R_f = 0.05$, and 100/100/1 hexane/toluene/Et_3N; $R_f = 0.20$) to afford 73.1 mg (0.183 mmol, 9.2%) of **22** as a colorless oil: ^1H NMR (400 MHz, C_6D_6) δ 8.24 (br s, 1H), 6.84 (d, J = 5.2 Hz, 2H), 6.71 (d, J = 5.2 Hz, 2H), 6.45 (d, J = 2.0 Hz, 2H), 2.62 (sept, J = 6.5 Hz, 1H), 2.55 (t, J = 7.6 Hz, 4H), 2.08 (t, J = 6.4 Hz 4H), 1.51 (quint, J = 7.3 Hz, 4H), 1.21 (quint, J = 6.9 Hz, 4H), 0.74 (d, J = 6.5 Hz, 6H); $^{13}C\{^1H\}$ NMR (100 MHz, C_6D_6) δ 139.3, 130.3, 129.6, 126.3, 123.9, 111.2, 50.4, 49.4, 29.3, 29.0, 28.9, 17.7; HRMS (APCI) Calcd. for $C_{23}H_{31}N_2S_2^+$: 399.1923 ([M+H]$^+$). Obsd. 399.1942.

Compound 23. To a solution of **22** (59.1 mg, 0.148 mmol) in acetonitrile (1.0 mL) was added di(*t*-butyl) dicarbonate (0.173 g, 0.791 mmol) and *N,N*-dimethyl-4-aminopyridine (25.9 mg, 0.212 mmol). The mixture was stirred at 80 °C for 1.5 h. After addition of ethyl acetate (5 mL) and water (5 mL), the organic layer was separated, and the aqueous layer was extracted with ethyl acetate (5 mL × 3). The combined organic layer was washed with brine, dried over anhydrous Na_2SO_4, filtered, and concentrated under reduced pressure. The crude mixture was subjected to silica gel column chromatography (ethyl acetate; $R_f = 0.15$) to afford 55.3 mg (0.111 mmol, 75%) of **23** as a colorless solid: mp 54.0–55.0 °C; ^1H NMR (400 MHz, C_6D_6) δ 6.90 (d, J = 5.2 Hz, 2H), 6.73 (d, J = 5.2 Hz, 2H), 6.24 (s, 2H), 2.74 (sept, J = 6.8 Hz, 1H) 2.56–2.68 (m, 4H), 2.14–2.28 (m, 4H), 1.46–1.63 (m, 4H), 1.26–1.42 (m, 4H), 1.11 (s, 9H), 0.83 (d, J = 6.8 Hz, 6H); $^{13}C\{^1H\}$ NMR (100 MHz, CD_2Cl_2) δ 149.1, 143.0, 129.7, 129.3, 127.9, 124.6, 115.3, 84.0, 49.6, 49.4, 29.9, 29.2, 28.2, 27.5, 17.7; HRMS (APCI) Calcd. for $C_{28}H_{39}N_2O_2S_2{}^+$: 499.2447 ([$M$+H]$^+$). Obsd. 499.2465.

Compound 24. To a solution of **23** (0.161 g, 0.322 mmol) in anhydrous THF (1.0 mL) was added a hexane solution of *n*-BuLi (1.62 M, 0.440 mL, 0.713 mmol), and the mixture was stirred for 50 min at –78 °C under a nitrogen atmosphere. Then, *N,N*-dimethylformamide (56.0 μL, 52.8 mg, 0.723 mmol) was added to the solution, and the resulting mixture was stirred for 2 h. After addition of water (2 mL) and ethyl acetate (5 mL), the organic layer was separated, and the aqueous layer was extracted with ethyl acetate (10 mL × 3). The combined organic layer was washed with brine, dried over anhydrous Na_2SO_4, filtered, and concentrated under reduced pressure. The crude product was recrystallized from ethyl acetate to afford 113 mg (0.204 mmol, 63%) of **24** as a yellow crystal: mp 149.3–150.0 °C; ^{1}H NMR (400 MHz, C_6D_6) δ 9.58, (s, 2H), 6.92 (s, 2H), 6.04 (s, 2H), 2.71 (sept, J = 6.7 Hz, 1H), 2.37–2.50 (m, 4H), 2.12–2.25 (m, 4H), 1.41 (quint, J = 7.5 Hz, 4H), 1.17–1.35 (m, 4H), 0.96 (s, 9H), 0.83 (d, J = 6.7 Hz, 6H); ^{13}C{^{1}H} NMR (100 MHz, C_6D_6) δ 182.0, 148.2, 144.0, 142.9, 139.4, 137.0, 127.7 116.2, 84.4, 49.9, 49.6, 29.9, 29.3, 27.9, 27.1, 17.7; HRMS (ESI) Calcd. for $C_{30}H_{39}N_2O_4S_2^+$ 555.2346 ([M+H]$^+$). Obsd. 555.2342.

Compound 6. Compound **24** (40.9 mg, 73.7 μmol) was heated neat for 2.5 h at 150 °C under a nitrogen atmosphere. The crude product was subjected to silica gel column chromatography (500/100/1 toluene/ethyl acetate/Et_3N; R_f = 0.15) to afford 30.8 mg (67.7 μmol, 92%) of **6** as a yellow solid: mp 142.1–143.0 °C; ^{1}H NMR (400 MHz, C_6D_6) δ 9.60 (s, 2H), 8.27 (br s, 1H), 6.91 (s, 2H), 6.31 (s, 2H), 2.60 (sept, J = 6.8 Hz, 1H), 2.36 (t, J = 7.8 Hz, 4H), 2.09 (t, J = 6.6 Hz, 4H), 1.40 (quint, J = 7.5 Hz, 4H), 1.14 (quint, J = 6.7 Hz, 4H), 0.75 (d, J = 6.8 Hz, 6H); ^{13}C{^{1}H} NMR (100 MHz, C_6D_6) δ 181.7, 141.5, 139.4, 139.1, 138.1, 127.3, 113.0, 50.7, 49.5, 29.2, 28.9, 28.6, 17.7; HRMS (APCI) Calcd. for $C_{25}H_{30}N_2O_2S_2$: 454.1743 ([M]$^+$). Obsd. 454.1757.

Scheme S6. Synthesis of **7**.

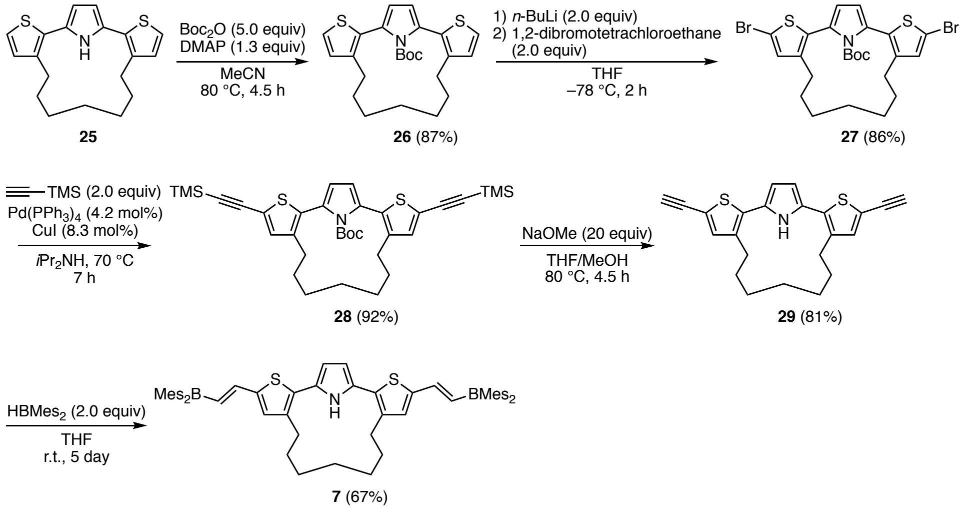

Compound 26. To a solution of **25** (0.199 g, 0.606 mmol) in acetonitrile (1.0 mL) was added di(t-butyl) dicarbonate (0.670 g, 3.06 mmol) and N,N-dimethyl-4-aminopyridine (94.3 mg, 0.771 mmol). The mixture was stirred at 80 °C for 4.5 h. After addition of ethyl acetate (2 mL) and water (5 mL), the organic layer was separated, and the aqueous layer was extracted with ethyl acetate (5 mL × 3). The combined organic layer was washed with brine, dried over anhydrous Na_2SO_4, filtered, and concentrated under reduced pressure. The crude mixture was subjected to silica gel column chromatography (30/1 hexane/ethyl acetate; R_f = 0.50) and further purified by HPLC (30/1 hexane/ethyl acetate) to afford 0.226 g (0.528 mmol, 87%) of **26** as a colorless crystal: mp. 79.0–79.8 °C; ^{1}H NMR (400 MHz, C_6D_6) δ 6.90 (d, J = 5.0 Hz, 2H), 6.68 (d, J = 5.0 Hz, 2H), 6.17 (s, 2H), 2.43–2.60 (m, 4H), 1.41–1.58 (m, 4H), 1.26–1.38 (m, 2H), 1.14–1.25 (m, 4H), 1.08 (s, 9H); ^{13}C{^{1}H} NMR (100 MHz, CD_2CL_2) δ 149.2, 143.6, 130.0, 129.4, 128.4, 124.7, 115.8, 84.3, 29.3, 28.4, 28.1, 27.5, 26.6; HRMS (ESI) Calcd. for $C_{24}H_{29}NO_2S_2Na^+$: 450.1532 ([M+Na]$^+$). Obsd. 450.1531.

Compound 27. To a solution of **26** (136 mg, 0.318 mmol) in anhydrous THF (1.0 mL) was added a hexane solution of *n*-BuLi (1.62 M, 0.400 mL, 0.648 mmol), and the mixture was stirred for 1 h at –78 °C under a nitrogen atmosphere. Then, a THF solution (1.0 mL) of 1,2-dibromotetrachloroethane (207 mg, 0.636 mmol) was added to the solution and the resulting mixture was stirred at –78 °C for 1 h. The mixture was allowed to warm to ambient temperature and quenched with water (2 mL). After addition of ethyl acetate (5 mL), the organic layer was separated, and the aqueous layer was extracted with ethyl acetate (5 mL × 3). The combined organic layer was washed with brine, dried over anhydrous Na_2SO_4, filtered, and concentrated under reduced pressure. The crude product was subjected to silica gel column chromatography (30/1 hexane/ethyl acetate; $R_f = 0.48$) to afford 160 mg (0.275 mmol, 86%) of **27** as a colorless solid: mp. 115.6–116.0 °C; ^{1}H NMR (400 MHz, C_6D_6) δ 6.58 (s, 2H), 6.02 (s, 2H), 2.30–2.39 (m, 2H), 2.16–2.24 (m, 2H), 1.28–1.42 (m, 4H), 1.16–1.26 (m, 2H), 0.96–1.10 (m, 12H), 0.82–0.94 (m, 1H); ^{13}C{^{1}H} NMR (100 MHz, C_6D_6) δ 148.4, 144.1, 131.7, 131.7, 127.3, 116.3, 111.9, 84.2, 29.4, 27.5, 27.3, 27.2, 26.4; HRMS (APCI) Calcd. for $C_{24}H_{27}Br_2NO_2S_2Na^+$: 605.9742 ([$M$+Na]$^+$). Obsd. 605.9743.

Compound 28. To a solution of **27** (81.8 mg, 0.140 mmol), $Pd(PPh_3)_4$ (6.82 mg, 5.90 μmol), and CuI (2.04 mg, 11.6 μmol) in degassed anhydrous *i*Pr_2NH (1.0 mL) was added trimethylsilylacetylene (40.0 μL, 0.283 mmol), and the mixture was stirred for 7 h at 70 °C under a nitrogen atmosphere. The mixture was cooled to ambient temperature. After addition of ethyl acetate (5 mL) and water (5 mL), the organic layer was separated, and the aqueous layer was extracted with ethyl acetate (5 mL × 3). The combined organic layer was washed with brine, dried over anhydrous Na_2SO_4, filtered, and concentrated under reduced pressure. The crude product was subjected to silica gel column chromatography (5/1 hexane/toluene; $R_f = 0.35$) to afford 80.4 mg (0.130 mmol, 92%) of **28** as a pale yellow solid: mp 77.0–78.0 °C; ^{1}H NMR (400 MHz, C_6D_6) δ 6.97 (s, 2H), 6.00 (s, 2H), 2.23–2.38 (m, 4H), 1.26–1.42 (m, 4H), 1.15–1.26 (m, 2H), 0.94–1.12 (m, 13H), 0.20 (s, 18H); ^{13}C{^{1}H} NMR (100 MHz, C_6D_6) δ 148.4, 143.3, 134.9, 132.1, 127.4, 122.8, 116.3, 99.1, 98.8, 84.1, 29.1, 27.8, 27.6, 27.2, 26.3 –0.05; HRMS (ESI) Calcd. for $C_{34}H_{45}NO_2S_2Si_2Na^+$: 642.2322 ([$M$+Na]$^+$). Obsd. 642.2321.

Compound 29. To a solution of **28** (44.6 mg, 71.9 μmol) in THF (1.0 mL) was added a methanol suspension (1.0 mL) of sodium methoxide (78.6 mg, 1.45 mmol), and the mixture was stirred at 80 °C for 4.5 h. The mixture was cooled to ambient temperature. After addition of ethyl acetate (5 mL) and water (5 mL), the organic layer was separated, and the aqueous layer was extracted with ethyl acetate (5 mL × 3). The combined organic layer was washed with brine, dried over anhydrous Na_2SO_4, filtered, and concentrated under reduced pressure. The crude mixture was subjected to silica gel column chromatography (4/1 hexane/toluene; $R_f = 0.46$) to afford 22.0 mg (58.6 μmol, 81%) of **29** as a pale yellow solid: mp. 154.0 °C (dec.); ^{1}H NMR (400 MHz, C_6D_6) δ 7.56 (br s, 1H), 6.87 (s, 2H), 6.24 (d, J = 2.4 Hz, 2H), 2.97 (s, 2H), 2.20 (t, J = 7.0 Hz, 4H), 1.17–1.26 (m, 4H), 0.85–0.97 (m, 6H); ^{13}C{^{1}H} NMR (100 MHz, C_6D_6) δ 139.7, 135.8, 132.0, 125.5, 120.8, 112.1, 82.3, 77.4, 29.6, 27.7, 27.0, 25.2; HRMS (ESI) Calcd. for $C_{23}H_{20}NS_2^-$: 374.1043 ([M–H]$^-$). Obsd. 374.1028.

Compound 7. To a solution of **29** (0.143 g, 0.381 mmol) in anhydrous THF was added a THF solution (10 mL) of dimesitylborane (0.190 g, 0.761 mmol), and the mixture was stirred for 5 days in the dark under a nitrogen atmosphere. All volatiles were removed under reduced pressure. The crude product was washed with ether (10 mL) to afford 225 mg (0.256 mmol, 67%) of **7** as a yellow powder: mp. 141.2 °C (dec.); ^{1}H NMR (400 MHz, C_6D_6) δ 7.87 (br s, 1H), 7.41 (d, J = 17 Hz, 2H), 7.32 (d, J = 17 Hz, 2H), 6.86 (s, 8H), 6.46 (d, J = 2.4 Hz, 2H), 6.26 (s, 2H), 2.38 (s, 24H), 2.27 (t, J = 7.6 Hz, 4H), 2.23 (s, 12H), 1.25–1.34 (m, 4H), 1.08–1.15 (m, 6H); ^{13}C{^{1}H} NMR (100 MHz, C_6D_6) δ 145.3, 142.9, 142.4, 141.0, 139.5, 138.7, 137.8, 134.1, 133.1, 128.9, 127.4, 112.4, 29.5, 28.5, 27.2, 24.9, 23.6, 21.3; ^{11}B{^{1}H} NMR (128 MHz, THF-d_8) δ 73.2; HRMS (ESI) Calcd. for $C_{59}H_{66}B_2NS_2$: 873.4865 ([M–H]$^-$). Obsd. 873.4851.

2. X-ray Crystallographic Analysis

Single crystals of **3** suitable for X-ray crystallographic analysis were obtained by slow cooling of a solution of **3** in ethyl acetate. Intensity data were collected at 123 K with Mo Kα radiation (λ = 0.71075 Å). A total of 9847 reflections were measured at a maximum 2θ angle of 52.7°, of which 4181 were independent reflections (R_{int} = 0.0183). The structure was solved be the direct method (SIR97)[4] and refined by full-matrix least-squares on F^2 (SHELXL-2013).[5] All non-hydrogen atoms were refined anisotropically, and all hydrogen atoms were placed using AFIX instructions. The crystal data are as follows: formula $C_{23}H_{26}N_2O_2S_2$, FW = 426.58, crystal size 0.30 mm × 0.08 mm × 0.06 mm, triclinic, P–1, a = 7.41480(10) Å, b = 10.3516(3) Å, c = 14.6348(3) Å, α = 82.054(8)°, β = 79.877(7)°, γ = 73.007(7)°, V = 1053.02(6) Å^3, Z = 4, D_{calcd} = 1.345 g cm^{-3}, μ = 0.275 mm^{-1}, R_1 = 0.0287 ($I > 2\sigma(I)$), wR_2 = 0.0816 (all data), GOF = 1.101. CCDC 1813601 contains the supplementary crystallographic data for this compound. This data can be obtained free of charge from The Cambridge Crystallographic Data Centre at www.ccdc.cam.ac.uk/data_request/cif.

Single crystals of **6** suitable for X-ray crystallographic analysis were obtained by slow diffusion of hexane vapor into a solution of **6** in ethyl acetate. Intensity data were collected at 123 K with Mo Kα radiation (λ = 0.71075 Å). A total of 18152 reflections were measured at a maximum 2θ angle of 55.0°, of which 5384 were independent reflections (R_{int} = 0.0214). The structure was solved be the direct method (SIR97)[4] and refined by full-matrix least-squares on F^2 (SHELXL-97).[6] All non-hydrogen atoms were refined anisotropically, and all hydrogen atoms were placed using AFIX instructions. The crystal data are as follows: formula $C_{25}H_{30}N_2O_2S_2$, FW = 454.63, crystal size 0.40 mm × 0.40 mm × 0.40 mm, monoclinic, $P2_1$/a, a = 10.7685(17) Å, b = 14.2394(19) Å, c = 16.386(3) Å, β = 108.7594(19)°, V = 2379.1(7) Å^3, Z = 4, D_{calcd} = 1.269 g cm^{-3}, μ = 0.248 mm^{-1}, R_1 = 0.0342 ($I > 2\sigma(I)$), wR_2 = 0.0865 (all data), GOF = 1.023. CCDC 1813602 contains the supplementary crystallographic data for this compound. This data can be obtained free of charge from The Cambridge Crystallographic Data Centre at www.ccdc.cam.ac.uk/data_request/cif.

3. Comparison of ^{1}H NMR spectra between 3 and 6

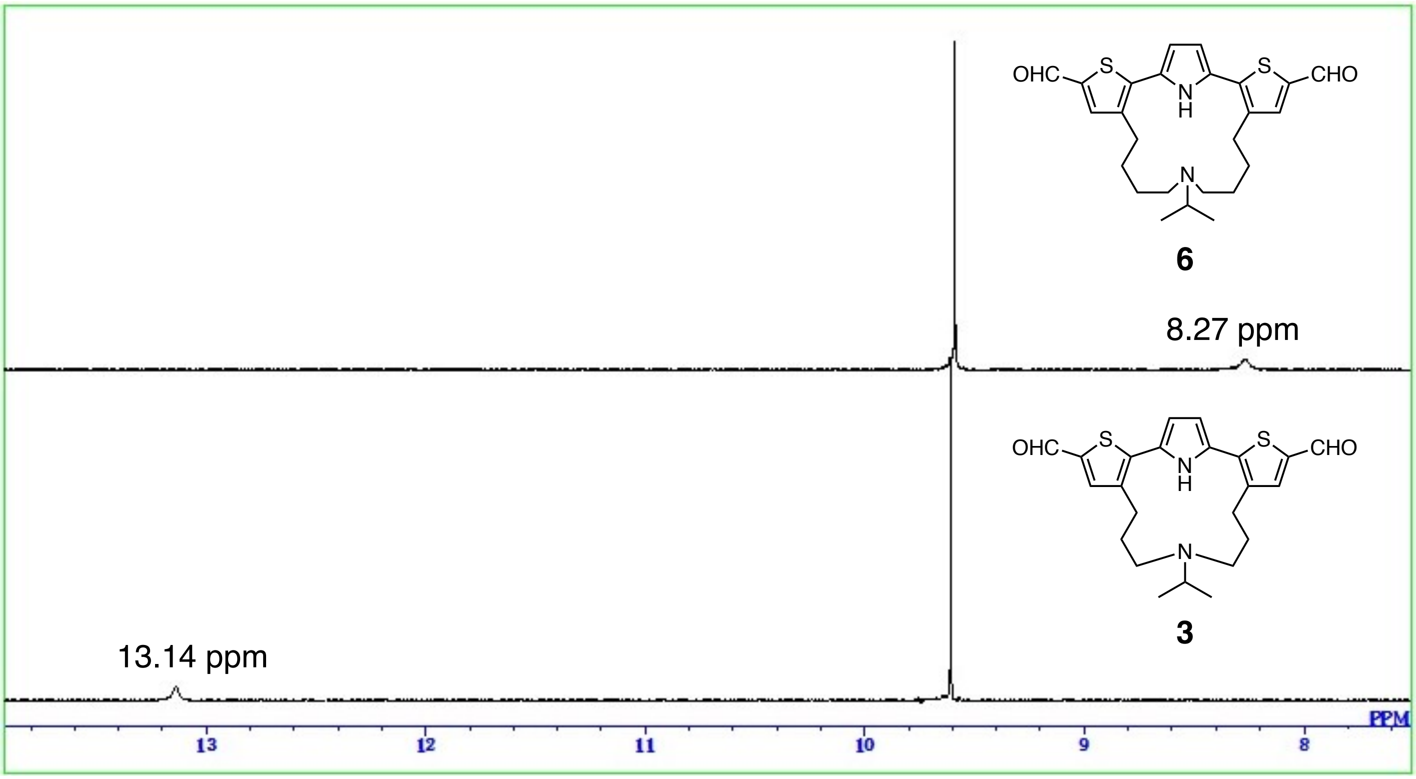

Fig. S1 Comparison of ^{1}H NMR spectra between **3** and **6** in C_6D_6.

4. Photophysical Properties

Measurements. UV/Vis absorption spectra of compounds **2–7** were measured with a Shimadzu UV-3150 spectrometer with a resolution of 0.2 nm using dilute sample solutions in spectral grade solvents in a 1 cm square quartz cuvette. Emission spectra of compounds **2**, **3**, **6**, and **7** were measured with a Hitachi F-4500 spectrometer with a resolution of 0.2 nm. Emission spectra of **4** and **5** were measured with Horiba SPEX Fluorolog 3 spectrofluorometer equipped with a Hamamatsu PMA R5509-73 and a cooling system C9940-01 with a resolution of 0.5 nm. Absolute fluorescence quantum yields were determined with a Hamamatsu Photonics C-9920-02 calibrated integrating sphere system. Self-absorption correction was carried out for all data.[7] The absorption and emission spectra of **2–7** are given in Fig. S2–S7. Excitation spectra of **2–5** are given in Fig. S8–S11. All photophysical properties are summarized in Table S1. Experimental details and photophysical properties of **1** are described in the previous paper.[1]

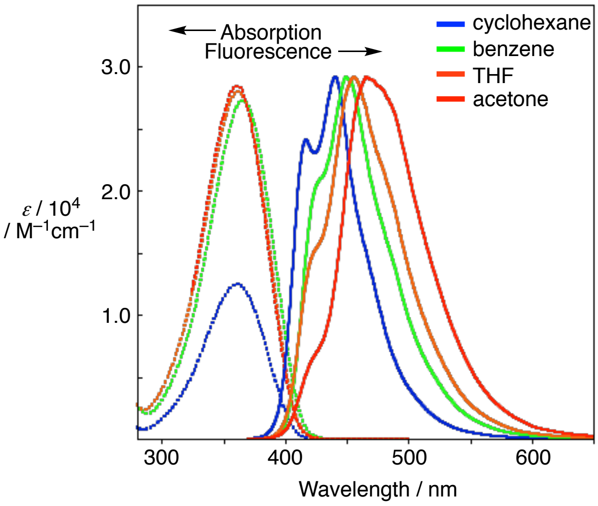

Fig. S2 Absorption and emission spectra of **2** in various solvents. The value of absorption coefficient in cyclohexane is underestimated due to low solubility of **2**.

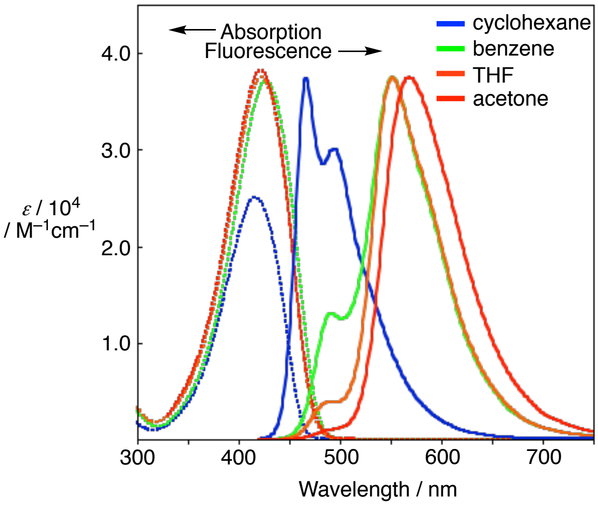

Fig. S3 Absorption and emission spectra of **3** in various solvents. The value of absorption coefficient in cyclohexane is underestimated due to low solubility of **3**.

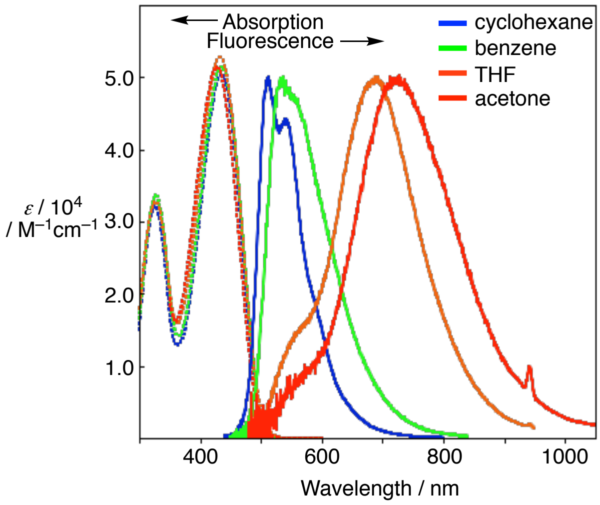

Fig. S4 Absorption and emission spectra of **4** in various solvents.

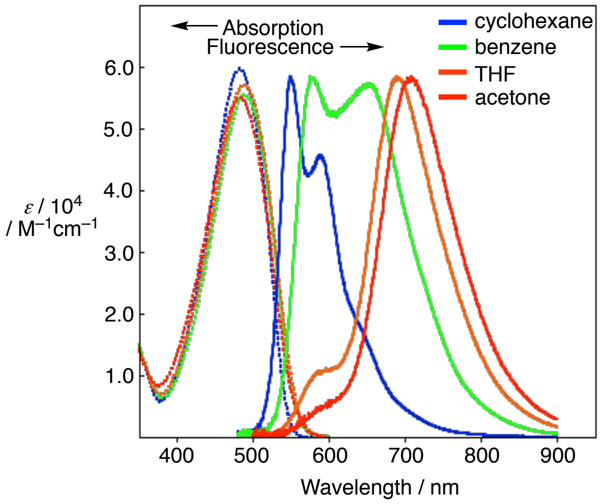

Fig S5 Absorption and emission spectra of **5** in various solvents.

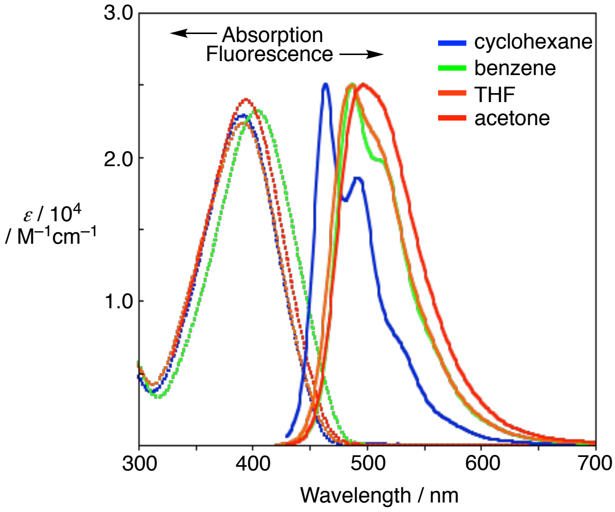

Fig. S6 Absorption and emission spectra of **6** in various solvents.

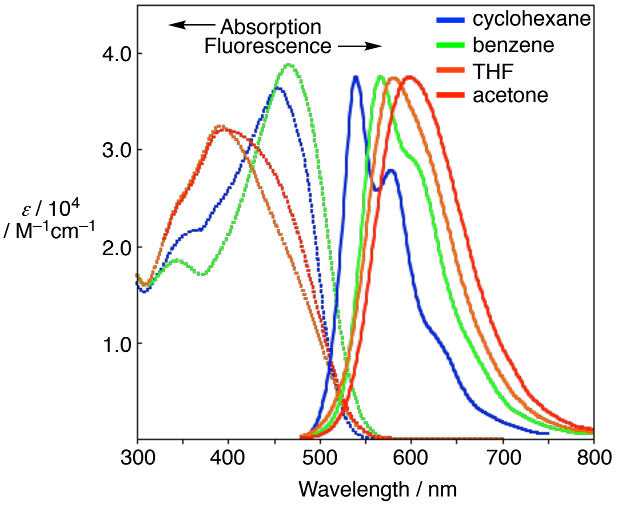

Fig. S7 Absorption and emission spectra of **7** in various solvents.

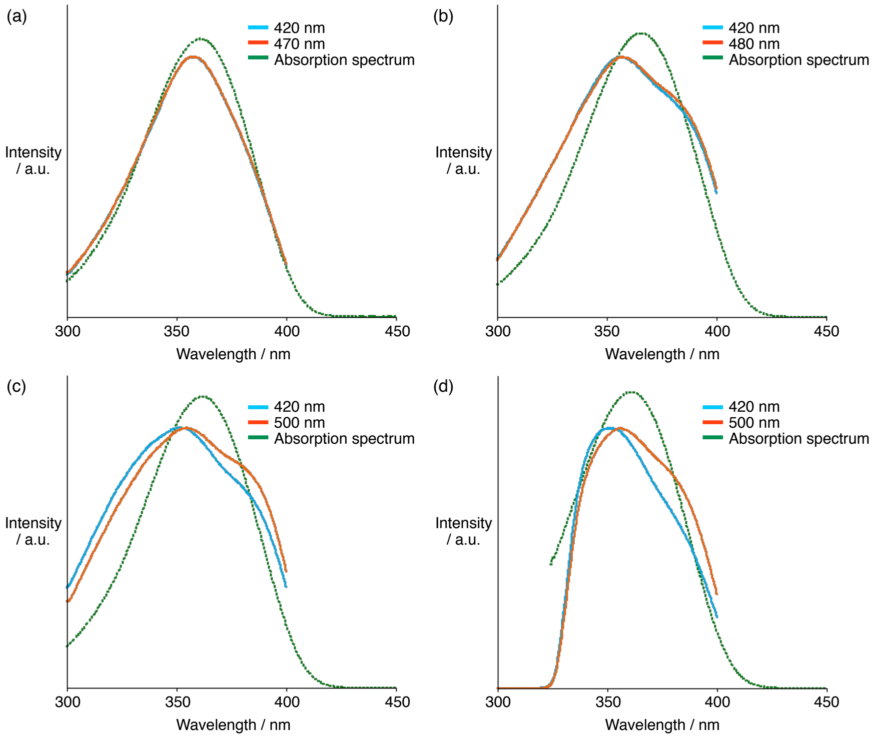

Fig. S8 Excitation spectra of **2** in (a) cyclohexane, (b) benzene, (c) THF, and (d) acetone.

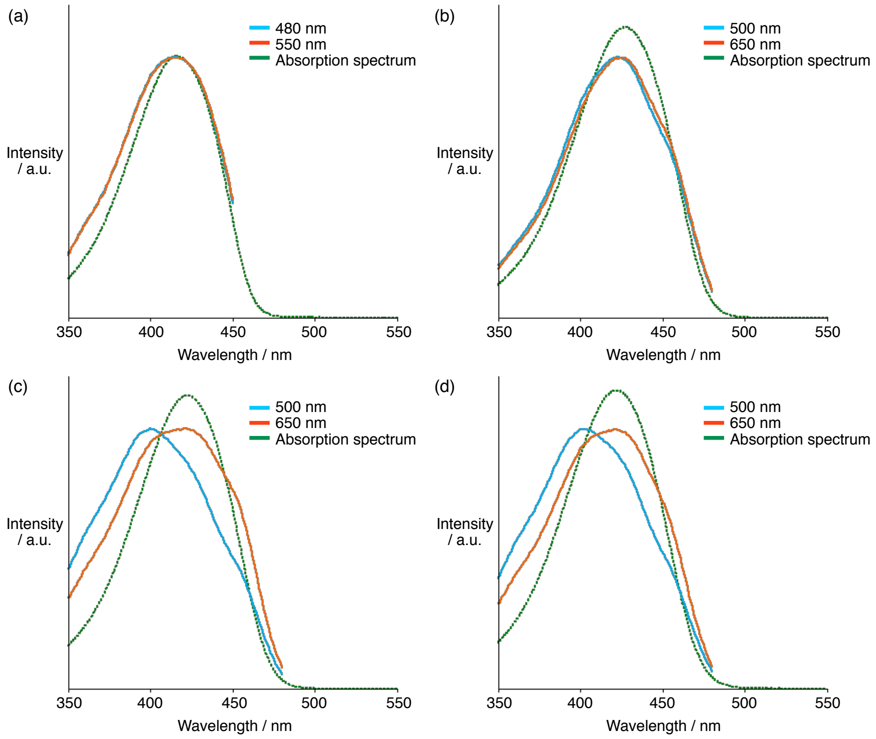

Fig. S9 Excitation spectra of **3** in (a) cyclohexane, (b) benzene, (c) THF, and (d) acetone.

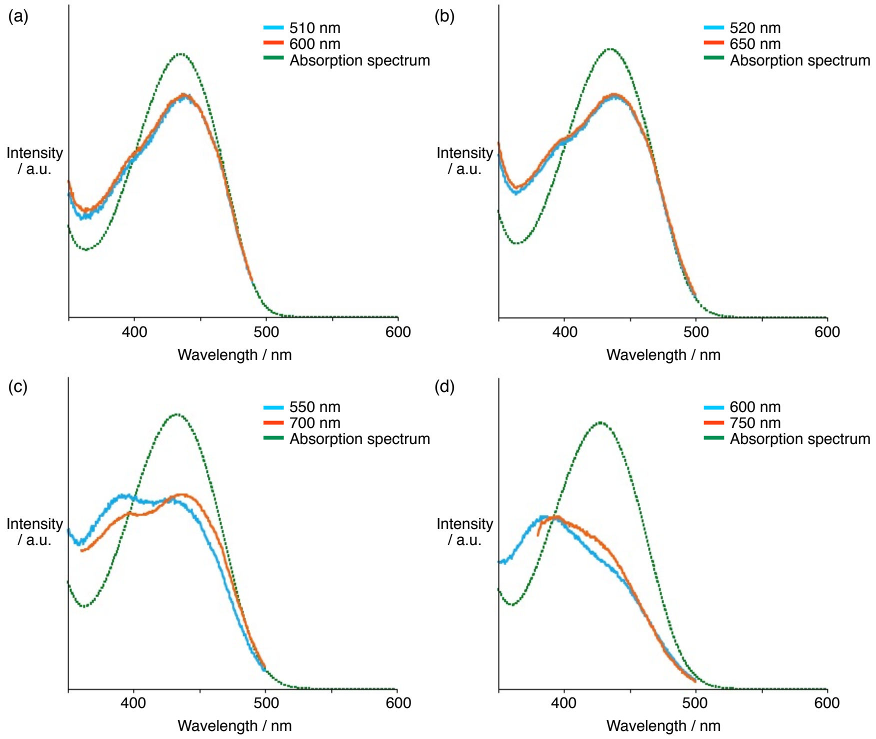

Fig. S10 Excitation spectra of **4** in (a) cyclohexane, (b) benzene, (c) THF, and (d) acetone.

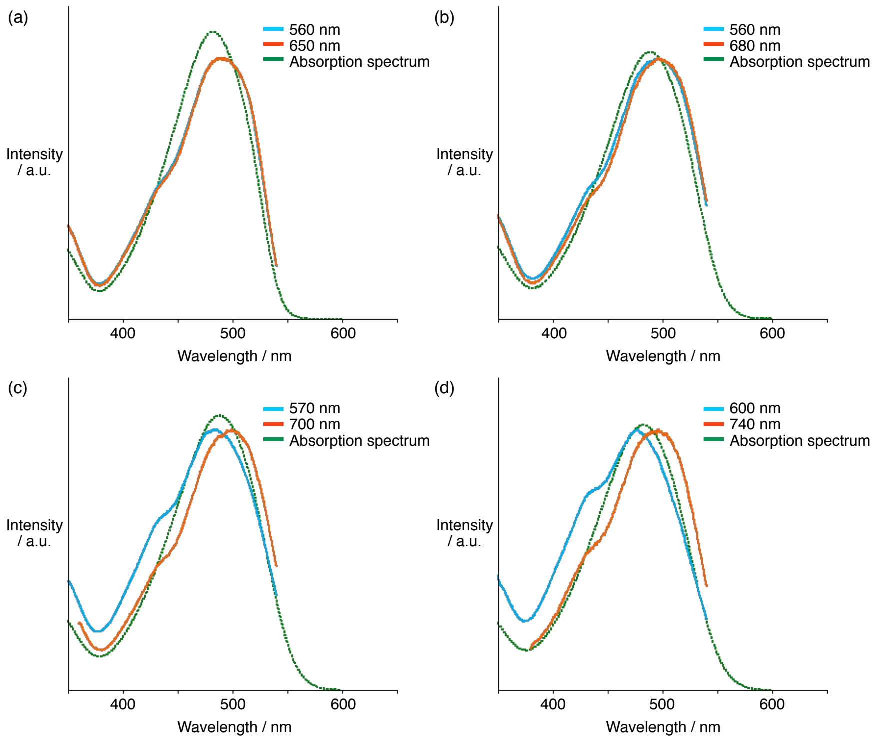

Fig. S11 Excitation spectra of **5** in (a) cyclohexane, (b) benzene, (c) THF, and (d) acetone.

Table S1. Summary of Photophysical Properties of **2–7**.

		Absorption		Fluorescence							
Cmpd	Solvent	λ_{abs}[a] [nm]	$\varepsilon/10^4$ [$M^{-1}cm^{-1}$]	λ_{em} [nm]	Φ_F[b]	τ_1 [ns]	τ_2 [ns]	A_1	A_2	k_r [10^9 s^{-1}]	k_{nr} [10^9 s^{-1}]
2	cyclohexane	361	–[c]	417	0.31	0.80	–[d]	0.08	–	0.39	0.86
	benzene	366	2.73	424, 485	0.33	0.84	–[d]	0.11	–	0.39	0.79
	THF	362	2.81	420, 487	0.28	0.74	0.97	0.13	0.03	–	–
	acetone	361	2.85	420, 490	0.27	0.86	1.1	0.11	0.04	–	–
3	cyclohexane	416	–[c]	466	0.37	0.90	–[d]	0.13	–	0.41	0.70
	benzene	427	3.71	491, 551	0.48	1.0	1.5	0.05	0.07	–	–
	THF	423	3.76	490, 552	0.52	0.73	1.7	0.02	0.10	–	–
	acetone	422	3.82	490, 568	0.60	–[d]	2.2	–	0.10	0.27	0.18
4	cyclohexane	435	5.05	513	0.72	1.2	–[d]	0.24	–	0.62	0.24
	benzene	435	5.19	536	0.71	1.2	2.0	0.20	0.03	–	–
	THF	433	5.28	550, 693	0.58	1.2	2.6	0.07	0.13	–	–
	acetone	429	5.14	560, 728	0.18	0.72	1.5	0.10	0.13	–	–
5	cyclohexane	482	5.99	547	0.68	1.4	1.7	0.08	0.01	–	–
	benzene	489	5.55	578, 653	0.67	1.4	1.7	0.04	0.05	–	–
	THF	488	5.73	585, 690	0.65	1.7	2.1	0.03	0.05	–	–
	acetone	483	5.54	585, 708	0.55	1.5	2.1	0.02	0.06	–	–
6	cyclohexane	391	2.29	463	0.28	0.90	–[d]	0.20	–	0.31	0.80
	benzene	404	2.32	486	0.30	1.0	–[d]	0.17	–	0.30	0.70
	THF	393	2.24	489	0.20	0.87	–[d]	0.15	–	0.23	0.90
	acetone	394	2.39	496	0.15	0.73	–[d]	0.14	–	0.20	1.2
7	cyclohexane	455	3.64	539	0.64	1.2	–[d]	0.13	–	0.52	0.29
	benzene	467	3.88	566	0.66	1.3	–[d]	0.15	–	0.50	0.26
	THF	391	3.25	583	0.58	1.4	–[d]	0.17	–	0.40	0.29
	acetone	395	3.21	599	0.56	1.5	–[d]	0.10	–	0.37	0.29

[a] Only the longest absorption maximum wavelengths are shown. [b] Absolute fluorescence quantum yields determined by a calibrated integrating sphere system within ±3% error. [c] Not dissolved. [d] Not observed.

Time-Resolved Fluorescence Measurement. Time-resolved fluorescence spectra were measured with a Hamamatsu Picosecond Fluorescence Measurement System C4780 equipped with a picosecond light pulser PLP-10 (excitation wavelength 377 nm for **2**, 400 nm for **3** and **4**, 464 nm for **5** and **7**, and 403 nm for **6** with a repetition rate of 10 Hz). All the decay profiles were fitted reasonably well using either a single exponential function or a double exponential function. The fluorescence decay profiles are shown in Fig. S12–S17.

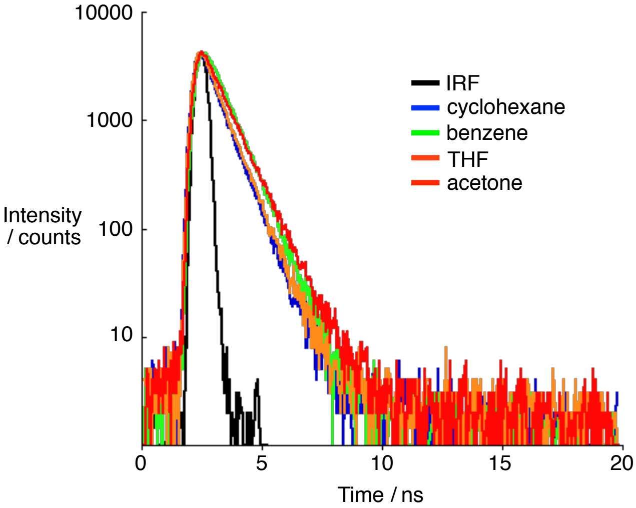

Fig. S12 Fluorescence decay profiles of **2** in cyclohexane ($\tau = 0.800$ ns, $\chi^2 = 1.127$), benzene ($\tau = 0.843$ ns, $\chi^2 = 1.178$), THF ($\tau_1 = 0.739$ ns, $\tau_2 = 0.972$ ns, $A_1 = 0.125$, $A_2 = 0.028$, $\chi^2 = 1.094$), and acetone ($\tau_1 = 0.855$ ns, $\tau_2 = 1.089$ ns, $A_1 = 0.107$, $A_2 = 0.039$, $\chi^2 = 0.976$). IRF represents the instrumental response.

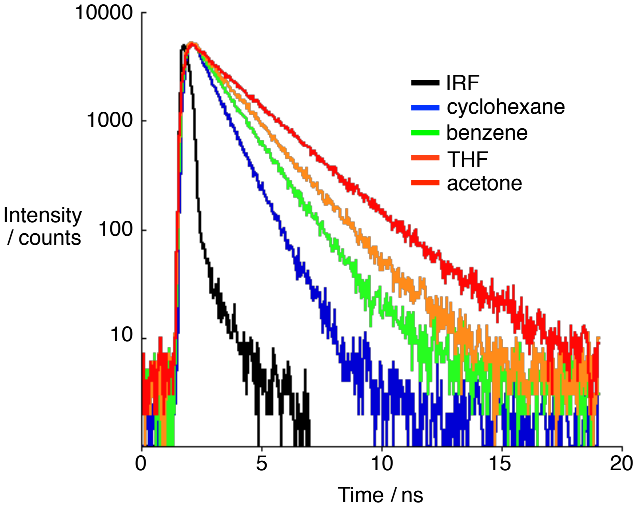

Fig. S13 Fluorescence decay profiles of **3** in cyclohexane ($\tau = 0.901$ ns, $\chi^2 = 1.002$), benzene ($\tau_1 = 1.033$ ns, $\tau_2 = 1.462$ ns, $A_1 = 0.047$, $A_2 = 0.073$, $\chi^2 = 1.146$), THF ($\tau_1 = 0.729$ ns, $\tau_2 = 1.710$ ns, $A_1 = 0.017$, $A_2 = 0.098$, $\chi^2 = 1.172$), and acetone ($\tau = 2.156$ ns, $\chi^2 = 1.172$). IRF represents the instrumental response.

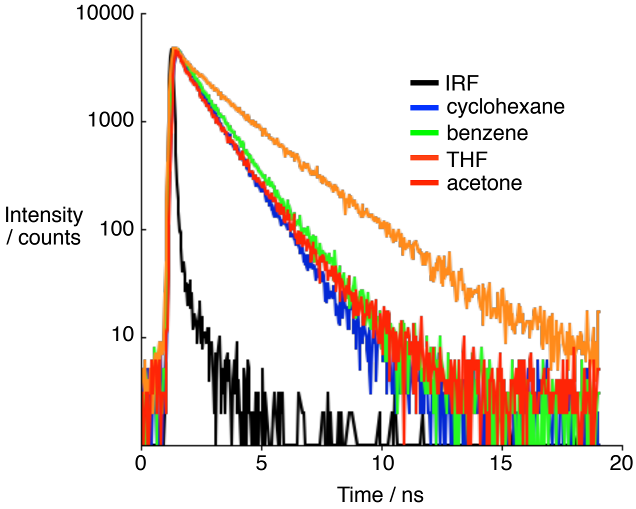

Fig. S14 Fluorescence decay profiles of **4** in cyclohexane ($\tau = 1.152$ ns, $\chi^2 = 1.195$), benzene ($\tau_1 = 1.197$ ns, $\tau_2 = 1.952$ ns, $A_1 = 0.196$, $A_2 = 0.031$, $\chi^2 = 1.160$), THF ($\tau_1 = 1.186$ ns, $\tau_2 = 2.553$ ns, $A_1 = 0.075$, $A_2 = 0.128$, $\chi^2 = 1.180$), and acetone ($\tau_1 = 0.718$ ns, $\tau_2 = 1.454$ ns, $A_1 = 0.096$, $A_2 = 0.135$, $\chi^2 = 1.190$). IRF represents the instrumental response.

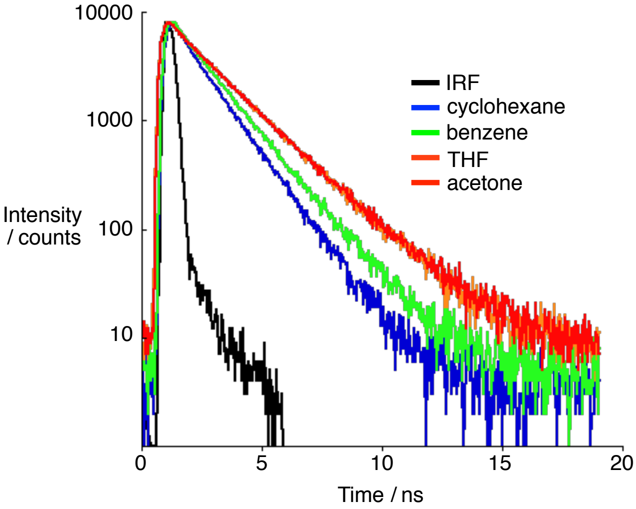

Fig. S15 Fluorescence decay profiles of **5** in cyclohexane ($\tau_1 = 1.361$ ns, $\tau_2 = 1.670$ ns, $A_1 = 0.077$, $A_2 = 0.009$, $\chi^2 = 1.051$), benzene ($\tau_1 = 1.350$ ns, $\tau_2 = 1.702$ ns, $A_1 = 0.038$, $A_2 = 0.050$, $\chi^2 = 1.108$), THF ($\tau_1 = 1.670$ ns, $\tau_2 = 2.133$ ns, $A_1 = 0.029$, $A_2 = 0.050$, $\chi^2 = 1.188$), and acetone ($\tau_1 = 1.502$ ns, $\tau_2 = 2.111$ ns, $A_1 = 0.017$, $A_2 = 0.062$, $\chi^2 = 1.191$). IRF represents the instrumental response.

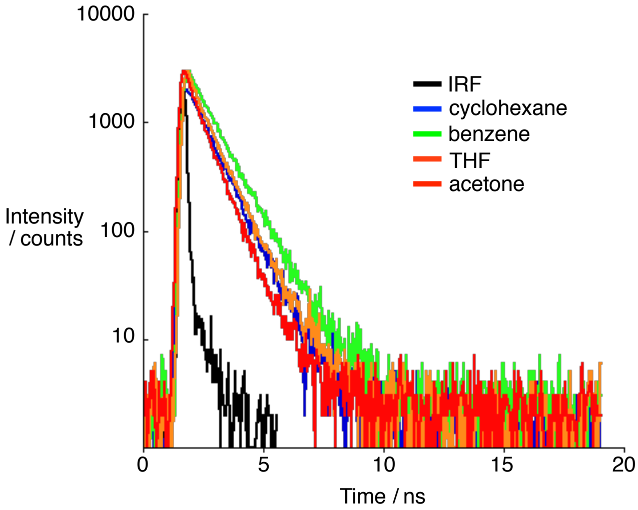

Fig. S16 Fluorescence decay profiles of **6** in cyclohexane ($\tau = 0.901$ ns, $\chi^2 = 1.173$), benzene ($\tau = 0.997$ ns, $\chi^2 = 1.175$), THF ($\tau = 0.885$ ns, $\chi^2 = 1.137$), and acetone ($\tau = 0.739$ ns, $\chi^2 = 1.056$). IRF represents the instrumental response.

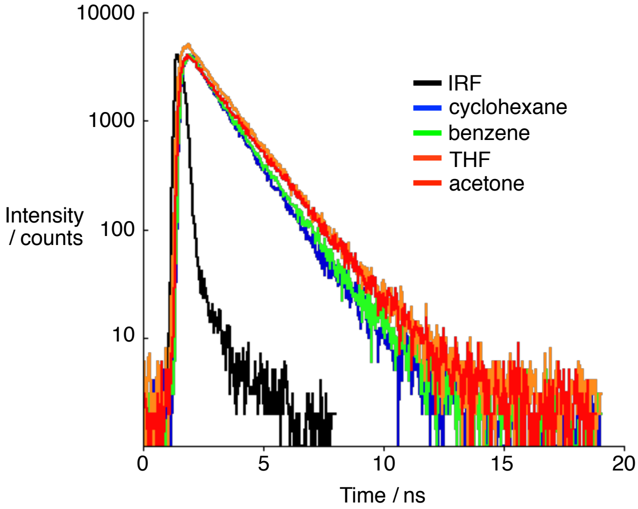

Fig. S17 Fluorescence decay profiles of **7** in cyclohexane ($\tau = 1.237$ ns, $\chi^2 = 1.137$), benzene ($\tau = 1.327$ ns, $\chi^2 = 1.196$), THF ($\tau = 1.440$ ns, $\chi^2 = 1.198$), and acetone ($\tau = 1.518$ ns, $\chi^2 = 1.101$). IRF represents the instrumental response.

Z-scan Measurements. A femtosecond optical parametric amplifier (*SpectraPhysics TOPAS Prime*, pumped by a regenerative amplifier, *Spitfire*, operating at 1 kHz) was used as the light source for the Z-scan measurements.[8] The pulse width varied depending on the wavelength selected but was in the range of 90-140 fs in full width at half maximum (FWHM). The sample solution was hold in a 2-mm quartz cuvette, which is much shorter that the Rayleigh range of the optical setup (8–10 mm)[9] and satisfies the thin-sample condition for the analysis. The pulse width and the Rayleigh range were measured at each selected wavelength to calculate the correct on-axis peak intensity of the incident pulse at the wavelength. The incident power (i.e., the average power) was verified in the range of 0.05–1 mW and the corresponding on-axis peak intensities were below 300 GWcm^2. The concentrations of the sample solutions were 2.8–2.9 mM for compound **1**, 2.6–2.8 mM for **5**, and 2.7 mM for **7** (all in spectroscopic grade THF). At least 400 shots of laser pulses whose fluctuation was smaller than 5% were averaged to obtain data points of each sample position of the Z-scan traces. Analysis of open-aperture Z-scan trace was performed by curve fitting of the theoretical equation that assumes spatial and temporal Gaussian pulses.[9, 10] Typical open-aperture Z-scan traces are presented in Fig. S18–S20. The TPA coefficient β was obtained from the slope of the plots of the two-photon absorbance q_0 and the on-axis peak intensity. The TPA cross section was obtained by using the convention, $\sigma^{(2)} = h\nu\beta/N$, where $h\nu$ is photon energy and N is the number density. The obtained $\sigma^{(2)}$ was corrected based on that of MPPBT[11] in DMSO (2.3 mM) measured at the same time.

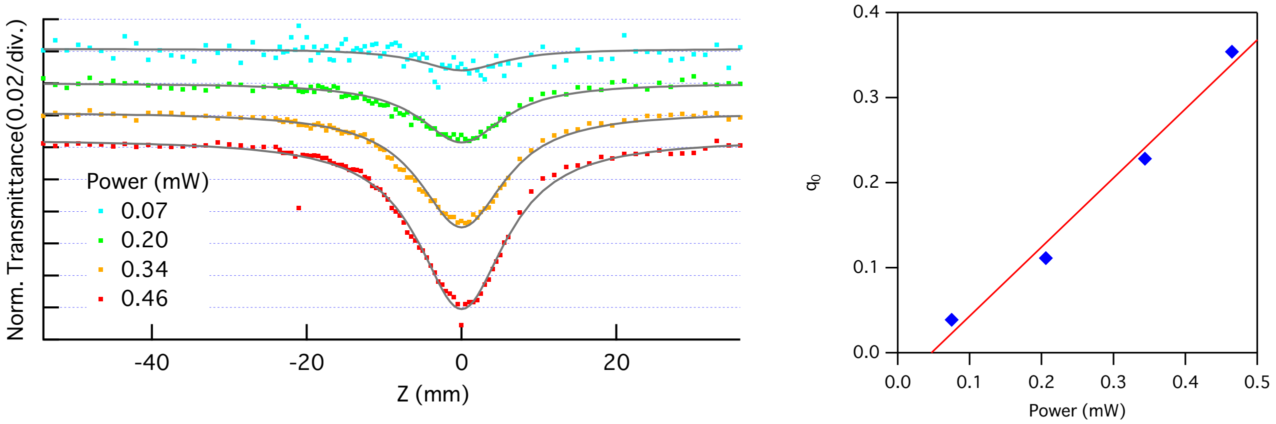

Fig. S18 (Left) Open-aperture Z-scan traces of **1** in THF with the various incident powers at 800 nm (dots) with the theoretical fits with the TPA model (solid curve). Each trace is sifted by one division for readability. (Right) The plot of the obtained two-photon absorbance q_0 from the traces versus the incident power (right).

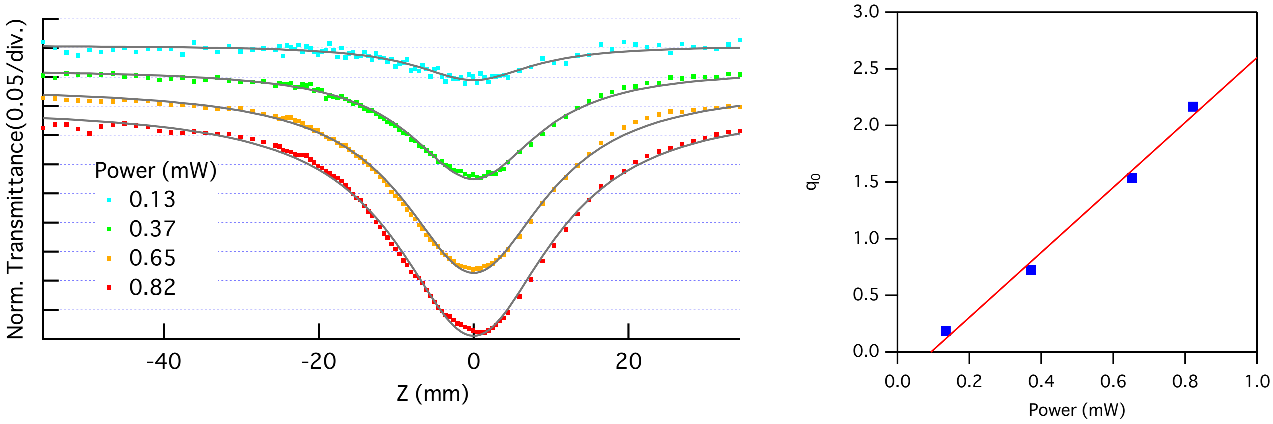

Fig. S19 (Left) Open-aperture Z-scan traces of **5** in THF with the various incident powers at 881 nm (dots) with the theoretical fits with the TPA model (solid curve). Each trace is sifted by one division for readability. (Right) The plot of the obtained two-photon absorbance q_0 from the traces versus the incident power (right).

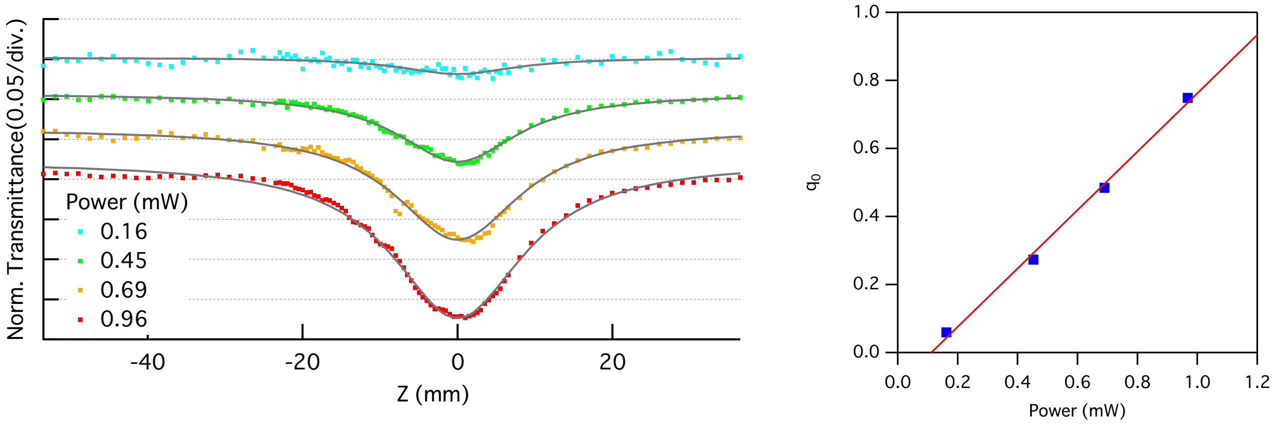

Fig. S20 (Left) Open-aperture Z-scan traces of **7** in THF with the various incident powers at 800 nm (dots) with the theoretical fits with the TPA model (solid curve). Each trace is sifted by one division for readability. (Right) The plot of the obtained two-photon absorbance q_0 from the traces versus the incident power (right).

Temperature-dependent Absorption Measurement. Temperature-dependent absorption spectra of **7** were recorded in 2-methyltetrahydrofran (2-MeTHF) with a Shimadzu UV-3150 spectrometer with a resolution of 0.2 nm. The sample solutions in a 1 cm square quarts cuvette equipped with J-Young® stopcock were cooled using an Oxford Optistat DN cryostat. The absorption spectra thus obtained are shown in Fig. S21.

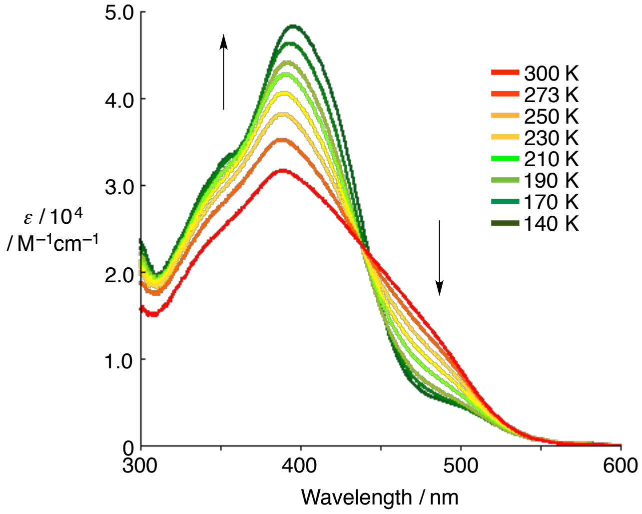

Fig. S21 Temperature-dependent absorption spectra of **7** in 2-MeTHF from 300 K to 140 K.

5. Theoretical Calculation

All quantum calculations were carried out using the GAUSSIAN 09 Revision D.01 suite of programs[12] with default thresholds and algorithms. The employed atomic basis sets were the 6-31G(d) set for H, B, C, P, and S atoms and 6-31+G(d) for N and O atoms, respectively. Furthermore, a set of *p* polarization function was added on the H atom attaching to a nitrogen atom (namely, the 6-31G(d,p) basis set was applied to the migrating H atom). Geometry optimizations in S_0 and S_1 were performed using density functional theory (DFT)/time-dependent DFT (TD-DFT) with the CAM-B3LYP range-separated exchange-correlation functional.[13] The X-ray crystallographic structure of **3** (see Fig. 3 and the CIF file) was used for the initial structures for the geometry optimizations of **2** and **3**. The geometry of **2** was optimized in gas phase and the geometry of **3** was optimized in gas phase, in cyclohexane, and in acetone. The solvation effects were included using the integral-equation-formalism polarizable continuum model (IEF-PCM)[14] and Truhlar's SMD solvation model.[15] For the evaluation of absorption and emission wavelengths of **3**, TD-DFT vertical excitation energy calculations were performed using the optimized structures obtained at S_0 and S_1 states, respectively. The lowest occupied molecular orbitals (LUMO) of **2** and **3** in the gas phase at S_0 state are shown in Fig. S22 and the Cartesian coordinates for the optimized geometries of **3** in S_0 and S_1 are given in Tables S2–S7. The corresponding optimized geometries are shown in Fig. S23 and S24.

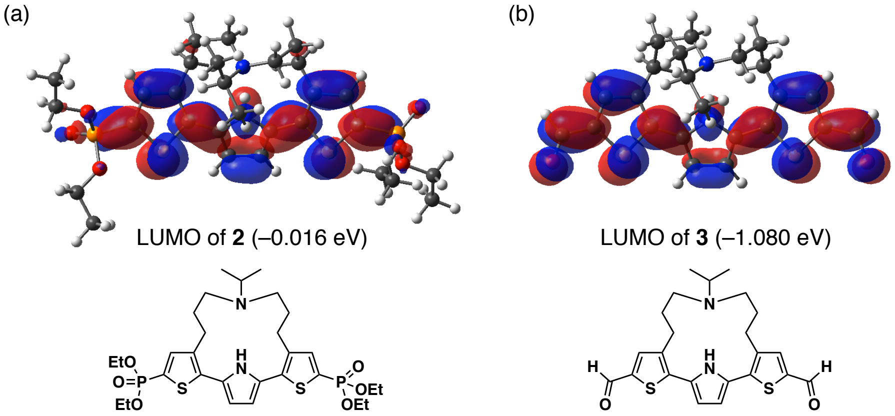

Fig. S22 Pictorial representation of the lowest occupied molecular orbitals (LUMO) of (a) **2** and (b) **3** in the gas phase at S_0 state.

Table S2. Cartesian Coordinates [Å] of the Optimized Structure for **3** in Cyclohexane in S_0[a]

atom	X	Y	Z
C	4.466442	0.470787	-0.476396
H	5.067304	1.339844	-0.726838
C	3.089767	0.356694	-0.798875
C	2.579063	-0.863616	-0.395099
S	-3.489179	-2.026335	0.383852
S	3.781285	-1.845766	0.388229
N	0.096335	-0.679769	-0.509916
H	0.037615	0.334009	-0.286759
N	-0.124193	2.132003	0.226696
C	-0.766229	2.951491	-0.811871
H	-0.140168	2.893270	-1.704807
H	-0.781687	4.012987	-0.514791
C	1.247452	-1.425951	-0.541982
C	0.885584	-2.759117	-0.675102
H	1.570957	-3.590227	-0.768250
C	-0.517477	-2.815956	-0.705195
H	-1.130441	-3.698717	-0.823771
C	2.155884	2.727692	-0.726311
H	3.130096	3.065309	-0.353234
H	1.809956	3.521403	-1.395487
C	-2.359055	-1.045435	-0.499054
C	-2.292211	1.139657	-1.876174
H	-2.891250	1.225780	-2.789437
H	-1.307156	0.792575	-2.199549

C	-1.328948	3.371971	2.099437
H	-0.451916	3.936300	2.431627
H	-1.951631	3.191162	2.980952
H	-1.903776	4.007961	1.420581
C	1.243346	2.613752	0.496003
H	1.704790	1.920227	1.202531
H	1.219753	3.601290	0.982931
C	-0.986977	-1.515771	-0.593986
C	-4.328577	0.150905	-0.684179
H	-4.985502	0.952594	-1.007908
C	-2.948291	0.095517	-1.010400
C	-0.943552	2.029347	1.467965
H	-1.866261	1.530757	1.157029
C	2.353544	1.440923	-1.541239
H	1.392277	1.066483	-1.901002
H	2.932876	1.696631	-2.436217
C	-0.290900	1.125900	2.514264
H	0.078918	0.193856	2.078567
H	-1.034421	0.862960	3.272243
H	0.537748	1.617098	3.033247
C	-2.176383	2.543450	-1.235505
H	-2.484691	3.293117	-1.971882
H	-2.883444	2.639716	-0.405707
C	4.990721	-0.628910	0.151158
C	6.367571	-0.796210	0.568413
H	7.015297	0.076656	0.359768
C	-4.775863	-0.916501	0.050197
C	-6.134388	-1.132028	0.506378
H	-6.844206	-0.331619	0.223013
O	-6.513547	-2.093808	1.153430
O	6.825690	-1.790564	1.106283

[a] Calculated with the CAM-B3LYP functional.

Table S3. Cartesian Coordinates [Å] of the LE state of **3** in Cyclohexane in S_1[a]

atom	X	Y	Z
C	4.467637	0.426908	-0.668365
H	5.067908	1.268293	-1.000453
C	3.082355	0.370431	-0.823863

C	2.554120	-0.850073	-0.331588
S	-3.588310	-2.040043	0.297493
S	3.833431	-1.886036	0.305736
N	0.087356	-0.598138	-0.499050
H	0.039331	0.431716	-0.318228
N	-0.094594	2.154971	0.308992
C	-0.747522	3.022981	-0.683224
H	-0.123667	3.020765	-1.579459
H	-0.776034	4.065986	-0.329838
C	1.236524	-1.341973	-0.298774
C	0.829924	-2.687535	-0.035306
H	1.503773	-3.521750	0.101569
C	-0.535448	-2.730366	-0.052820
H	-1.160504	-3.604478	0.066417
C	2.177880	2.748815	-0.645073
H	3.167781	3.044698	-0.279788
H	1.842738	3.570263	-1.285823
C	-2.357210	-0.997918	-0.415229
C	-2.229555	1.218048	-1.800725
H	-2.781653	1.328909	-2.739961
H	-1.230092	0.882812	-2.088024
C	-1.287206	3.317129	2.238596
H	-0.407842	3.876180	2.573876
H	-1.891846	3.100299	3.124493
H	-1.880414	3.971665	1.594165
C	1.278366	2.618756	0.583695
H	1.737811	1.905451	1.271345
H	1.265622	3.594638	1.093021
C	-1.015292	-1.414332	-0.334520
C	-4.324992	0.158061	-0.854445
H	-4.961922	0.939939	-1.256357
C	-2.936625	0.153876	-1.003221
C	-0.903855	2.000760	1.554011
H	-1.828031	1.511422	1.232344
C	2.325677	1.480706	-1.502554
H	1.348159	1.134978	-1.845563
H	2.879524	1.755993	-2.407199
C	-0.238566	1.063598	2.561598
H	0.143486	0.154104	2.090835
H	-0.977829	0.761691	3.308955

H	0.584761	1.544301	3.098421
C	-2.150234	2.607084	-1.117046
H	-2.478451	3.371425	-1.828890
H	-2.856664	2.656856	-0.283444
C	5.037531	-0.694658	-0.080114
C	6.430624	-0.908315	0.194543
H	7.091712	-0.069866	-0.095804
C	-4.844911	-0.939505	-0.181634
C	-6.227498	-1.198946	0.106187
H	-6.927592	-0.419838	-0.250281
O	-6.650334	-2.190872	0.697550
O	6.901374	-1.921405	0.708905

[a] Calculated with the CAM-B3LYP functional.

Table S4. Cartesian Coordinates [Å] of the ESIPT state of **3** in Cyclohexane in S_1[a]

atom	X	Y	Z
C	4.512519	0.486386	-0.657279
H	5.115812	1.332447	-0.972738
C	3.124879	0.442109	-0.800947
C	2.581386	-0.779443	-0.339467
S	-3.514458	-2.025608	0.283797
S	3.858077	-1.837944	0.268125
N	0.120157	-0.504544	-0.521739
H	-0.065607	1.057171	-0.063350
N	-0.172188	2.056218	0.360583
C	-0.755750	2.951067	-0.688164
H	-0.068402	2.922131	-1.531904
H	-0.749121	3.970036	-0.293376
C	1.247697	-1.258177	-0.309200
C	0.879088	-2.621752	-0.006424
H	1.566076	-3.438301	0.170423
C	-0.477110	-2.679770	-0.035537
H	-1.102237	-3.550420	0.110541
C	2.146739	2.762678	-0.437428
H	3.110701	3.034306	0.006018
H	1.817515	3.645816	-0.993184
C	-2.307177	-0.980888	-0.467725
C	-2.230956	1.197331	-1.897993

H	-2.801330	1.325920	-2.823436
H	-1.235776	0.859228	-2.197622
C	-1.500220	3.205558	2.195680
H	-0.648224	3.769748	2.586678
H	-2.157528	2.987912	3.041789
H	-2.058350	3.847176	1.510223
C	1.216341	2.486508	0.738317
H	1.630343	1.684069	1.348595
H	1.130859	3.380488	1.359680
C	-0.942477	-1.354163	-0.366002
C	-4.309620	0.109991	-0.942338
H	-4.964248	0.862305	-1.372222
C	-2.920451	0.130496	-1.088561
C	-1.082128	1.881590	1.569305
H	-1.964426	1.386367	1.159785
C	2.363535	1.587811	-1.408854
H	1.412497	1.233512	-1.813282
H	2.938458	1.971059	-2.258723
C	-0.457027	0.948205	2.599994
H	-0.061292	0.037242	2.145520
H	-1.234971	0.650955	3.307858
H	0.338640	1.433724	3.172088
C	-2.139917	2.577319	-1.200417
H	-2.382413	3.361475	-1.925218
H	-2.895578	2.656285	-0.413863
C	5.077724	-0.652391	-0.096396
C	6.466830	-0.879405	0.168158
H	7.130821	-0.040140	-0.116292
C	-4.805186	-0.974233	-0.226784
C	-6.175334	-1.249153	0.081345
H	-6.893218	-0.502743	-0.310692
O	-6.581507	-2.218049	0.726919
O	6.941133	-1.900540	0.668625

[a] Calculated with the CAM-B3LYP functional.

Table S5. Cartesian Coordinates [Å] of the Optimized Structure for **3** in Acetone in S_0[a]

atom	X	Y	Z
C	4.470390	0.477784	-0.477050

H	5.070392	1.348003	-0.724558
C	3.092832	0.364885	-0.798118
C	2.581035	-0.854911	-0.396332
S	-3.487413	-2.023159	0.382910
S	3.784835	-1.843157	0.382659
N	0.097436	-0.671460	-0.510747
H	0.036157	0.349862	-0.290783
N	-0.126881	2.112063	0.232872
C	-0.759812	2.936895	-0.809520
H	-0.130415	2.874052	-1.699314
H	-0.769440	3.997047	-0.509718
C	1.248411	-1.416492	-0.539141
C	0.889071	-2.752775	-0.665417
H	1.574596	-3.584935	-0.754977
C	-0.514437	-2.811150	-0.695719
H	-1.125947	-3.696108	-0.810387
C	2.156117	2.729704	-0.699631
H	3.128767	3.062819	-0.318661
H	1.809456	3.529427	-1.360724
C	-2.357260	-1.040520	-0.502383
C	-2.294013	1.140818	-1.885004
H	-2.903686	1.232030	-2.790391
H	-1.311649	0.794219	-2.217464
C	-1.343451	3.354752	2.096633
H	-0.467144	3.917925	2.433016
H	-1.972095	3.172246	2.974112
H	-1.913936	3.988473	1.412124
C	1.238446	2.595874	0.515921
H	1.698211	1.896060	1.217735
H	1.206771	3.576698	1.014446
C	-0.983843	-1.508620	-0.591473
C	-4.328999	0.151512	-0.694366
H	-4.986047	0.951926	-1.020199
C	-2.947750	0.096431	-1.018821
C	-0.955747	2.011940	1.467627
H	-1.878250	1.516798	1.150972
C	2.358518	1.455348	-1.531862
H	1.399463	1.086292	-1.903081
H	2.946907	1.723191	-2.416905
C	-0.311654	1.107960	2.518929

H	0.059649	0.175259	2.084546
H	-1.061226	0.849070	3.272968
H	0.516278	1.598227	3.040147
C	-2.170893	2.540631	-1.238822
H	-2.468433	3.292230	-1.977307
H	-2.882631	2.640808	-0.413565
C	4.995887	-0.623418	0.147694
C	6.370577	-0.788241	0.558896
H	7.015883	0.084010	0.353903
C	-4.776756	-0.913687	0.043599
C	-6.132846	-1.125360	0.496538
H	-6.841280	-0.327746	0.212234
O	-6.512892	-2.090820	1.147993
O	6.832152	-1.790083	1.092604

[a] Calculated with the CAM-B3LYP functional.

Table S6. Cartesian Coordinates [Å] of the LE state of **3** in Acetone in S_1[a]

atom	X	Y	Z
C	4.464587	0.404335	-0.718374
H	5.066540	1.233831	-1.076081
C	3.079305	0.363679	-0.842659
C	2.541228	-0.845353	-0.319570
S	-3.603942	-2.031715	0.292626
S	3.824388	-1.888704	0.307636
N	0.079133	-0.577653	-0.481870
H	0.036045	0.462794	-0.310352
N	-0.075654	2.143753	0.322948
C	-0.734166	3.020693	-0.659983
H	-0.119007	3.020424	-1.561564
H	-0.755332	4.060157	-0.297776
C	1.224648	-1.318079	-0.256641
C	0.812705	-2.658429	0.057971
H	1.480545	-3.492659	0.224183
C	-0.546976	-2.697408	0.042309
H	-1.170728	-3.568148	0.192389
C	2.187742	2.741378	-0.646533
H	3.182471	3.032807	-0.290760
H	1.846035	3.564313	-1.281077

C	-2.361970	-0.981299	-0.397424
C	-2.229772	1.235861	-1.787369
H	-2.788347	1.364314	-2.720024
H	-1.232965	0.900443	-2.083513
C	-1.251279	3.305283	2.262955
H	-0.367598	3.866636	2.582953
H	-1.842505	3.085823	3.157805
H	-1.855956	3.954874	1.624262
C	1.300631	2.604793	0.589279
H	1.764161	1.887076	1.269709
H	1.291467	3.577383	1.103844
C	-1.024657	-1.384456	-0.288813
C	-4.329809	0.160669	-0.883854
H	-4.962769	0.936751	-1.302735
C	-2.942217	0.165645	-1.004560
C	-0.874276	1.989364	1.574573
H	-1.802000	1.501741	1.261394
C	2.323114	1.478322	-1.513022
H	1.341863	1.140761	-1.853351
H	2.878023	1.755783	-2.415858
C	-0.200109	1.052625	2.576957
H	0.181075	0.144213	2.102501
H	-0.934797	0.751287	3.329707
H	0.626895	1.535872	3.106041
C	-2.141866	2.613552	-1.081806
H	-2.476454	3.386411	-1.780951
H	-2.839255	2.652688	-0.240146
C	5.037696	-0.716425	-0.123039
C	6.426820	-0.936391	0.124142
H	7.088624	-0.110449	-0.191235
C	-4.860170	-0.938792	-0.216085
C	-6.241724	-1.200194	0.036656
H	-6.934478	-0.424977	-0.335577
O	-6.681194	-2.199385	0.620681
O	6.904951	-1.952164	0.647297

[a] Calculated with the CAM-B3LYP functional.

Table S7. Cartesian Coordinates [Å] of the ESIPT state of **3** in Acetone in S_1[a]

atom	X	Y	Z
C	4.462056	0.360311	-0.804503
H	5.067204	1.172565	-1.195777
C	3.073621	0.338859	-0.891350
C	2.520883	-0.841734	-0.326040
S	-3.598919	-2.018347	0.286660
S	3.803717	-1.888996	0.300600
N	0.074580	-0.536635	-0.505628
H	-0.019505	1.159558	-0.043493
N	-0.066630	2.139908	0.362641
C	-0.741646	3.019779	-0.648200
H	-0.113877	3.005362	-1.536901
H	-0.731462	4.036091	-0.250540
C	1.185162	-1.279811	-0.211871
C	0.793058	-2.596998	0.262725
H	1.462307	-3.399672	0.543260
C	-0.558611	-2.630216	0.247394
H	-1.194892	-3.464808	0.510964
C	2.197710	2.719670	-0.658185
H	3.197015	3.003268	-0.310523
H	1.845048	3.557395	-1.265765
C	-2.354079	-0.964044	-0.399555
C	-2.229296	1.243162	-1.798823
H	-2.776977	1.404839	-2.732225
H	-1.229116	0.910459	-2.083147
C	-1.221510	3.327661	2.286781
H	-0.332538	3.900583	2.565223
H	-1.782413	3.125462	3.203658
H	-1.854286	3.947550	1.647853
C	1.353824	2.571775	0.601496
H	1.797281	1.821465	1.255039
H	1.322286	3.521126	1.138318
C	-1.002548	-1.335535	-0.241872
C	-4.335676	0.125209	-0.967965
H	-4.969260	0.882160	-1.420398
C	-2.946163	0.153088	-1.046730
C	-0.866930	1.990938	1.652133

H	-1.783714	1.494381	1.330890
C	2.315469	1.465133	-1.541359
H	1.329488	1.126053	-1.864969
H	2.857221	1.759502	-2.446466
C	-0.157972	1.071446	2.639598
H	0.217418	0.162208	2.162736
H	-0.882850	0.772381	3.401510
H	0.670105	1.570701	3.149988
C	-2.146936	2.600874	-1.051371
H	-2.489384	3.395392	-1.721321
H	-2.831112	2.616703	-0.199000
C	5.033852	-0.753969	-0.190769
C	6.419441	-0.989936	0.029358
H	7.086373	-0.186131	-0.331640
C	-4.868429	-0.967108	-0.284361
C	-6.245740	-1.244154	-0.059711
H	-6.940554	-0.492864	-0.476713
O	-6.693247	-2.230936	0.547978
O	6.902064	-1.995760	0.576180

[a] Calculated with the CAM-B3LYP functional.

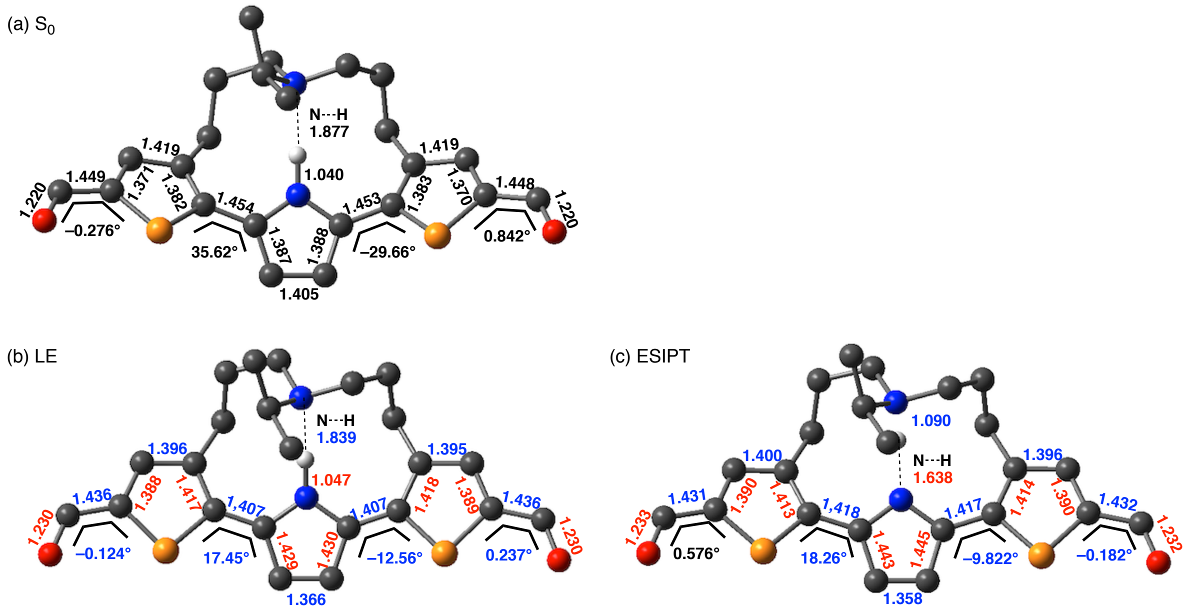

Fig. S23 Optimized geometries of **3** in cyclohexane (a) in S_0, (b) in S_1 corresponding to the locally excited state (LE), and (c) in S_1 corresponding to ESIPT state calculated using the CAM-B3LYP functional with the 6-31G+(d) (for N atoms), 6-31(d,p) (for the migrating H atom), and 6-31G(d) basis sets (for other atoms). Solvents were considered by using IEF-PCM model.

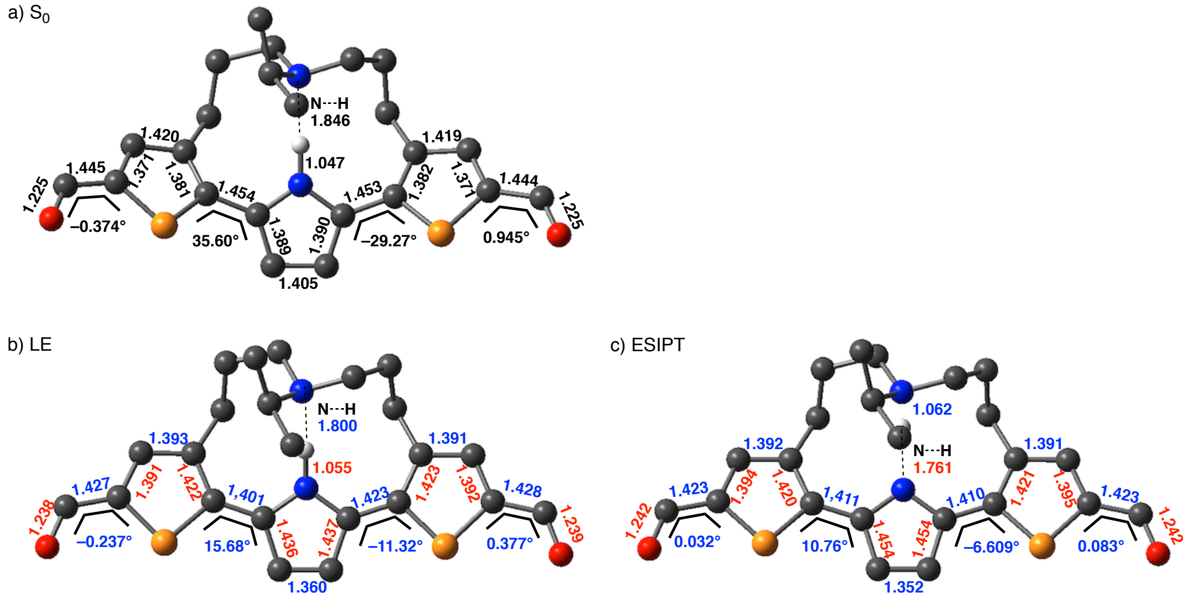

Fig. S24 Optimized geometries of **3** in acetone (a) in S$_0$, (b) in S$_1$ corresponding to the locally excited state (LE), and (c) in S$_1$ corresponding to ESIPT state calculated using the CAM-B3LYP functional with the 6-31G+(d) (for N atoms), 6-31(d,p) (for the migrating H atom), and 6-31G(d) basis sets (for other atoms). Solvent effects were included using IEF-PCM model.

6. References

(1) N. Suzuki, A. Fukazawa, K. Nagura, S. Saito, H. Kitoh-Nishioka, D. Yokogawa, S. Irle, S. Yamaguchi, *Angew. Chem. Int. Ed.*, **2014**, *53*, 8231–8235.

(2) Y. Hu, Y. Ishikawa, K. Hirai, H. Tomioka, *Bull. Chem. Soc. Jpn.*, **2001**, *74*, 2207–2218.

(3) M. Takahachi, K. Masui, H. Sekiguchi, N. Kobayashi, A. Mori, M. Funahashi, N. Tamaoki, *J. Am. Chem. Soc.*, **2006**, *128*, 10930–10933.

(4) A. Altomare, G. Cascarano, C. Giacovazzo, A. Gualiardi, A. G. G. Moliterni, M. C. Burla, G. Polidori, M. Camalli, R. Spagna, *SIR 97*, 1997.

(5) G. M. Sheldrick, *SHELX-2013, Program for the Refinement of Crystal Structures*; University of Gottingen, Germany, 2013.

(6) G. M. Sheldrick, *SHELX-97, Program for the Refinement of Crystal Structures*; University of Gottingen, Germany, 1997.

(7) T.-S. Ahn, R. O. Al-Kaysi, A. M. Müller, K. M. Wentz, C. J. Bardeen, *Rev. Sci. Instrum.*, **2007**, *78*, 086105.

(8) M. Sheik-Bahae, A. A. Said, T. H. Wei, D. J. Hagan, E. W. Van Stryland, *IEEE J. Quantum Electron.*, **1990**, *26*, 760–769.

(9) K. Kamada, K. Matsunaga, A. Yoshino, K. Ohta, *J. Opt. Soc. Am. B*, **2003**, *20*, 529–537.

(10) R. L. Sutherland, "Handbook of Nonliner Optics", 2nd Ed. (Mercel Dekker Inc. 2003, New York)

(11) K. Kamada, Y. Iwase, K. Sakai, K. Kondo, K. Ohta, *J. Phys. Chem. C*, **2009**, *113*, 11469–11474.

(12) M. J. Frisch, G. W. Trucks, H. B. Schlegel, G. E. Scuseria, M. A. Robb, J. R. Cheeseman, G. Scalmani, V. Barone, B. Mennucci, G. A. Petersson et al. Gaussian 09, revision D.01; Gaussian, Inc.: Wallingford, CT, 2010.

(13) T. Yanai, D. Tew, N. Handy, *Chem. Phys. Lett.*, **2004**, *393*, 51–57.

(14) (*a*) S. Miertuš, E. Scrocco, J. Tomasi, *Chem. Phys.*, **1981**, *55*, 117–129; (*b*) M. Cossi, V. Barone, R. Cammi, J. Tomasi, *Chem. Phys. Lett.*, **1996**, *255*, 327–335; (*c*) J. Tomasi, B. Mennucci, R. Cammi, *Chem. Rev.*, **2005**, *105*, 2999–3093.

(15) A. V. Marenich, C. J. Cramer, D. G. Truhlar, *J. Phys. Chem. B*, **2009**, *113*, 6378–6396.

7. NMR Spectra for New Compounds

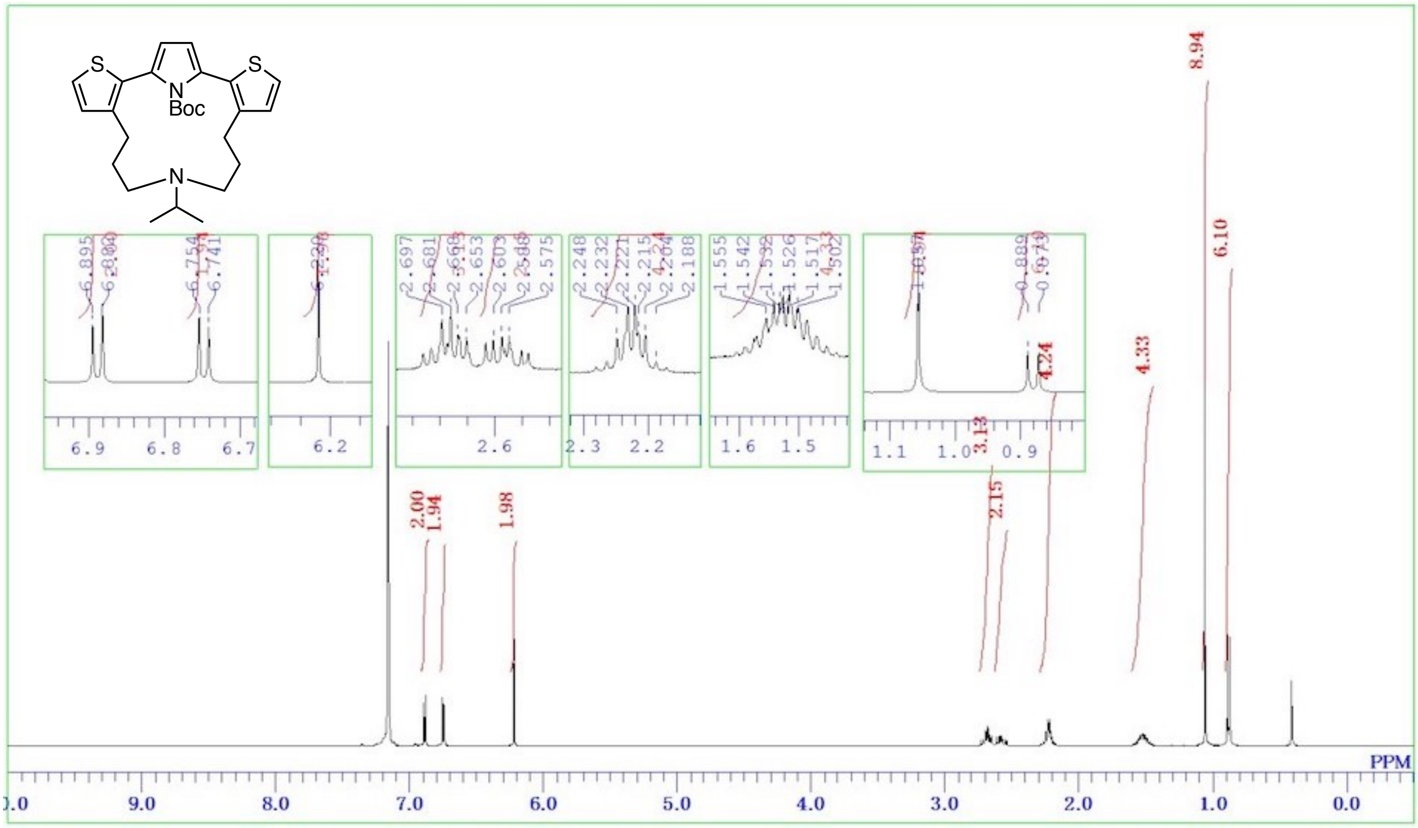

Fig. S25 ^{1}H NMR spectrum of **9** (400 MHz, C_6D_6).

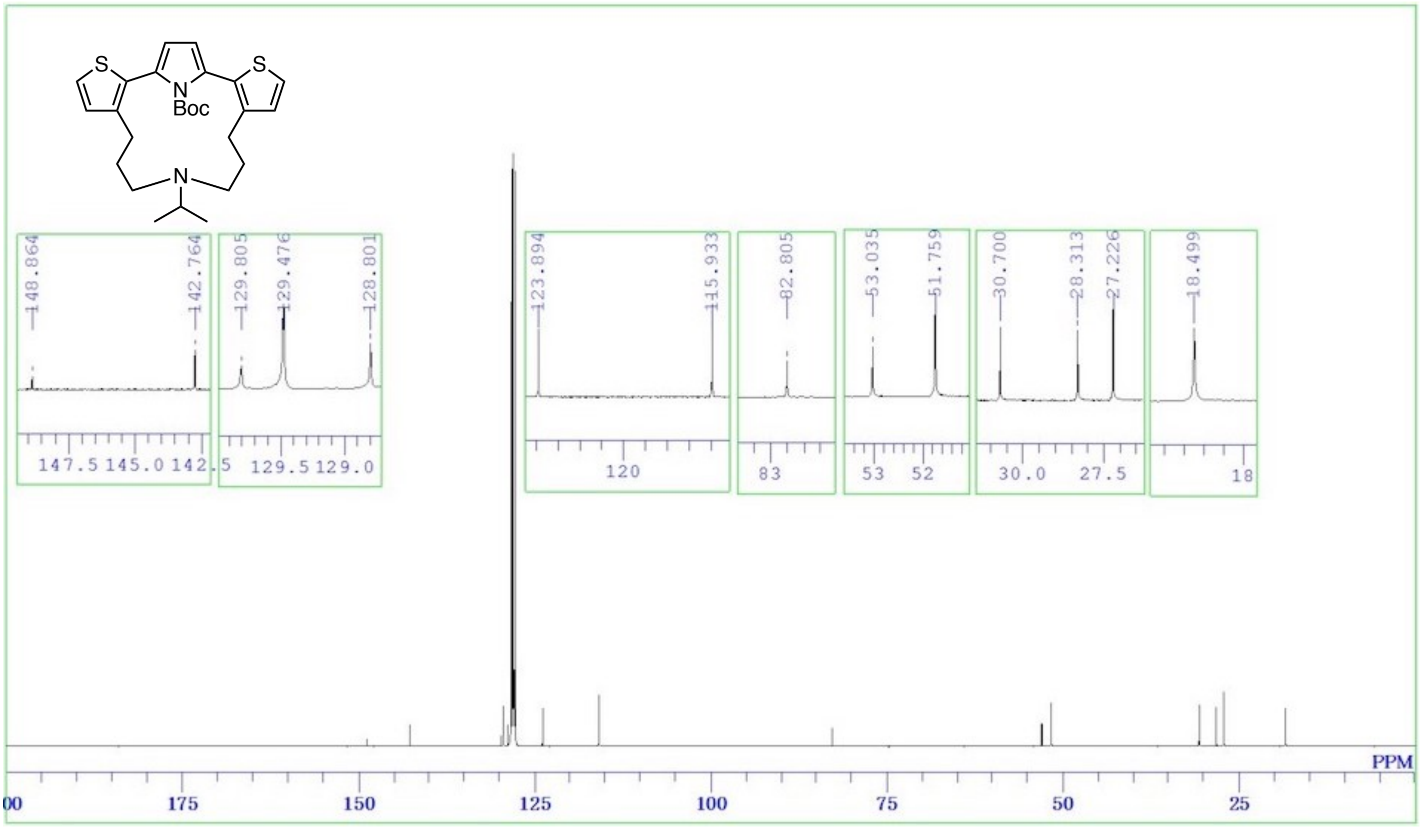

Fig. S26 ^{13}C NMR spectrum of **9** (100 MHz, C_6D_6).

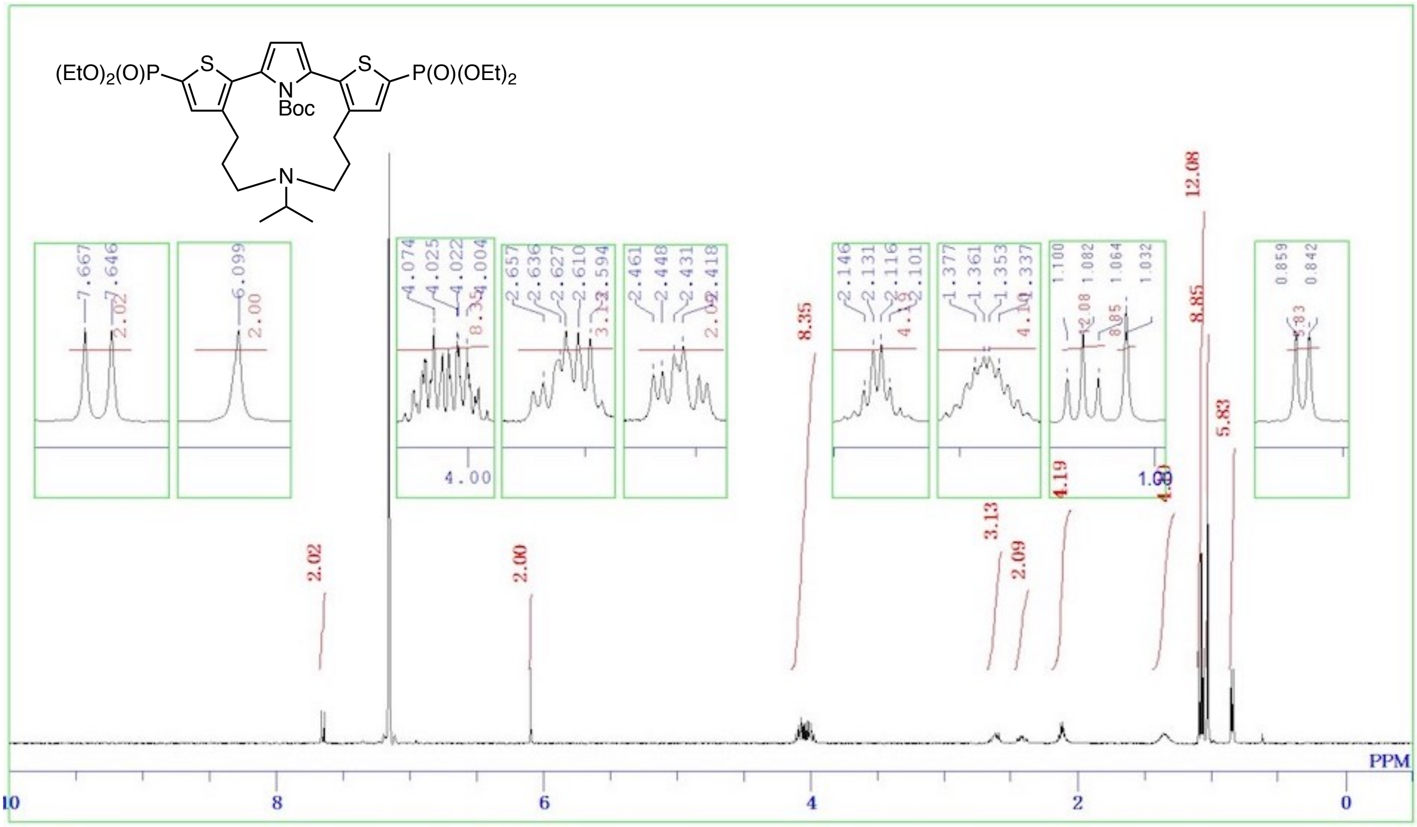

Fig. S27 ^{1}H NMR spectrum of **10** (400 MHz, C_6D_6).

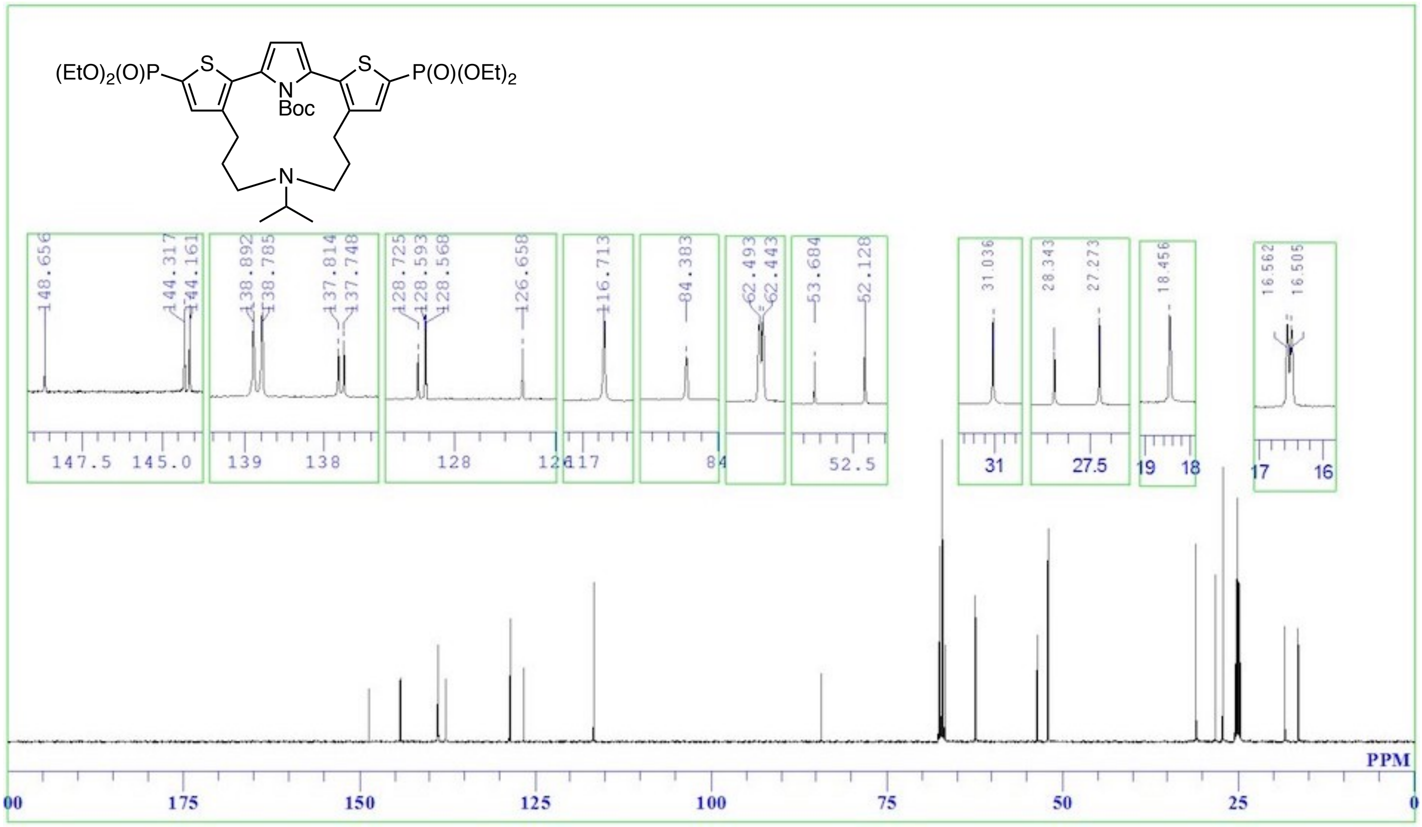

Fig. S28 ^{13}C NMR spectrum of **10** (100 MHz, THF-d_8).

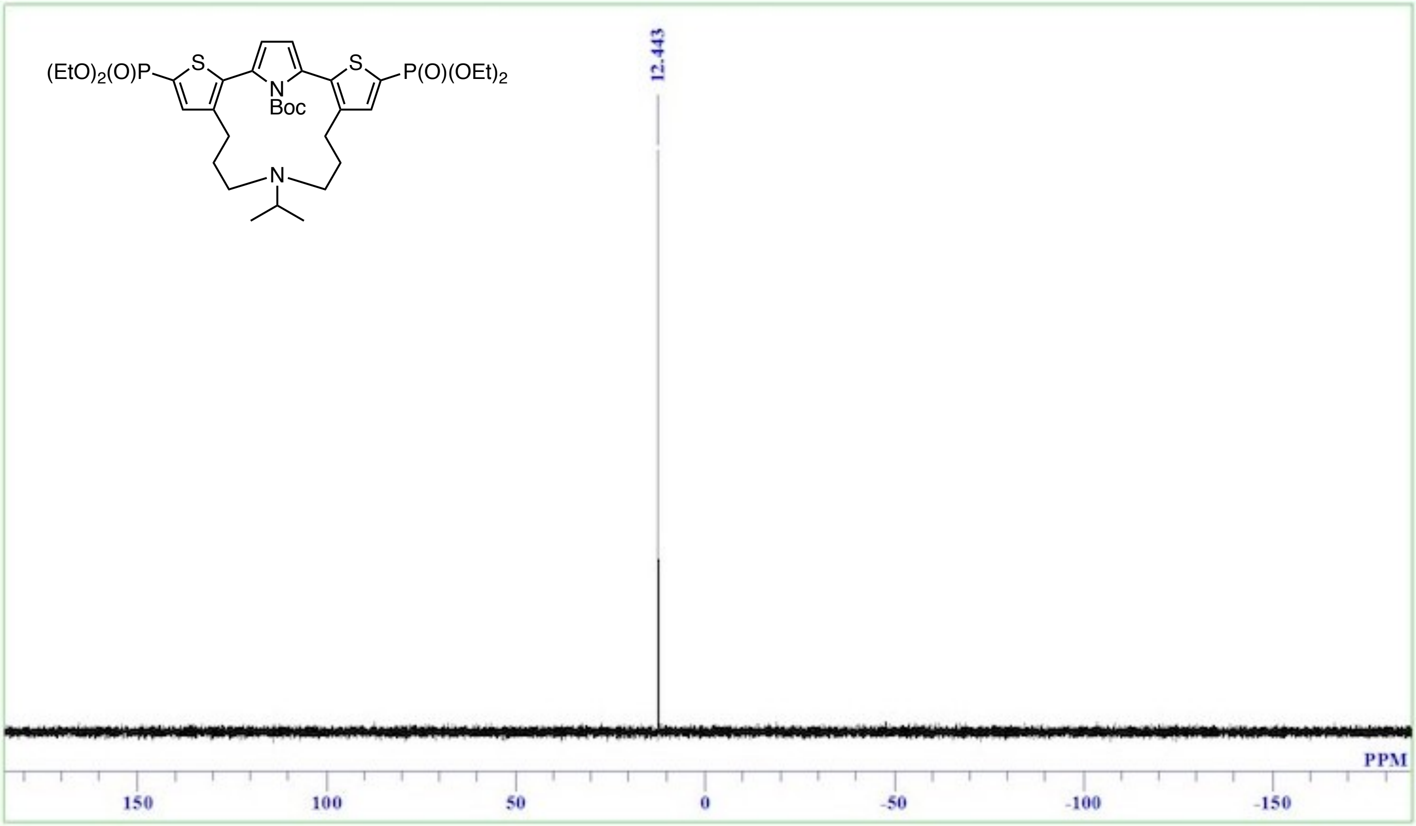

Fig. S29 ^{31}P NMR spectrum of **10** (162 MHz, C_6D_6).

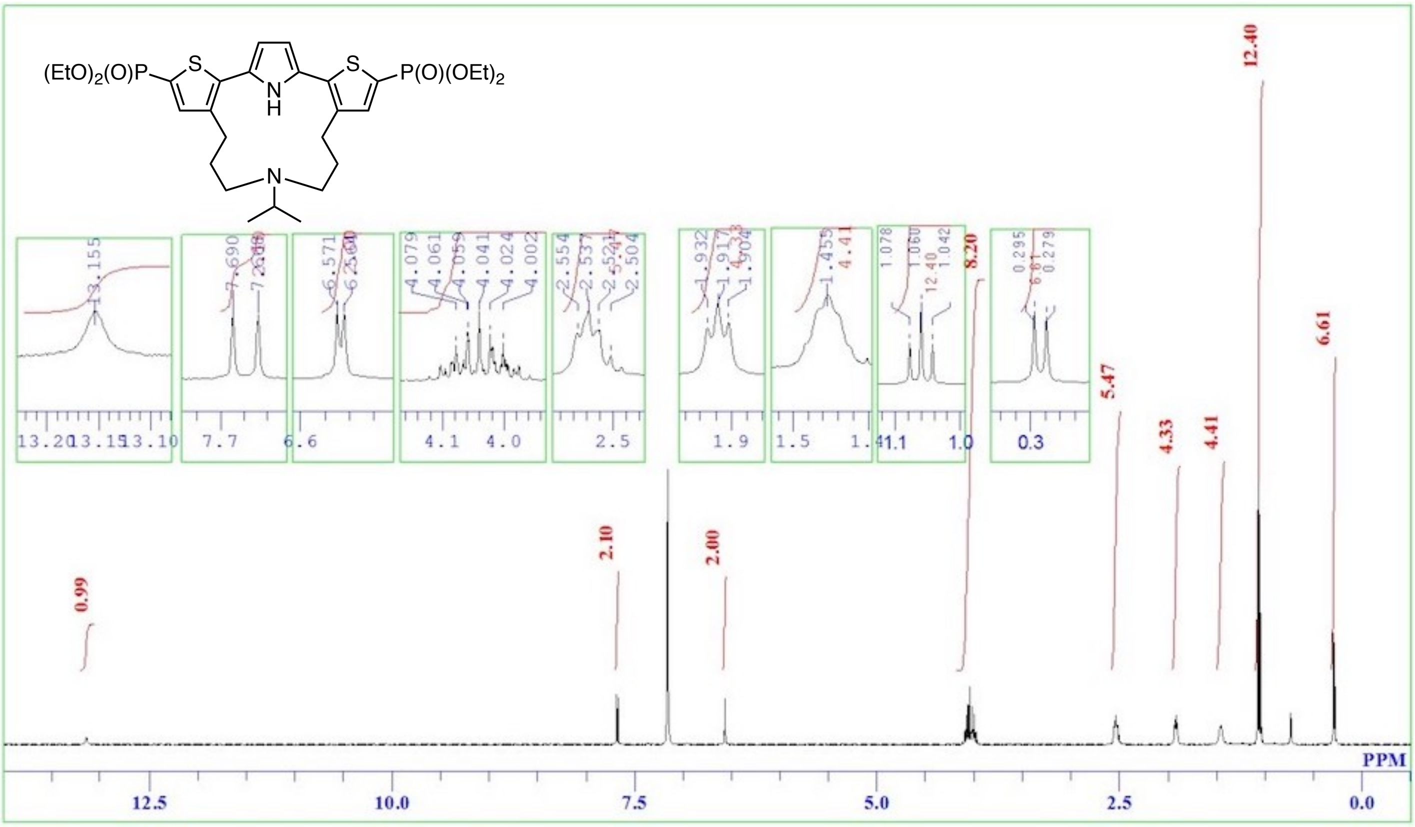

Fig. S30 ^{1}H NMR spectrum of **2** (400 MHz, C_6D_6).

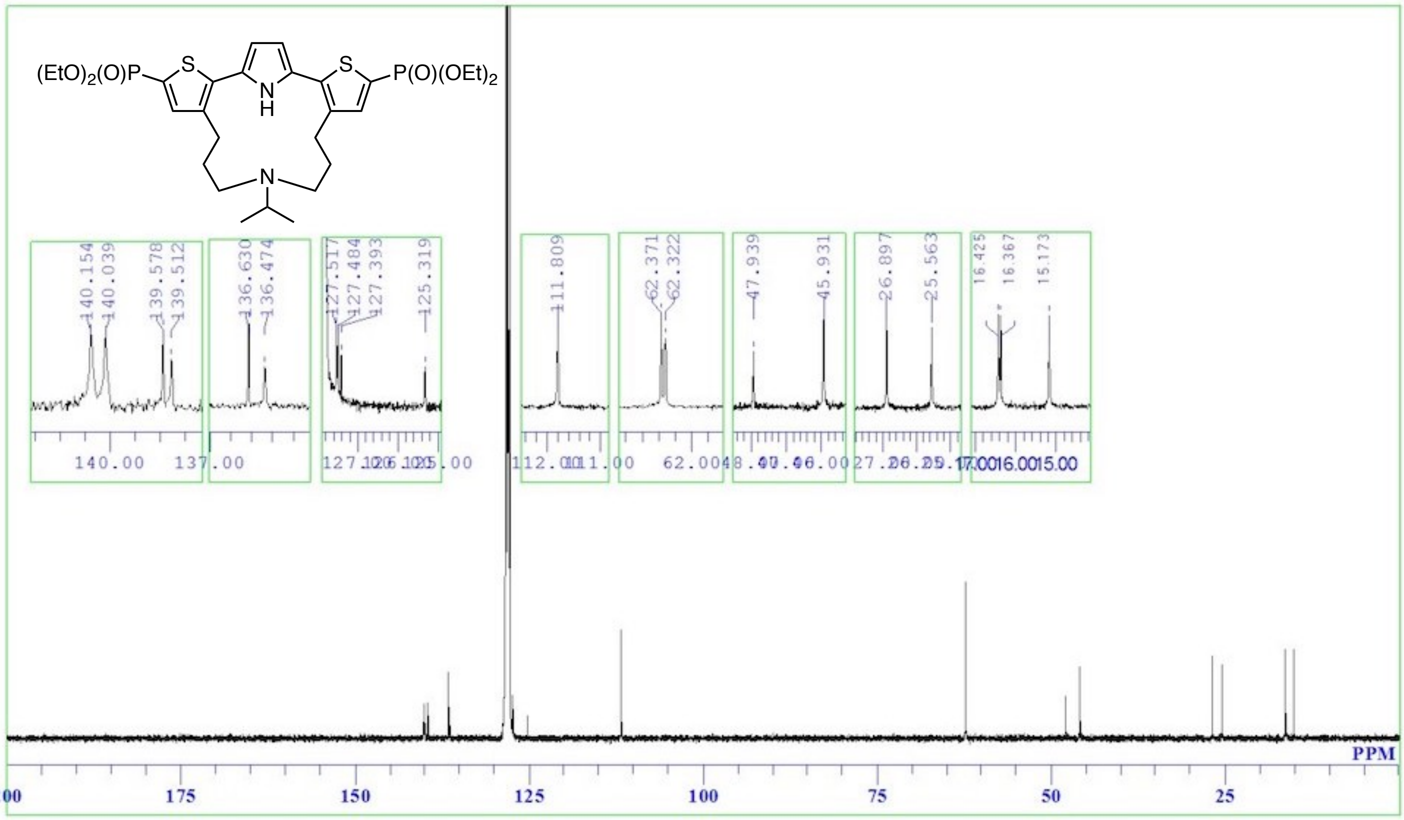

Fig. S31 ^{13}C NMR spectrum of **2** (100 MHz, C_6D_6).

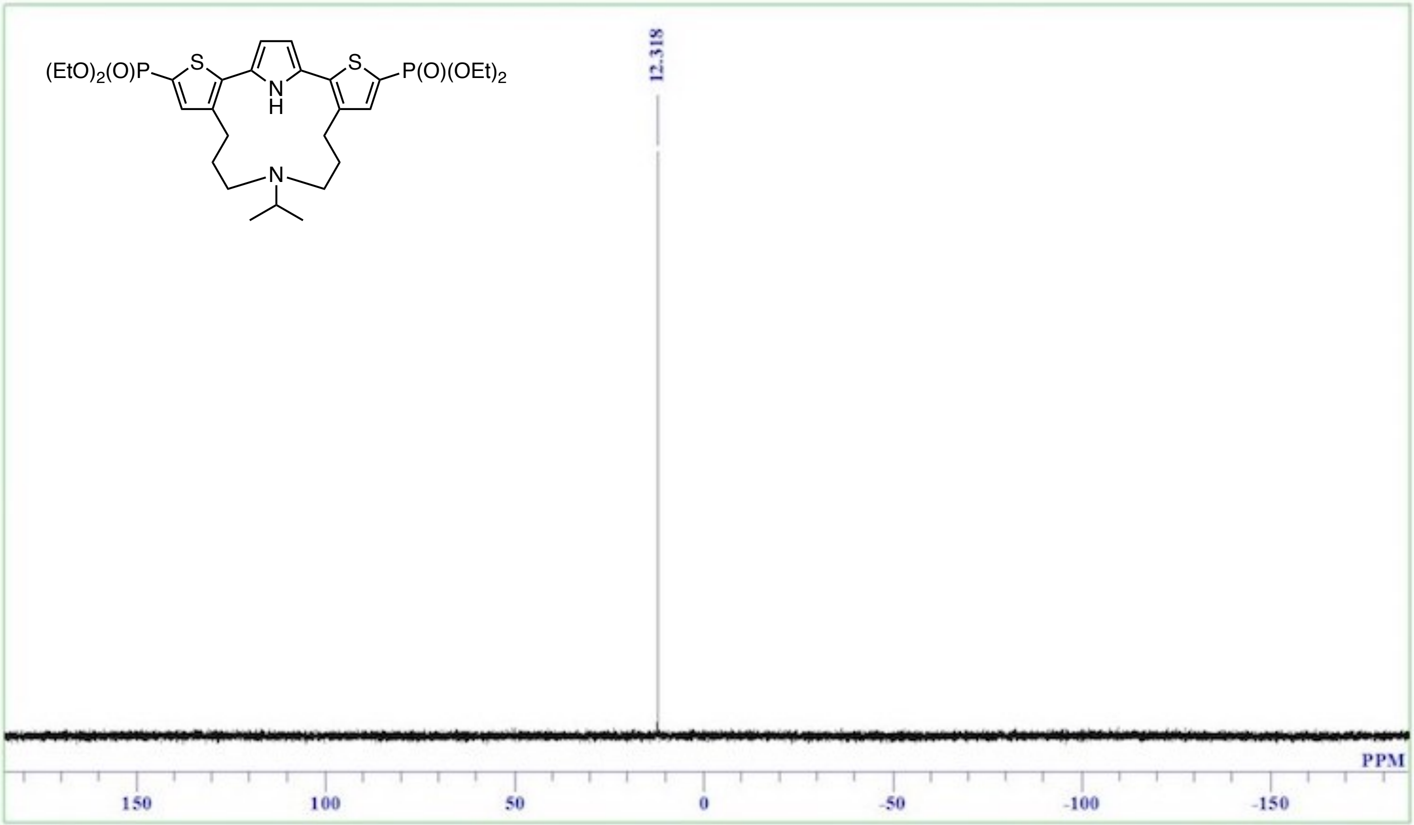

Fig. S32 ^{31}P NMR spectrum of **2** (162 MHz, C_6D_6).

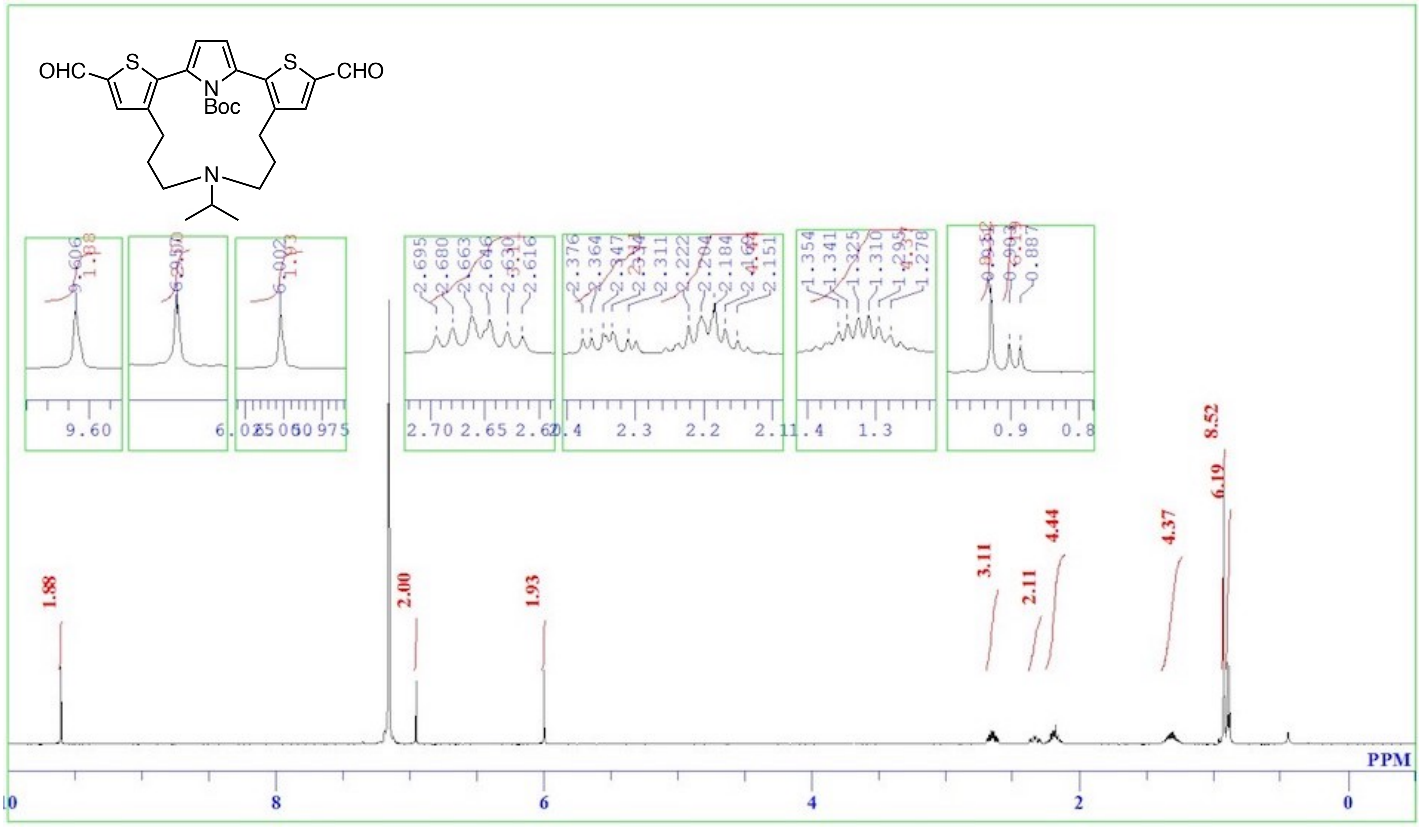

Fig. S33 ^{1}H NMR spectrum of **11** (400 MHz, C_6D_6).

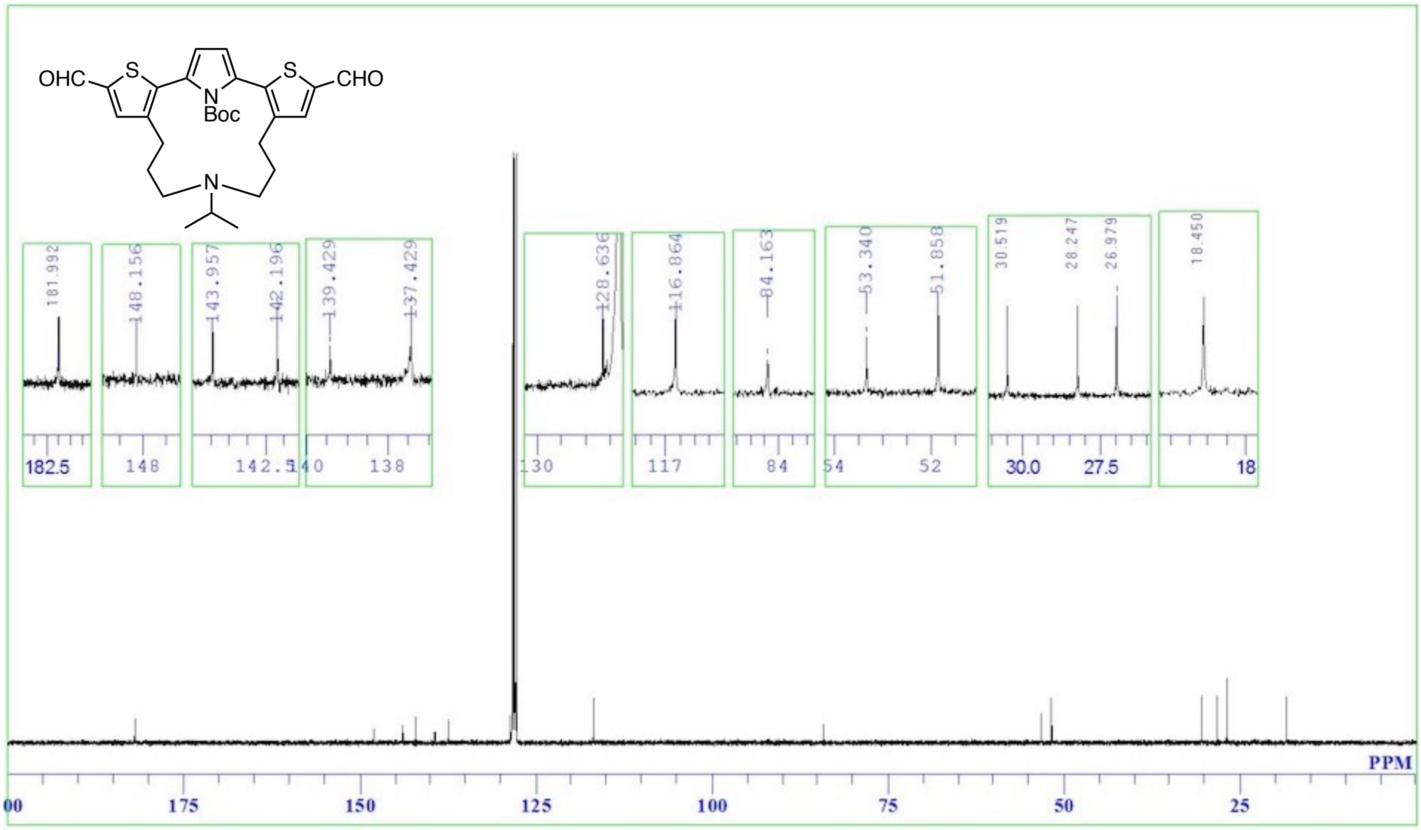

Fig. S34 ^{13}C NMR spectrum of **11** (100 MHz, C_6D_6).

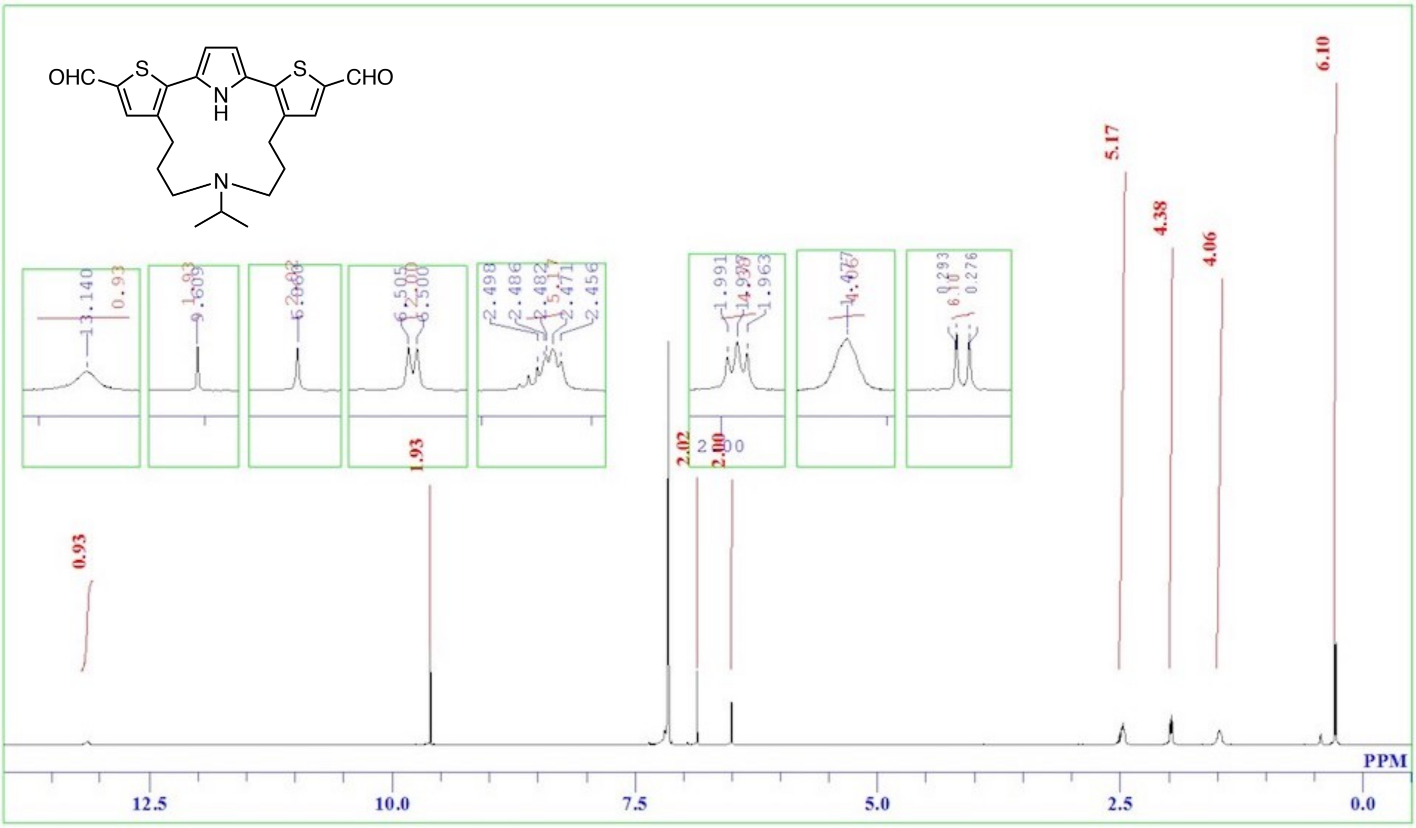

Fig. S35 ^{1}H NMR spectrum of **3** (400 MHz, C_6D_6).

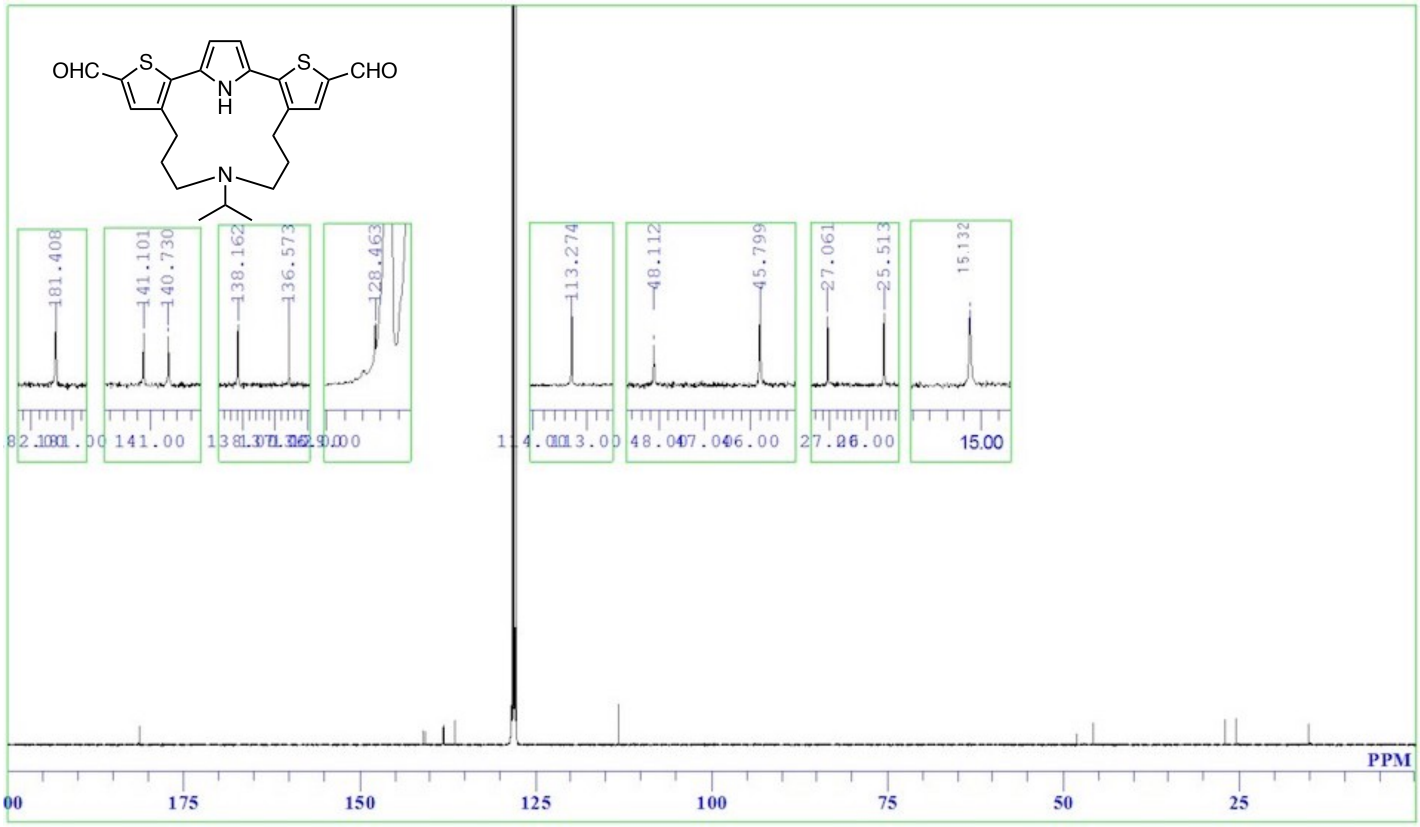

Fig. S36 ^{13}C NMR spectrum of **3** (100 MHz, C_6D_6).

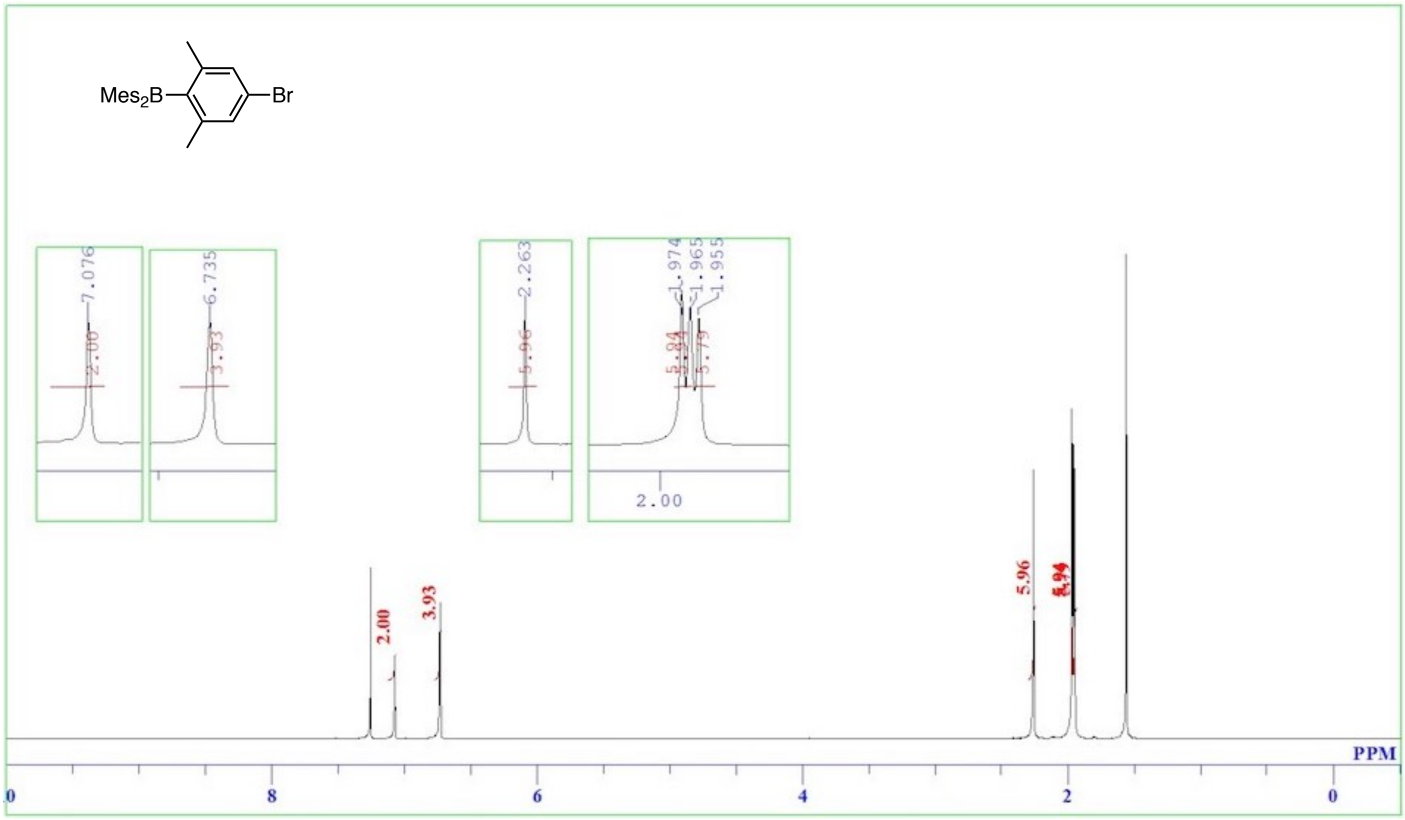

Fig. S37 ^{1}H NMR spectrum of **15** (400 MHz, CDCl$_3$).

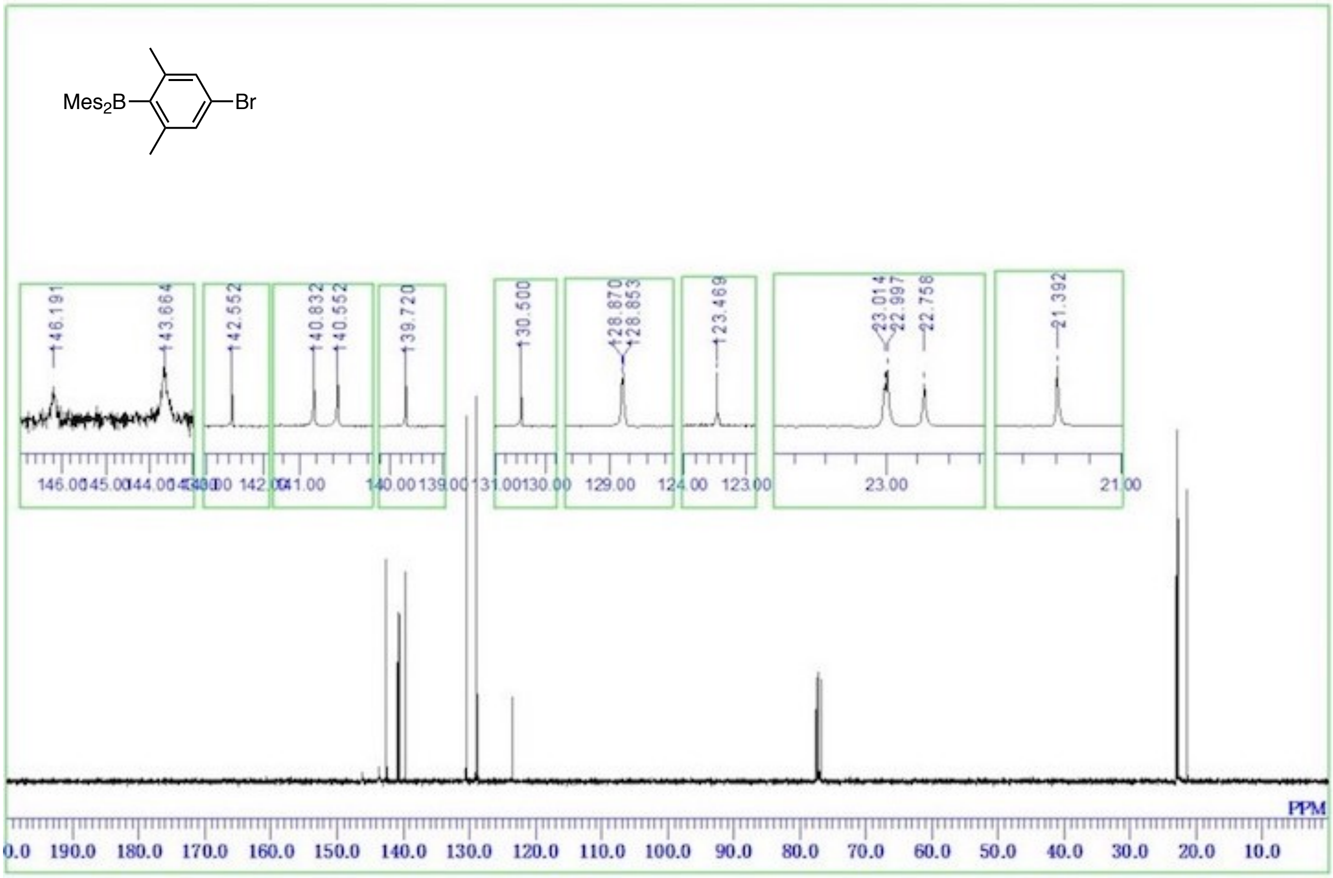

Fig. S38 ^{13}C NMR spectrum of **15** (100 MHz, CDCl$_3$).

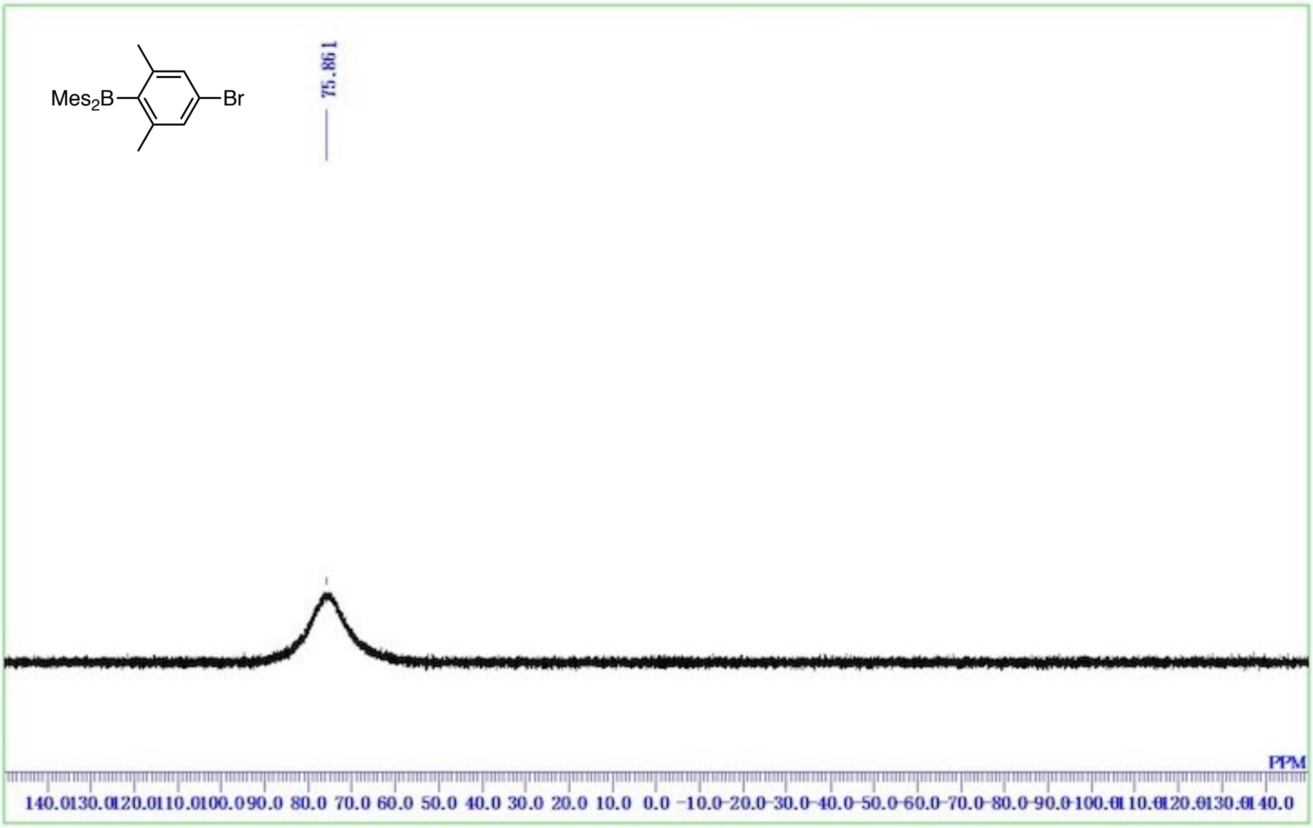

Fig. S39 ^{11}B NMR spectrum of **15** (128 MHz, CDCl$_3$).

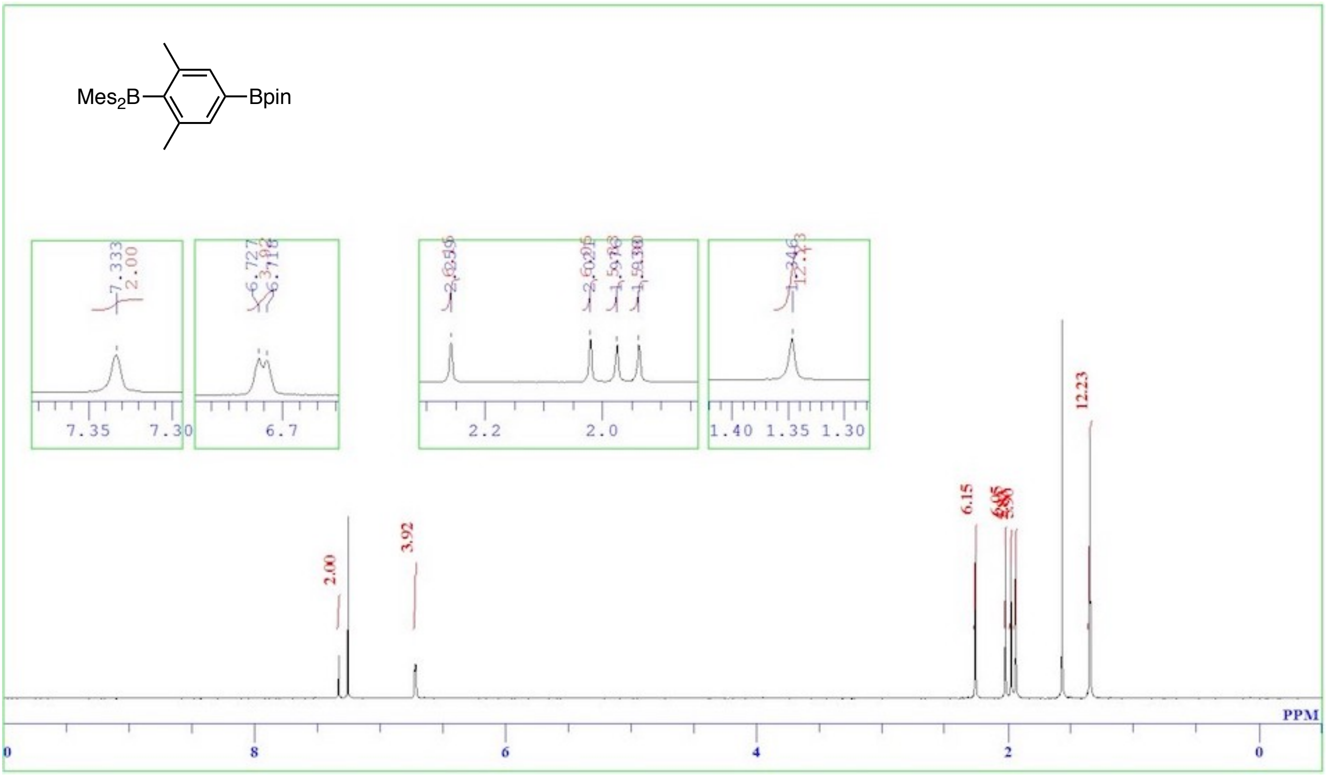

Fig. S40 ^{1}H NMR spectrum of **16** (400 MHz, CDCl$_3$).

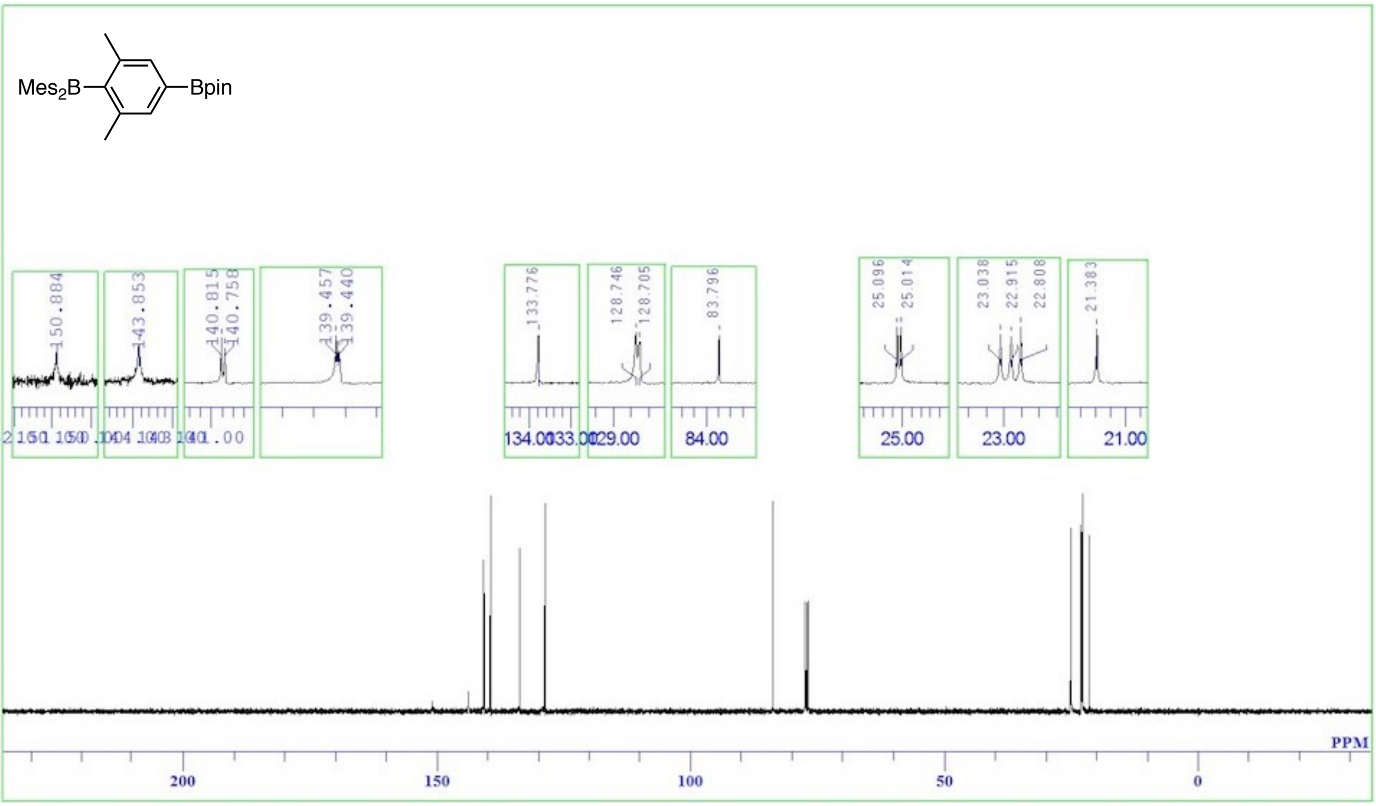

Fig. S41 ^{13}C NMR spectrum of **16** (100 MHz, CDCl$_3$).

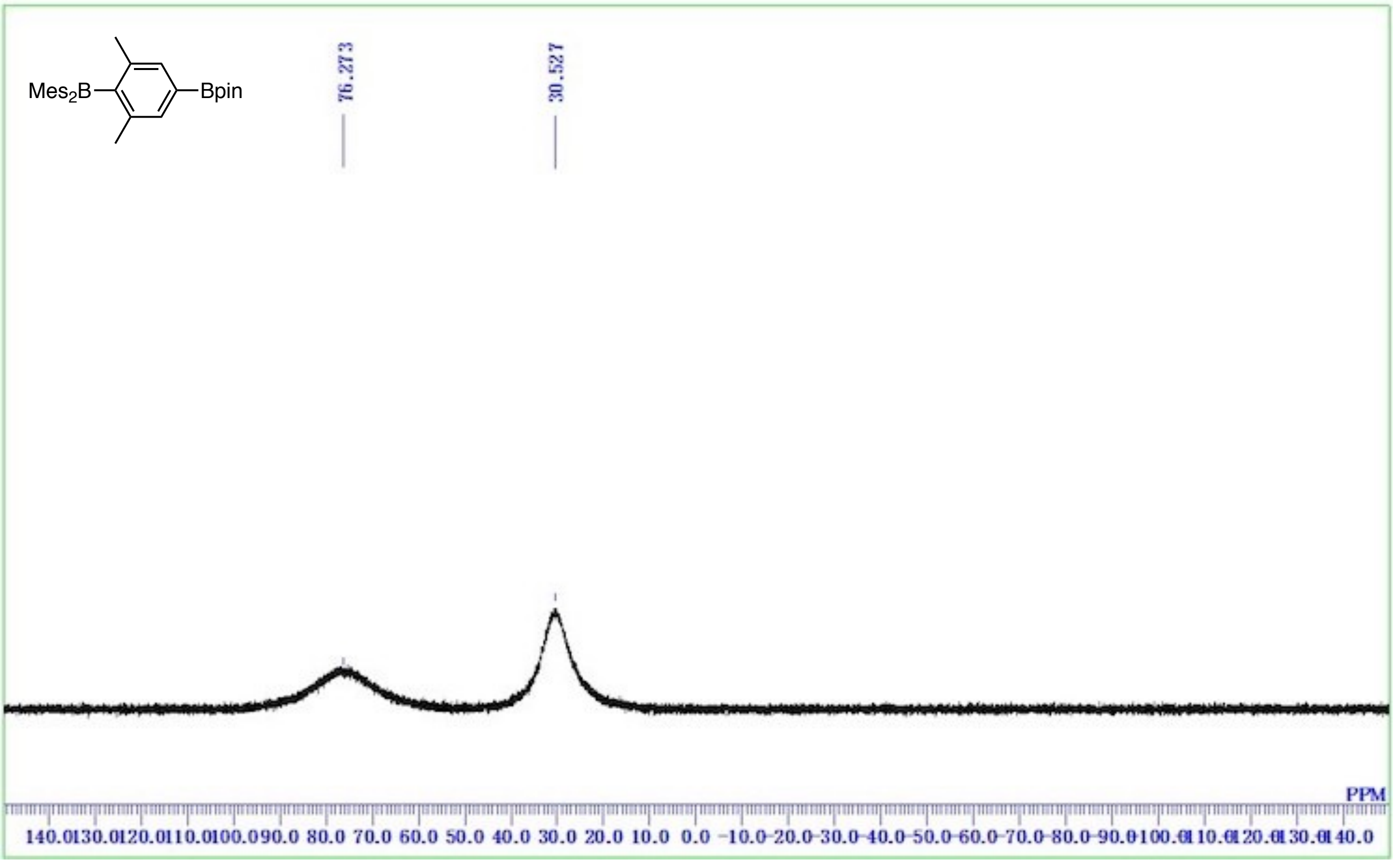

Fig. S42 ^{11}B NMR spectrum of **16** (128 MHz, CDCl$_3$).

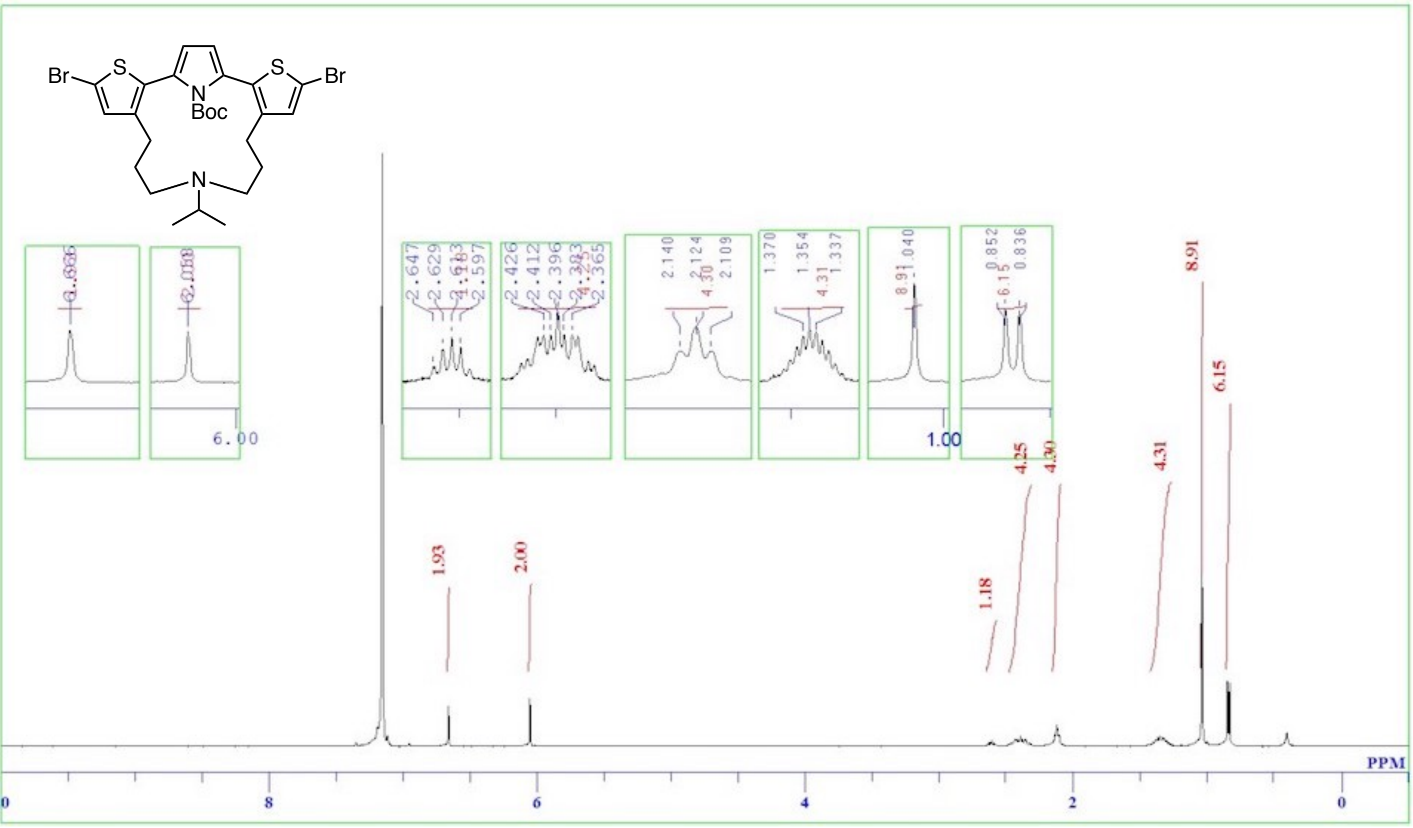

Fig. S43 ^{1}H NMR spectrum of **12** (400 MHz, C_6D_6).

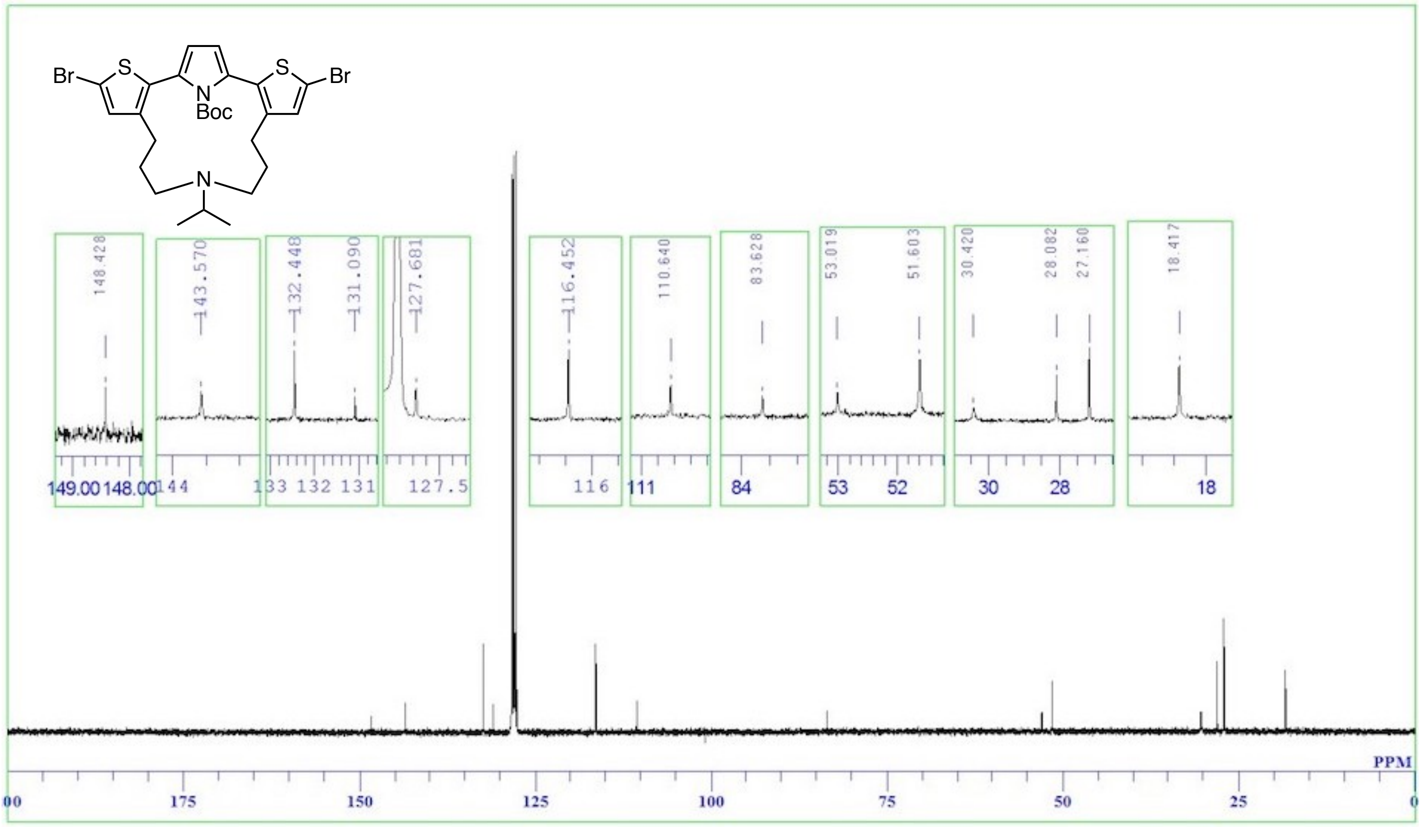

Fig. S44 ^{13}C NMR spectrum of **12** (100 MHz, C_6D_6).

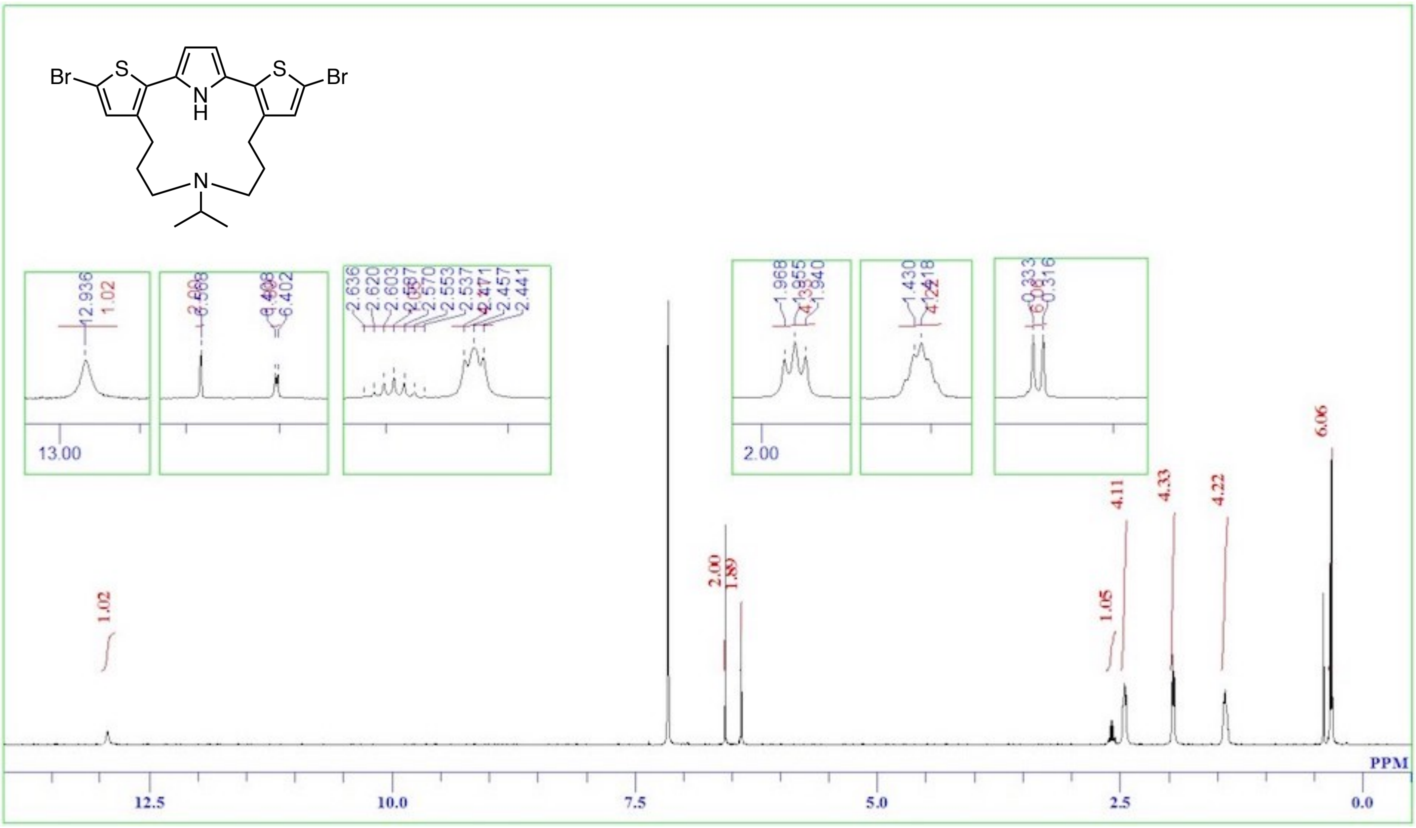

Fig. S45 ^{1}H NMR spectrum of **17** (400 MHz, C_6D_6).

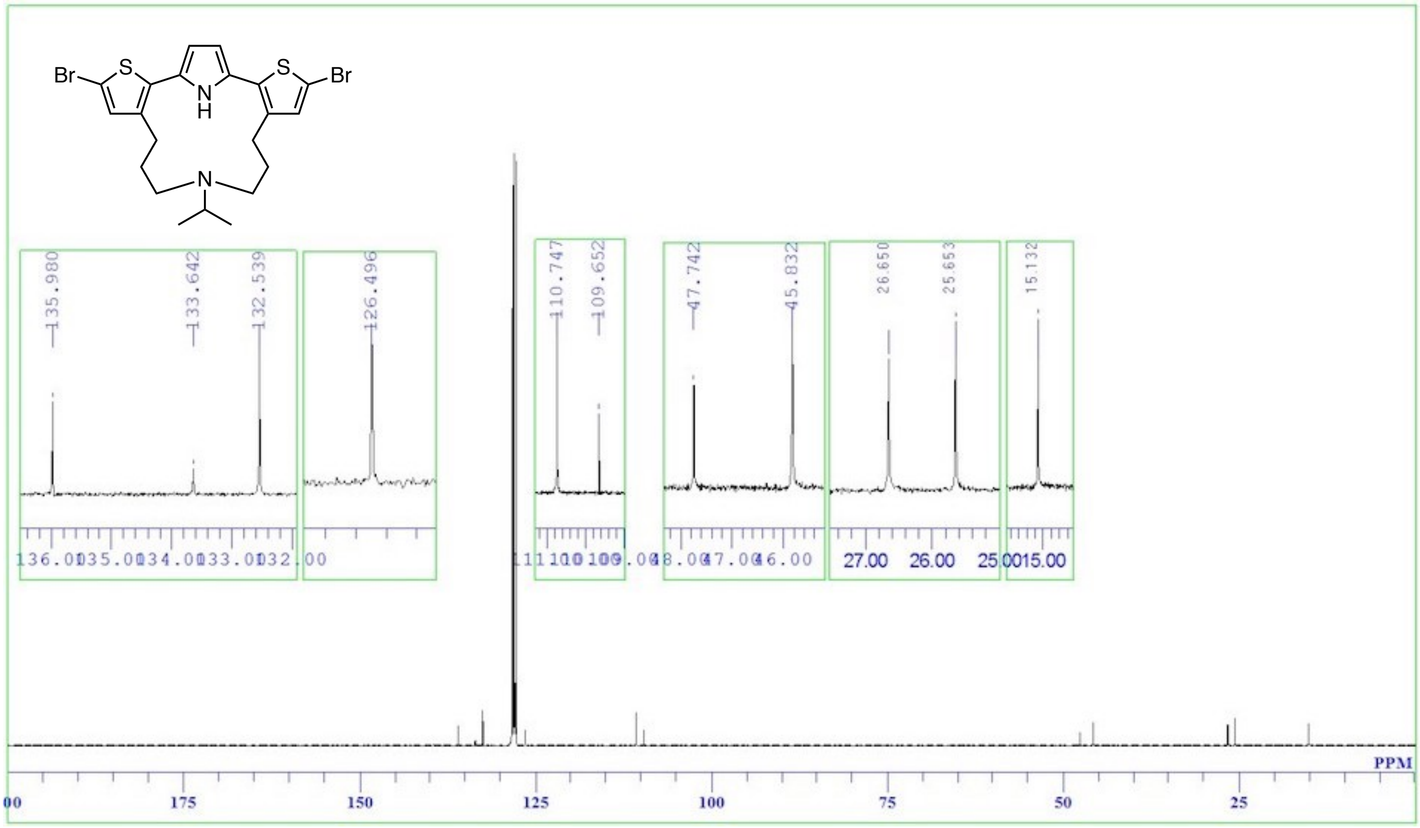

Fig. S46 ^{13}C NMR spectrum of **17** (100 MHz, C_6D_6).

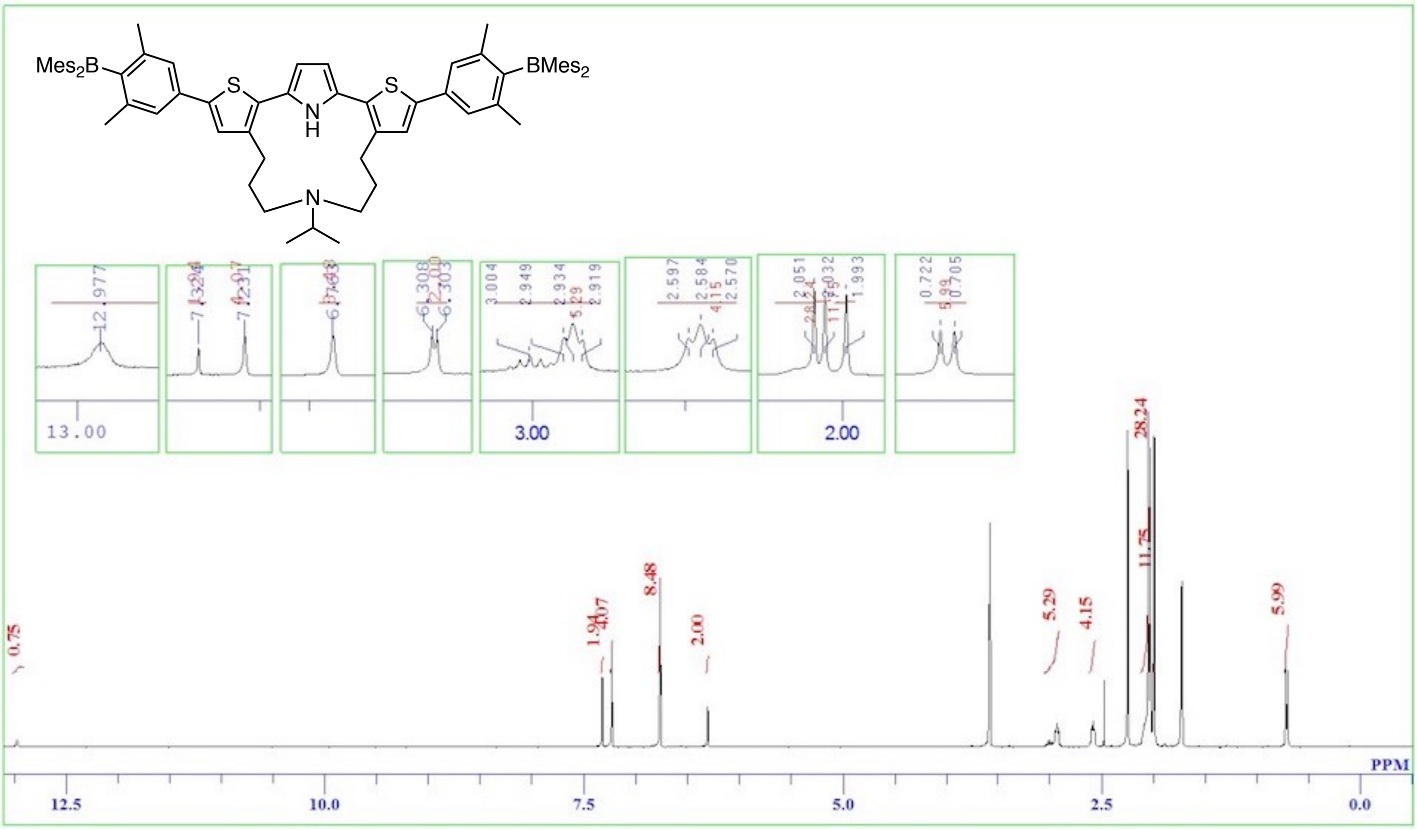

Fig. S47 ^{1}H NMR spectrum of **4** (400 MHz, THF-d_6).

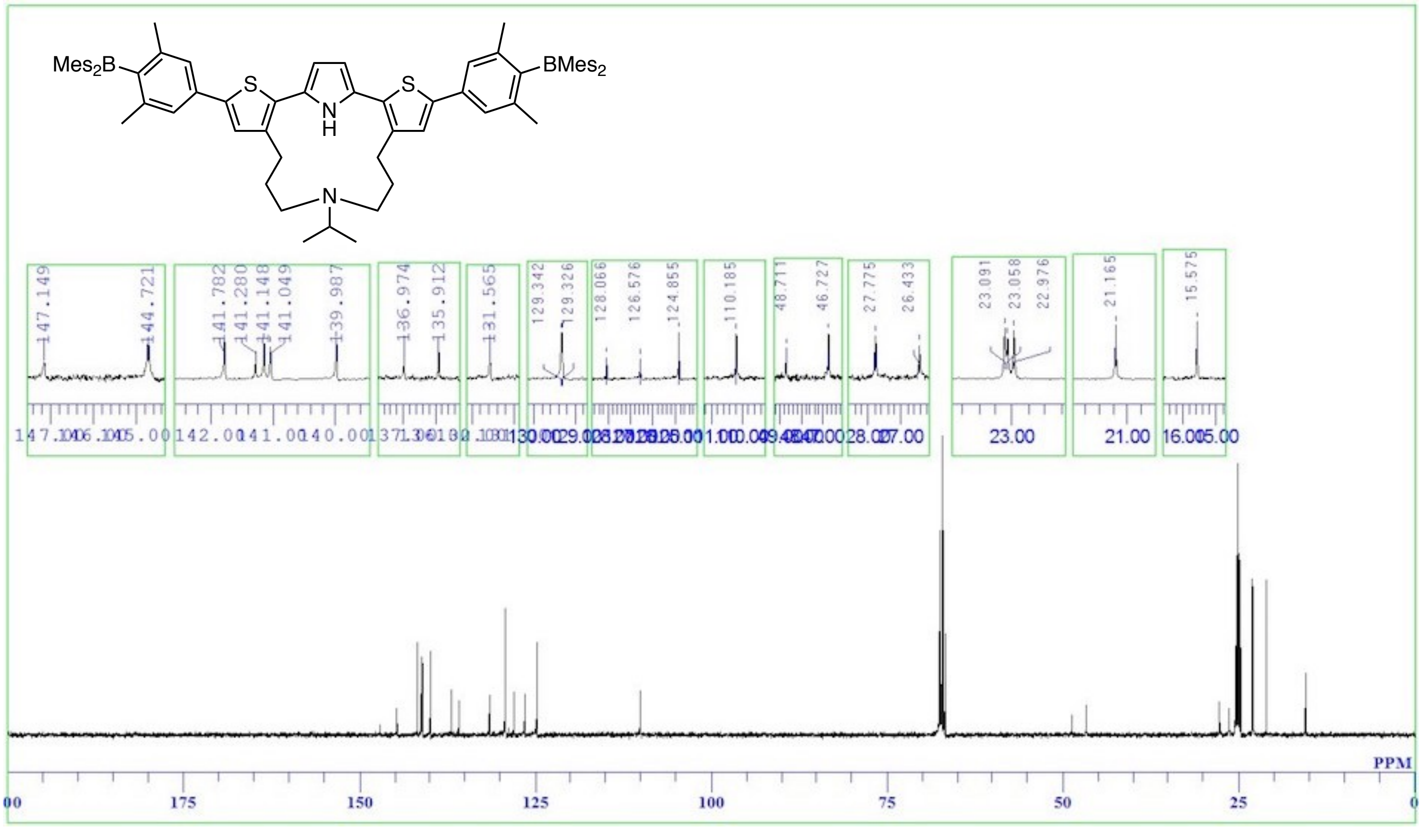

Fig. S48 ^{13}C NMR spectrum of **4** (100 MHz, THF-d_8).

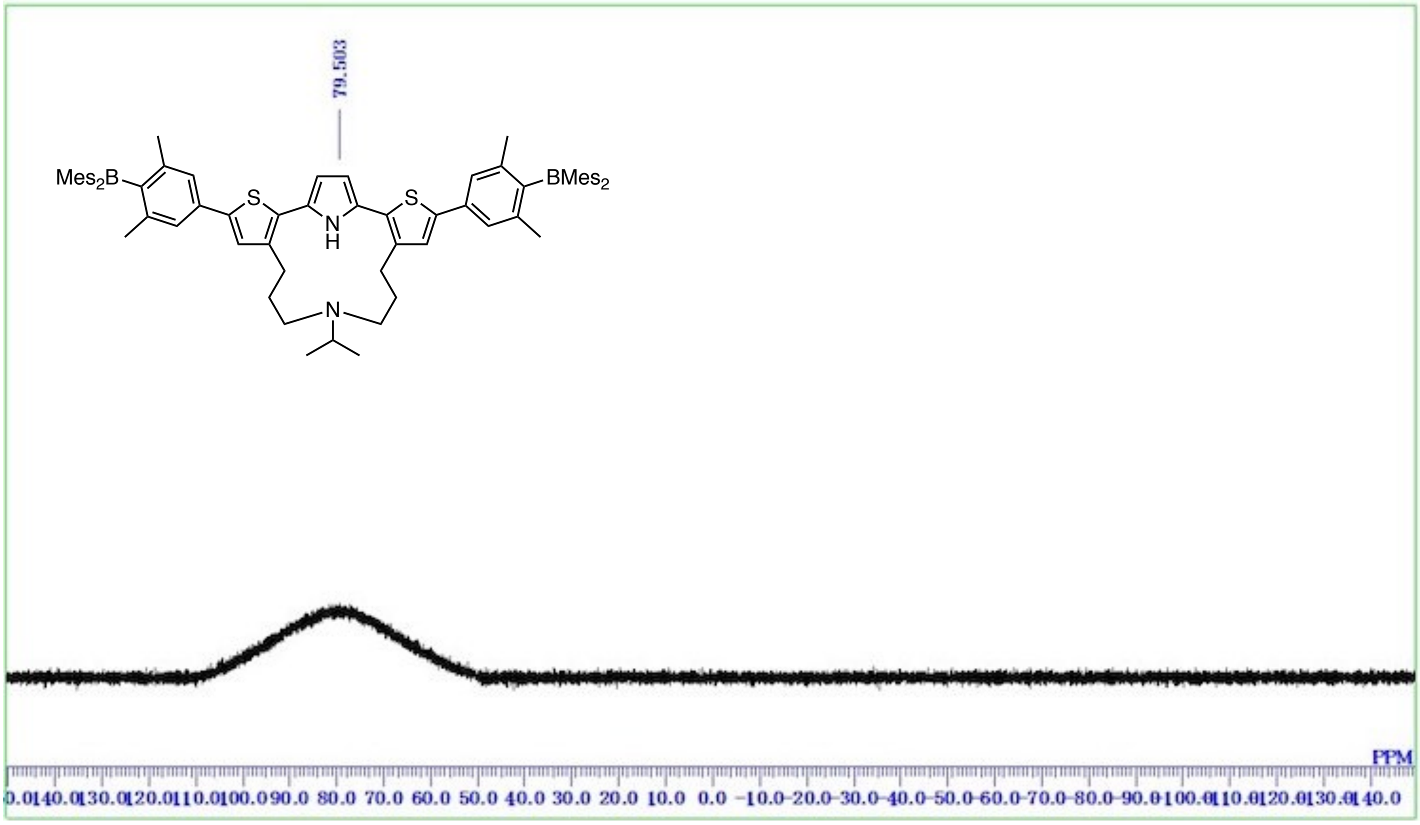

Fig. S49 ^{11}B NMR spectrum of **4** (128 MHz, THF-d_8).

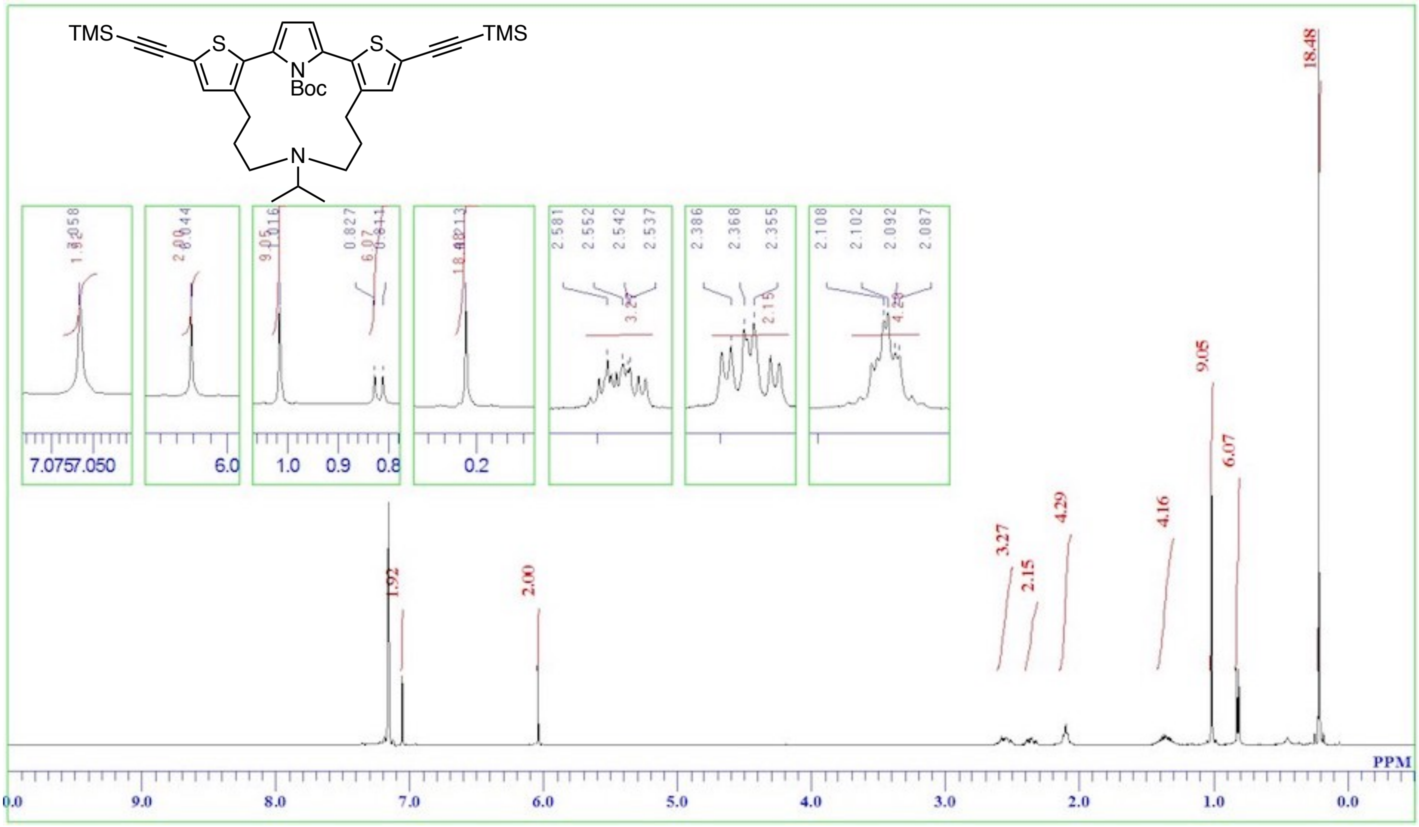

Fig. S50 ^{1}H NMR spectrum of **13** (400 MHz, C_6D_6).

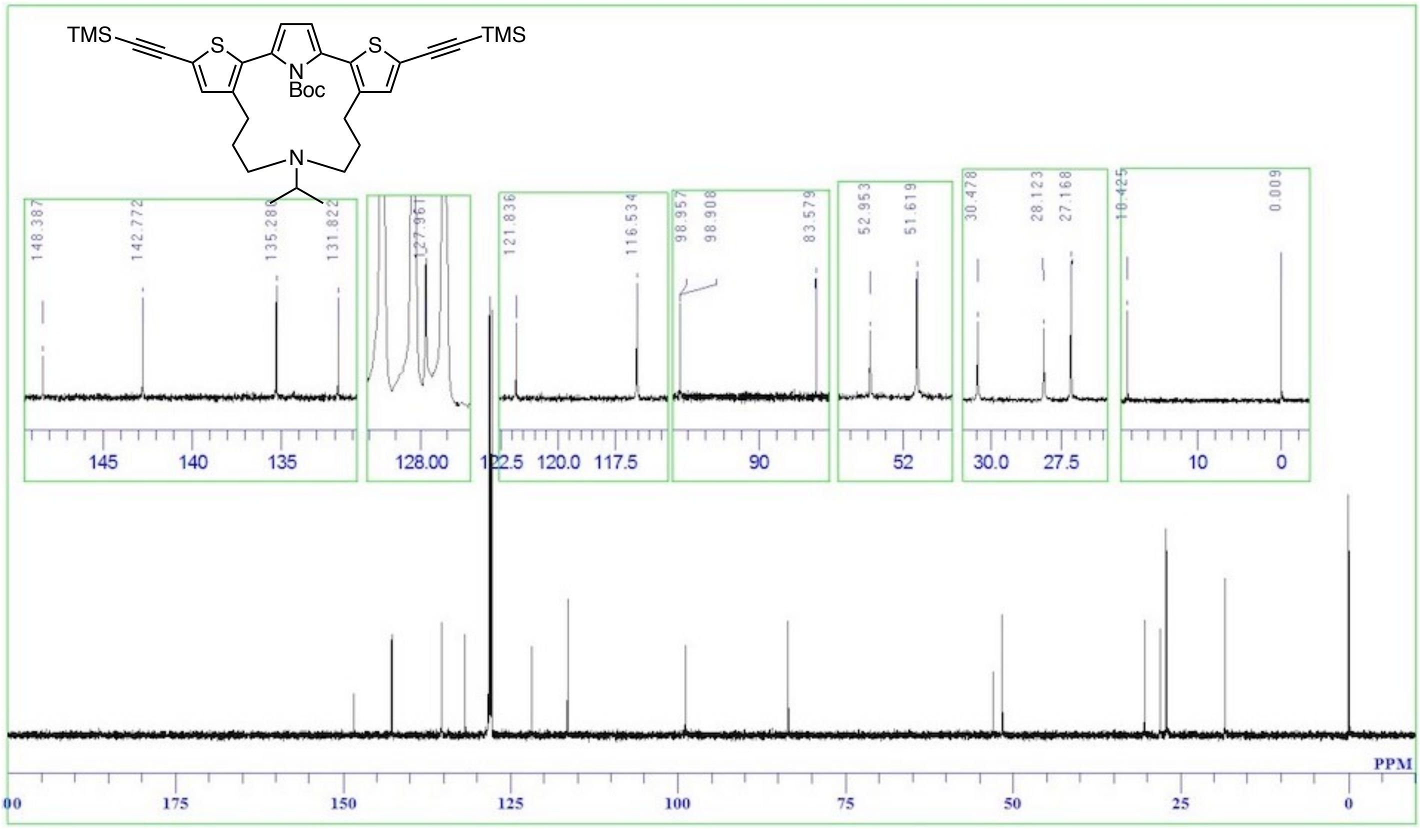

Fig. S51 ^{13}C NMR spectrum of **13** (100 MHz, C_6D_6).

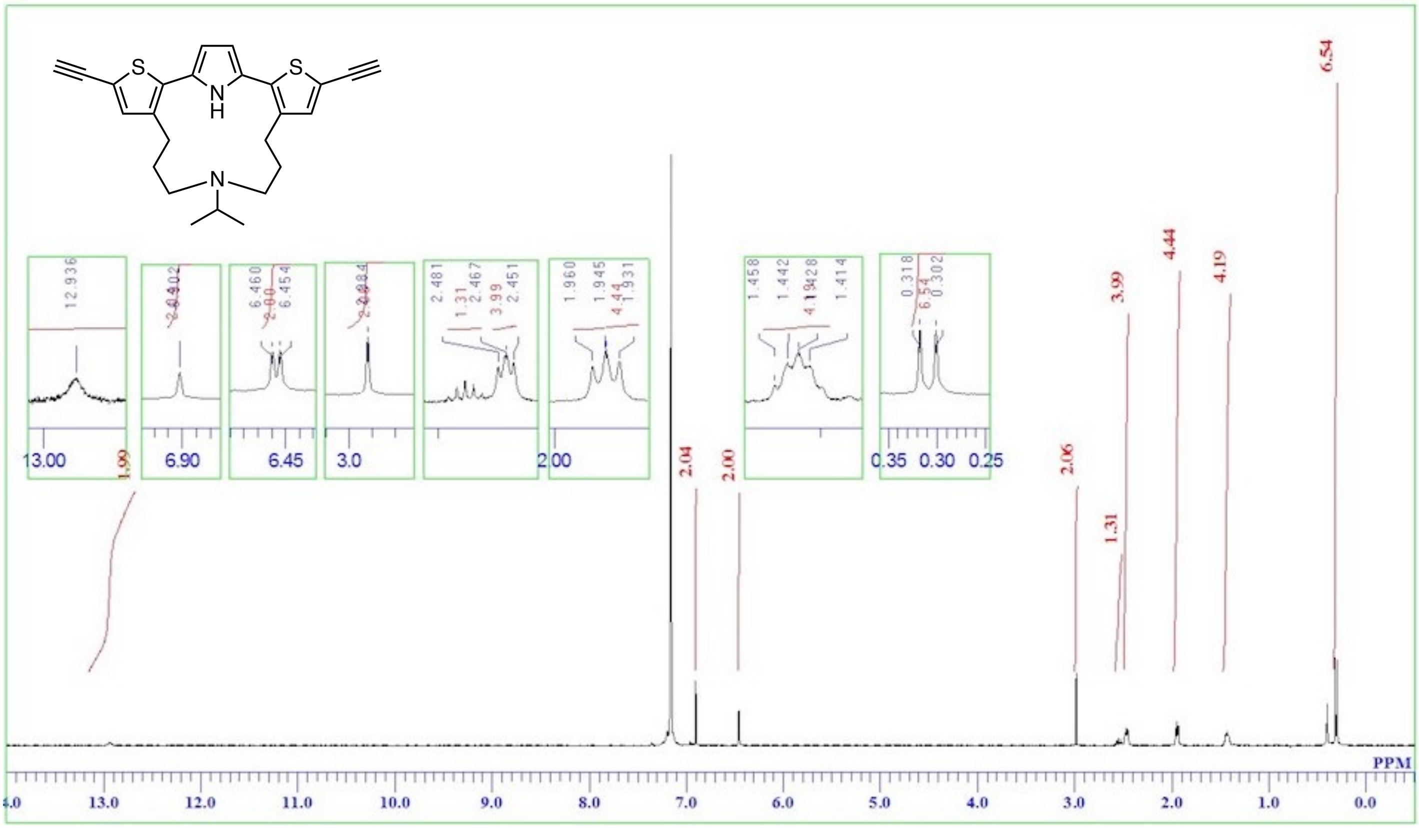

Fig. S52 ^{1}H NMR spectrum of **14** (400 MHz, C_6D_6).

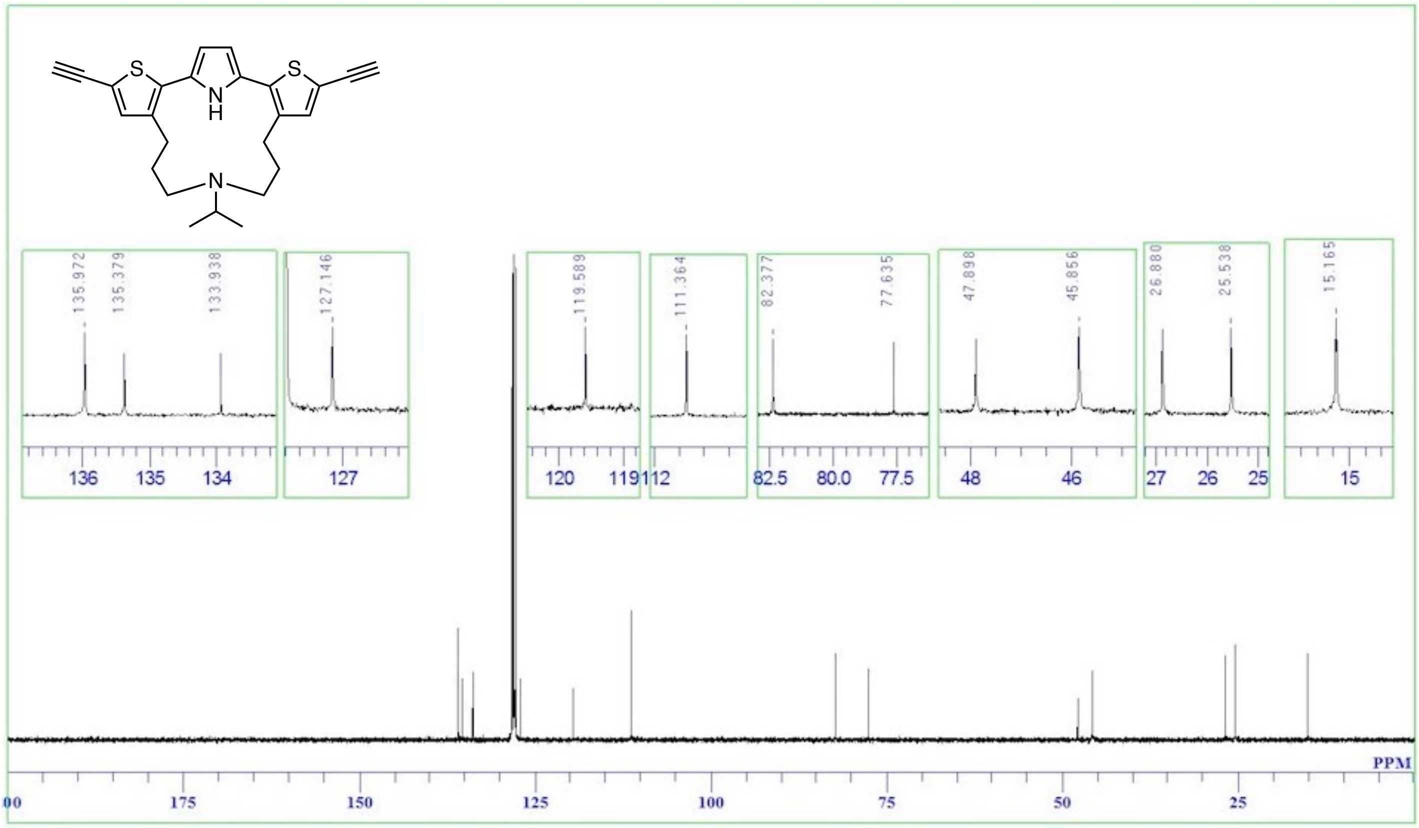

Fig. S53 ^{13}C NMR spectrum of **14** (100 MHz, C_6D_6).

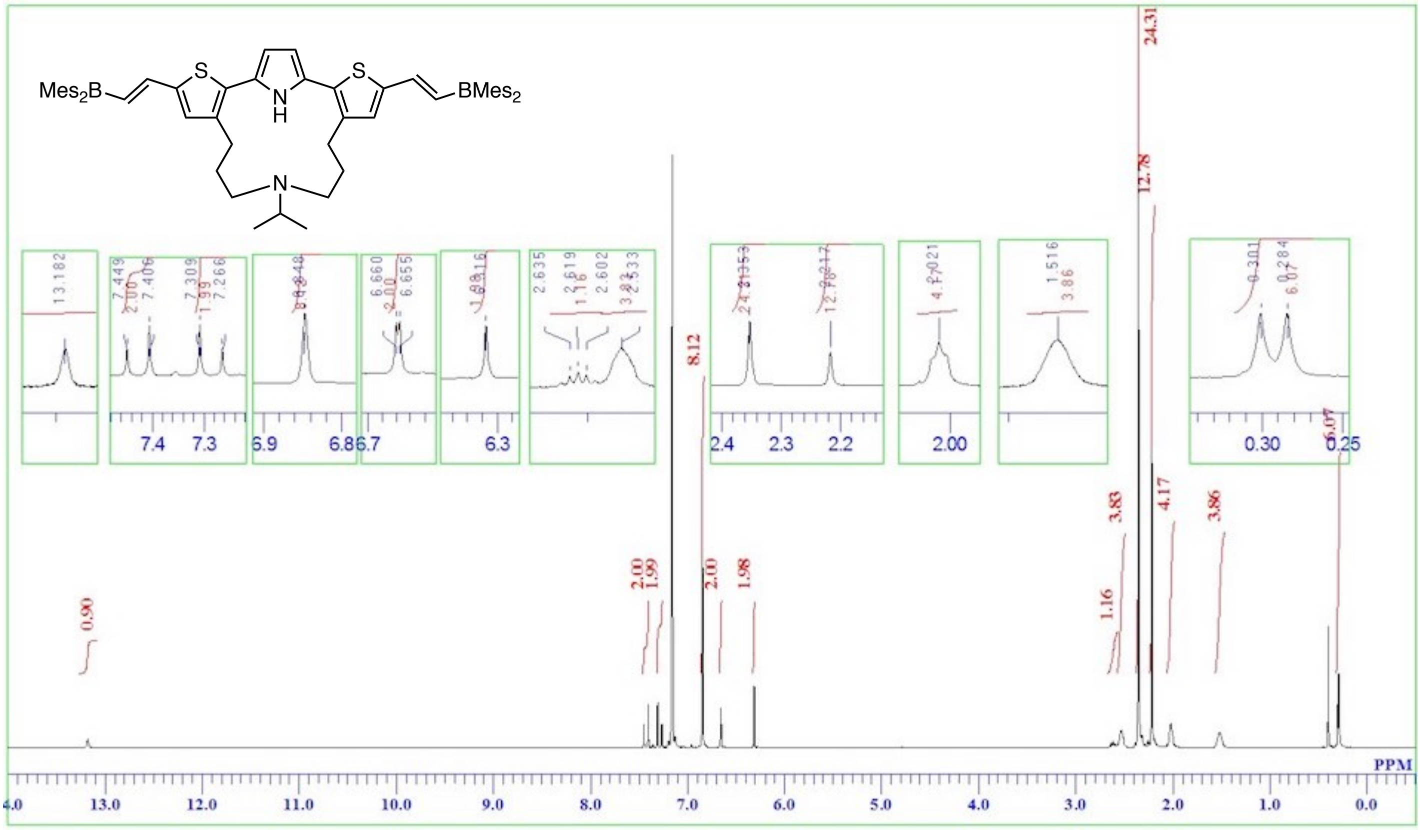

Fig. S54 ^{1}H NMR spectrum of **5** (400 MHz, C_6D_6).

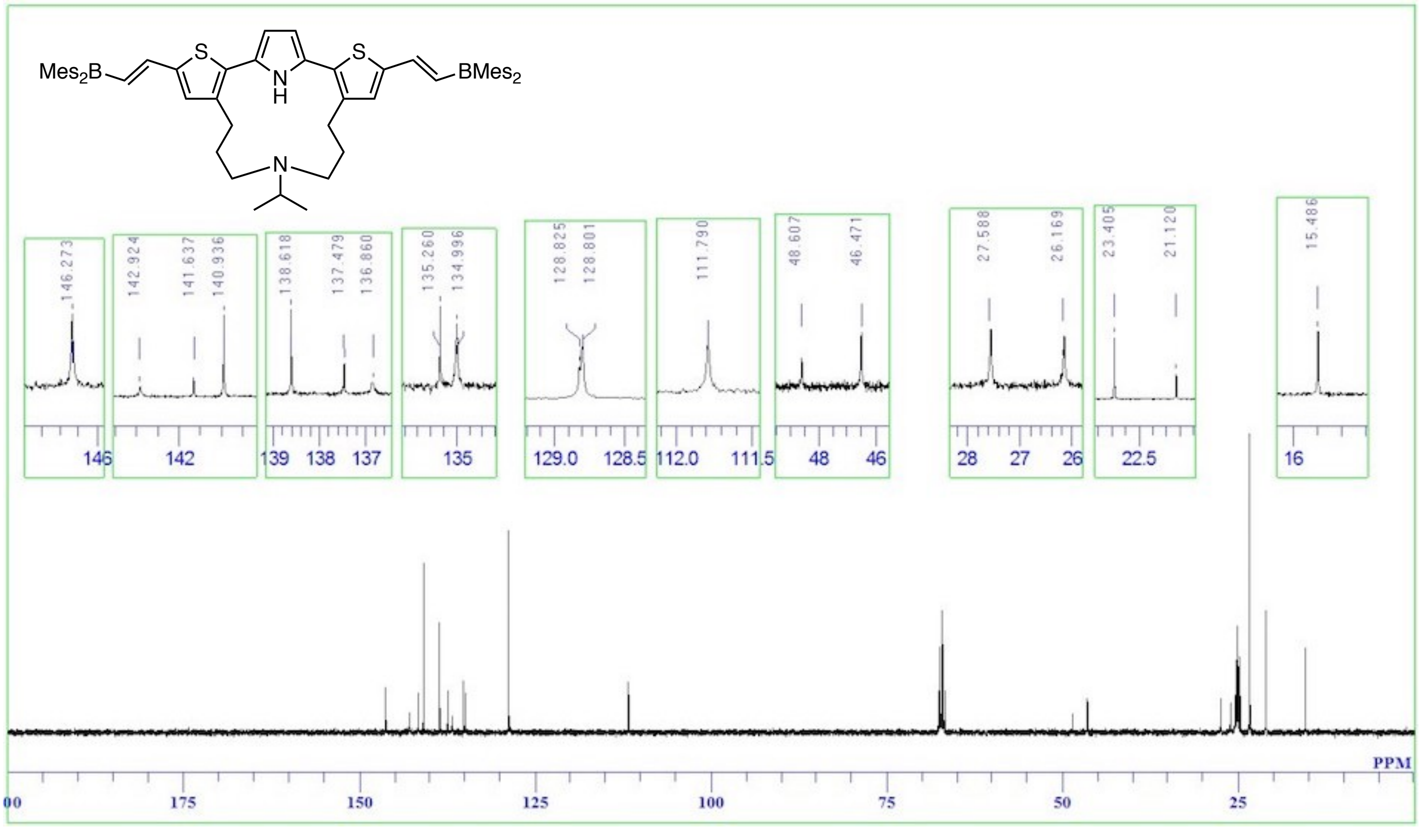

Fig. S55 ^{13}C NMR spectrum of **5** (100 MHz, THF-d_8).

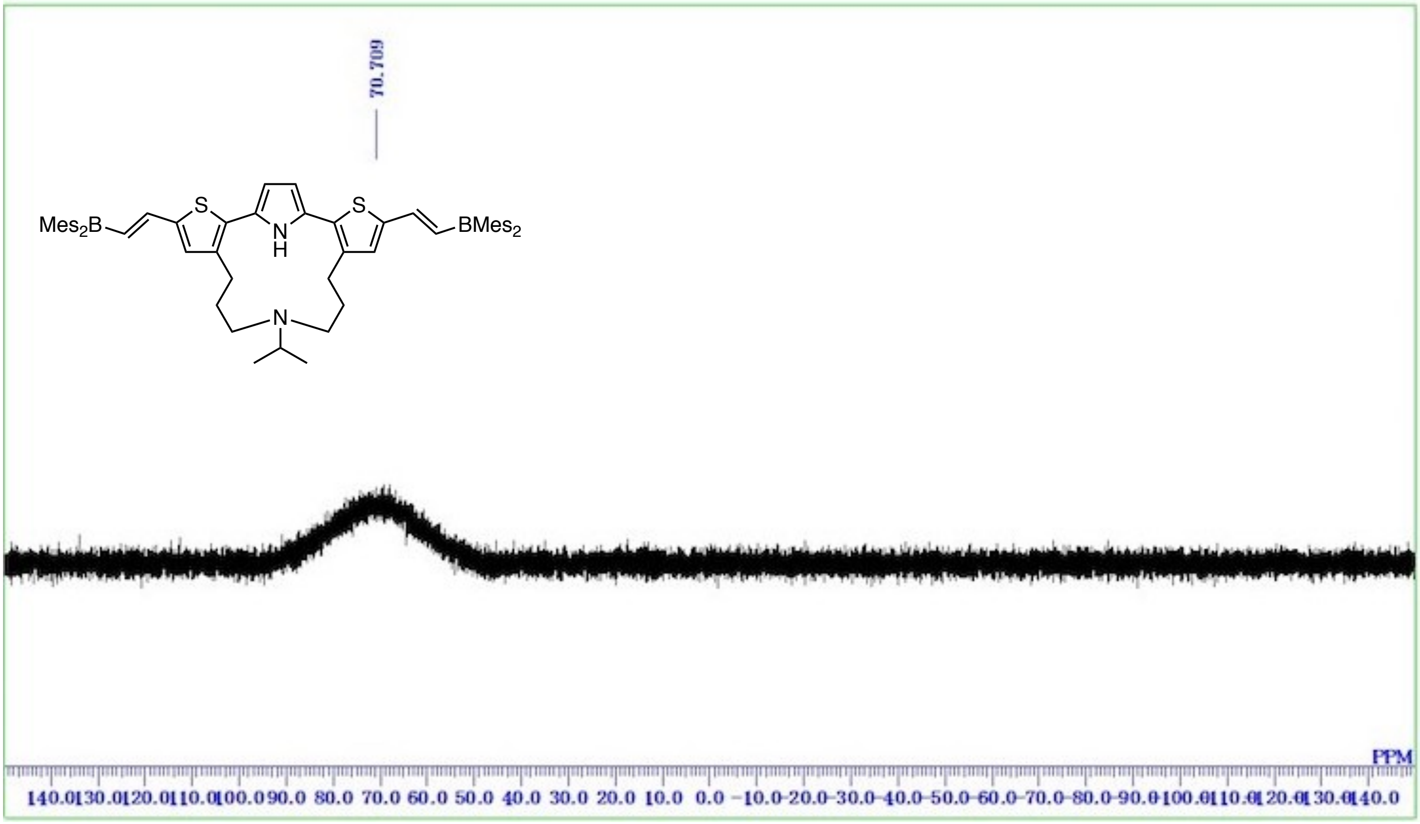

Fig. S56 ^{11}B NMR spectrum of **5** (128 MHz, C_6D_6).

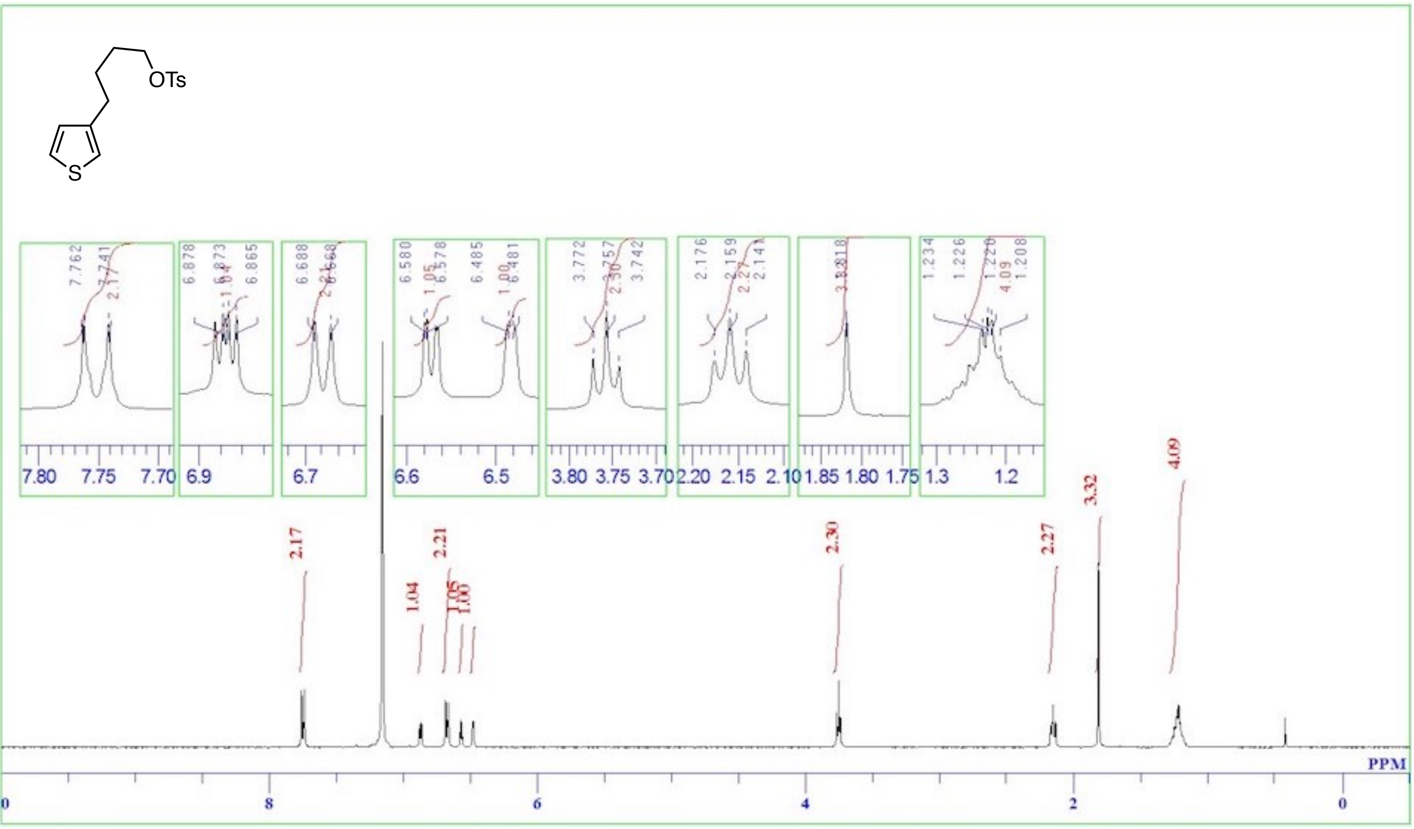

Fig. S57 ^{1}H NMR spectrum of **18** (400 MHz, C_6D_6).

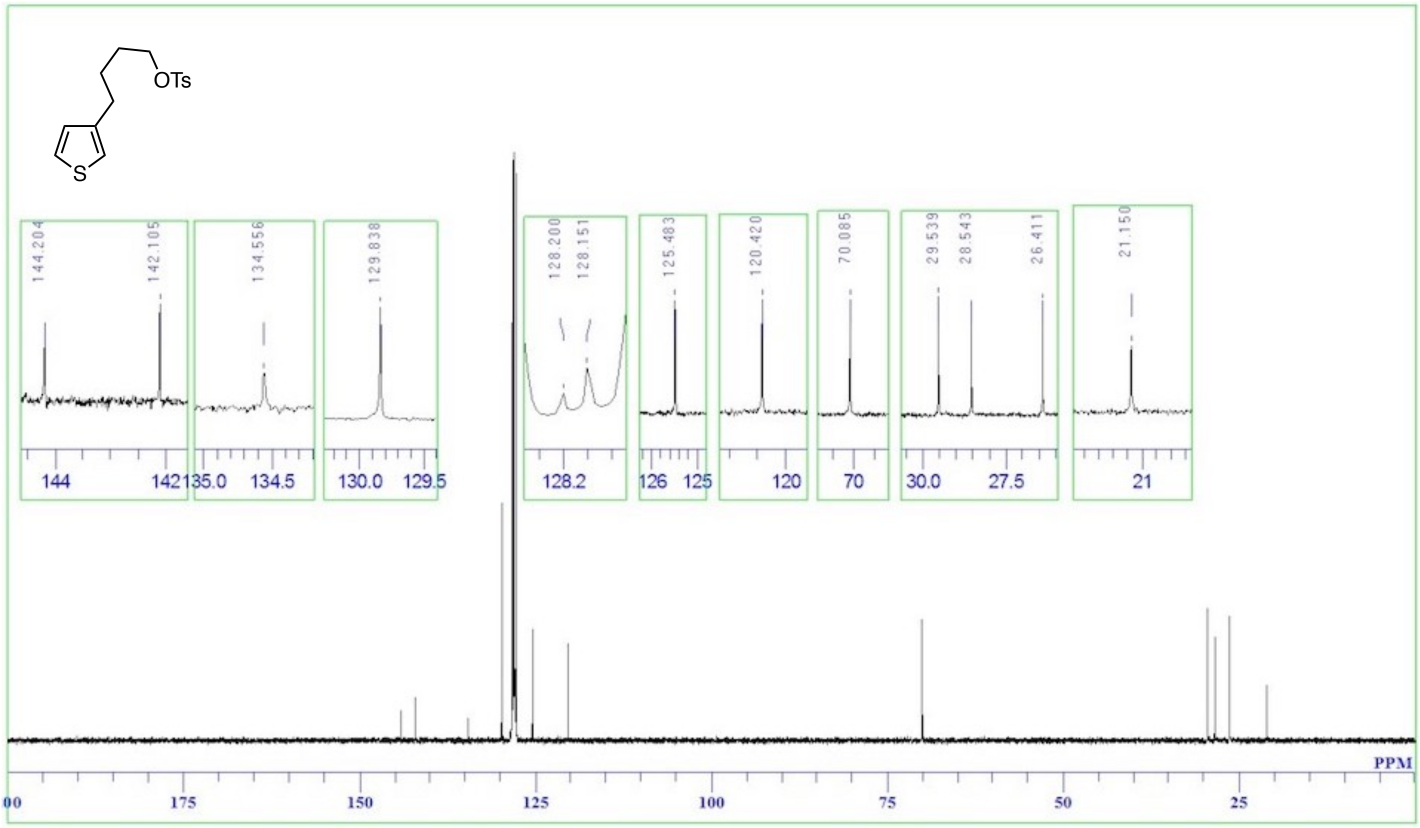

Fig. S58 ^{13}C NMR spectrum of **18** (100 MHz, C_6D_6).

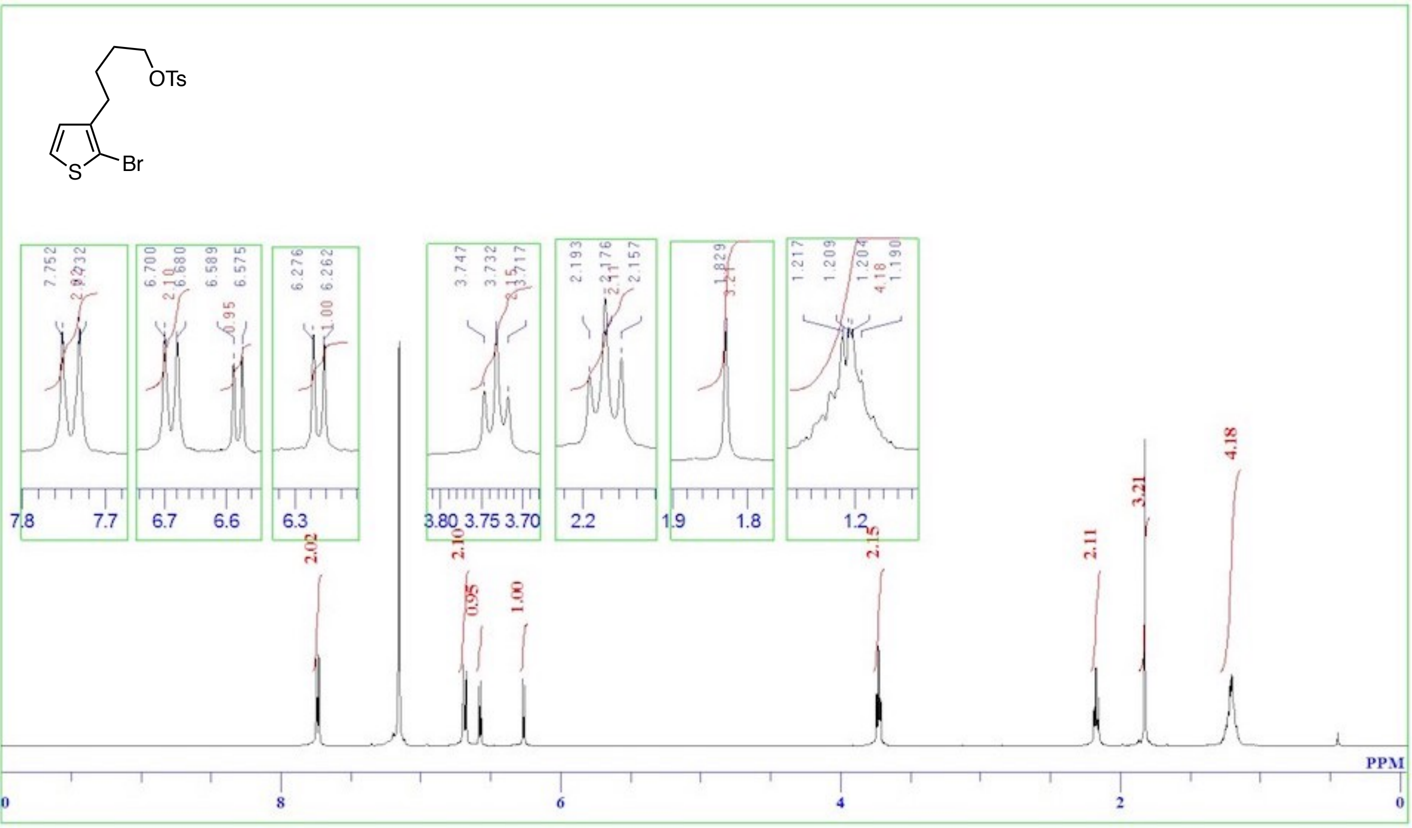

Fig. S59 ^{1}H NMR spectrum of **19** (400 MHz, C_6D_6).

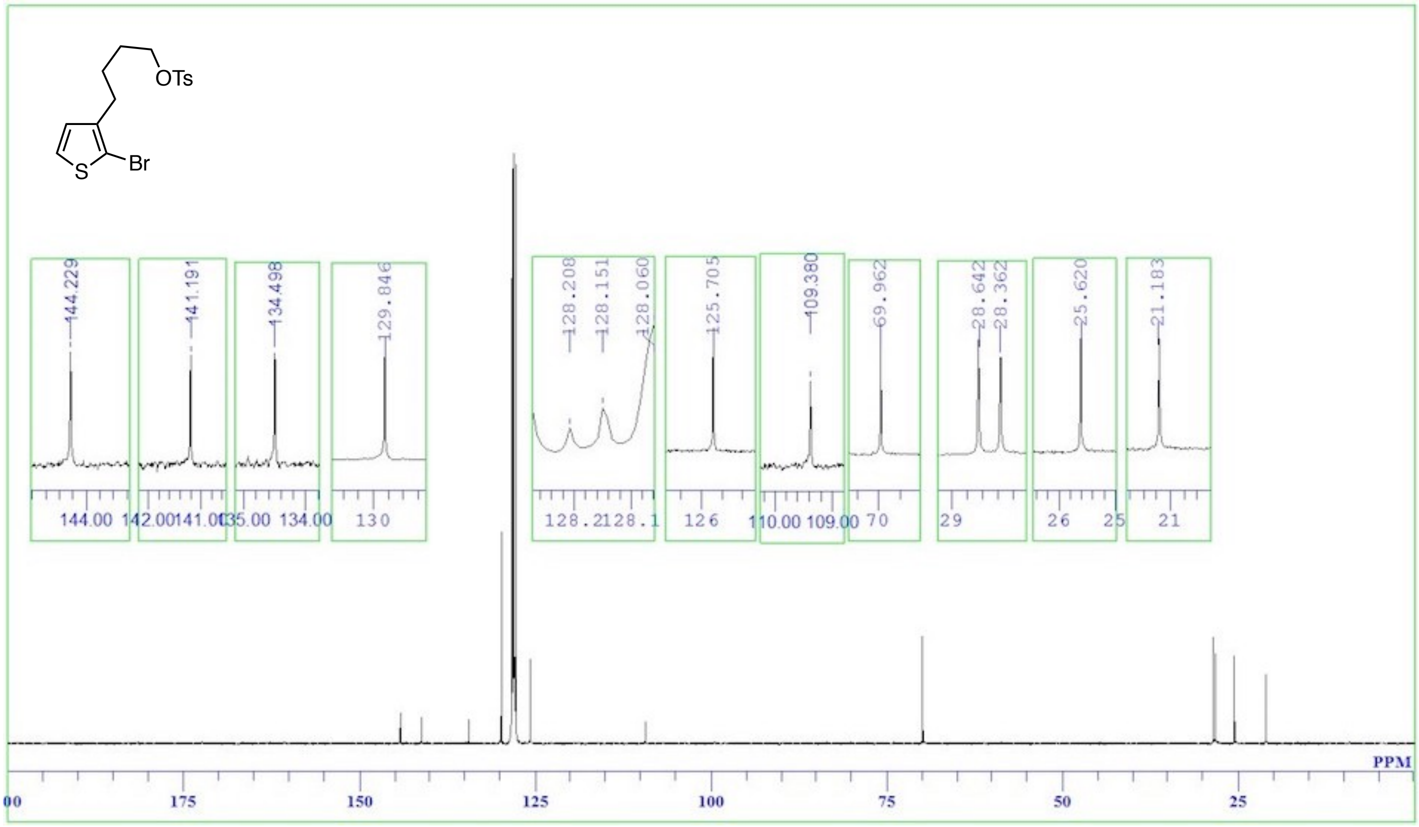

Fig. S60 ^{13}C NMR spectrum of **19** (100 MHz, C_6D_6).

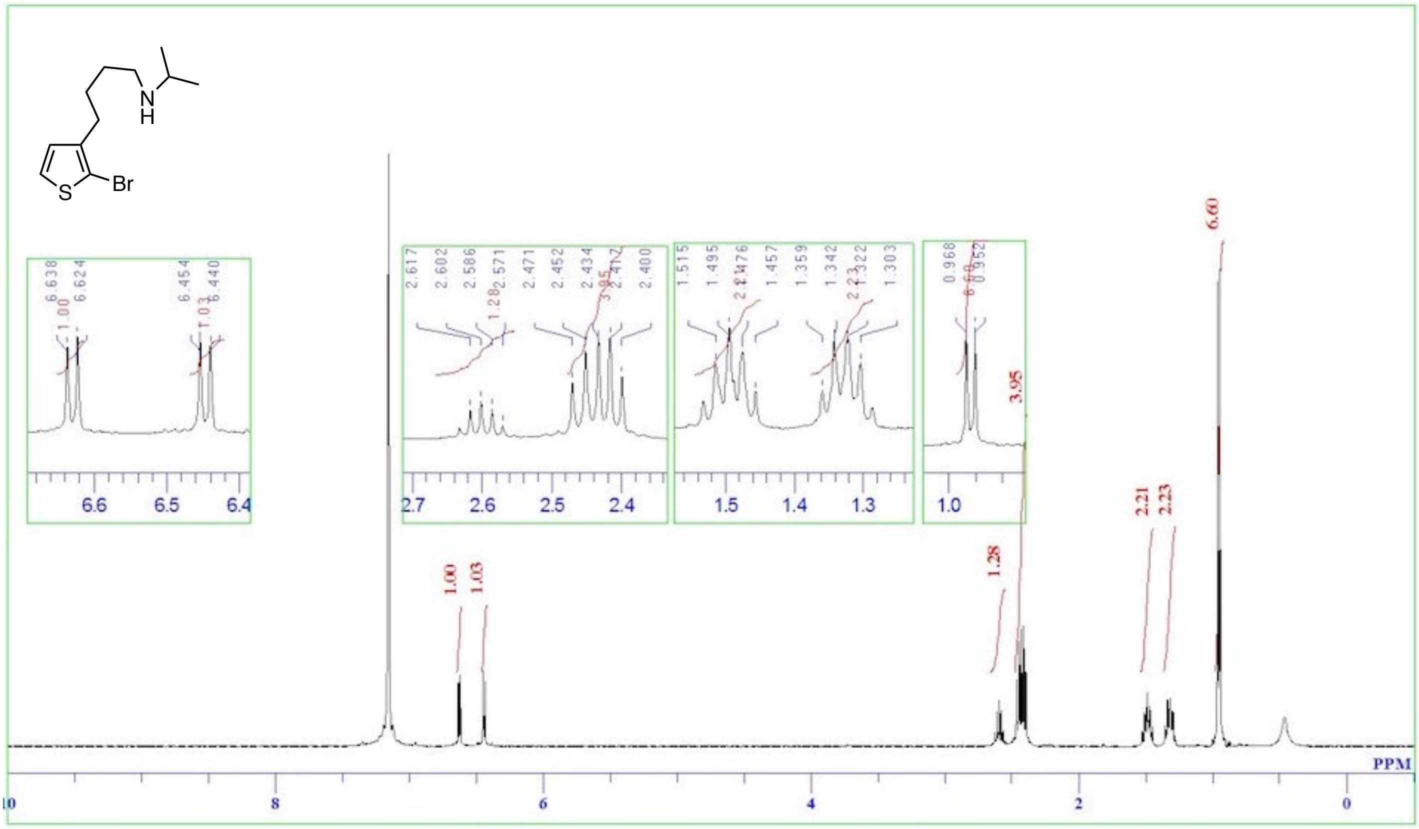

Fig. S61 ^{1}H NMR spectrum of **20** (400 MHz, C_6D_6).

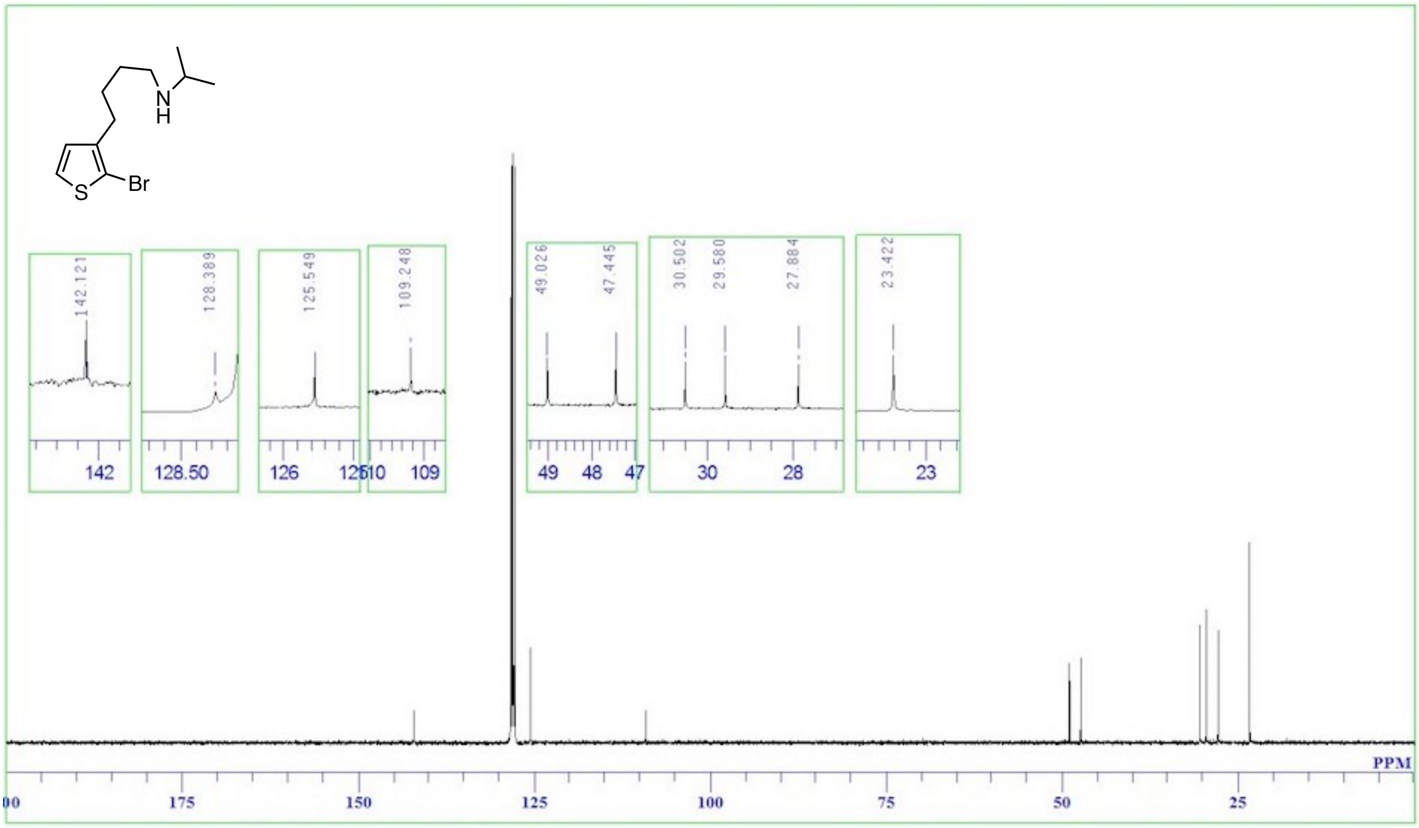

Fig. S62 ^{13}C NMR spectrum of **20** (100 MHz, C_6D_6).

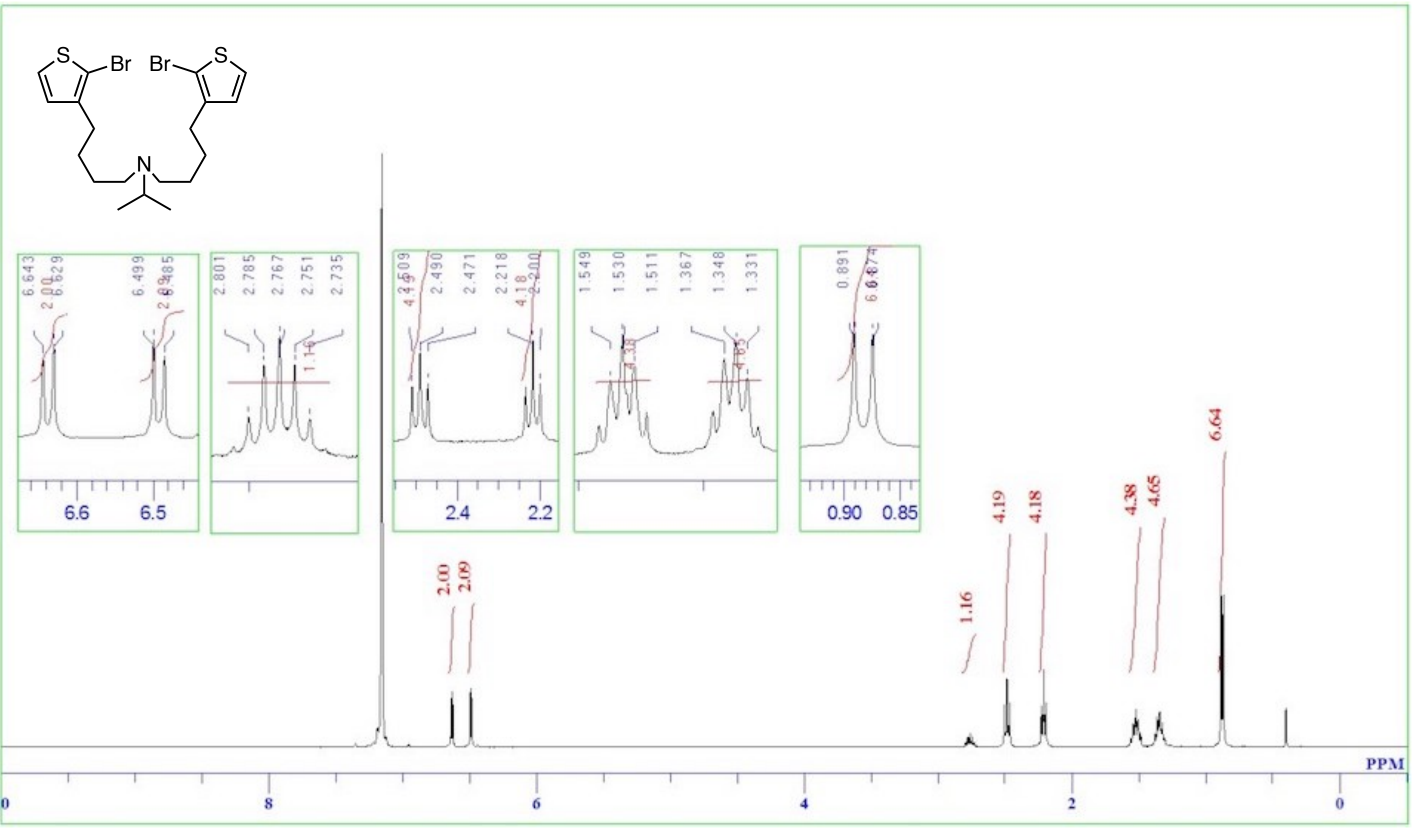

Fig. S63 ^{1}H NMR spectrum of **21** (400 MHz, C_6D_6).

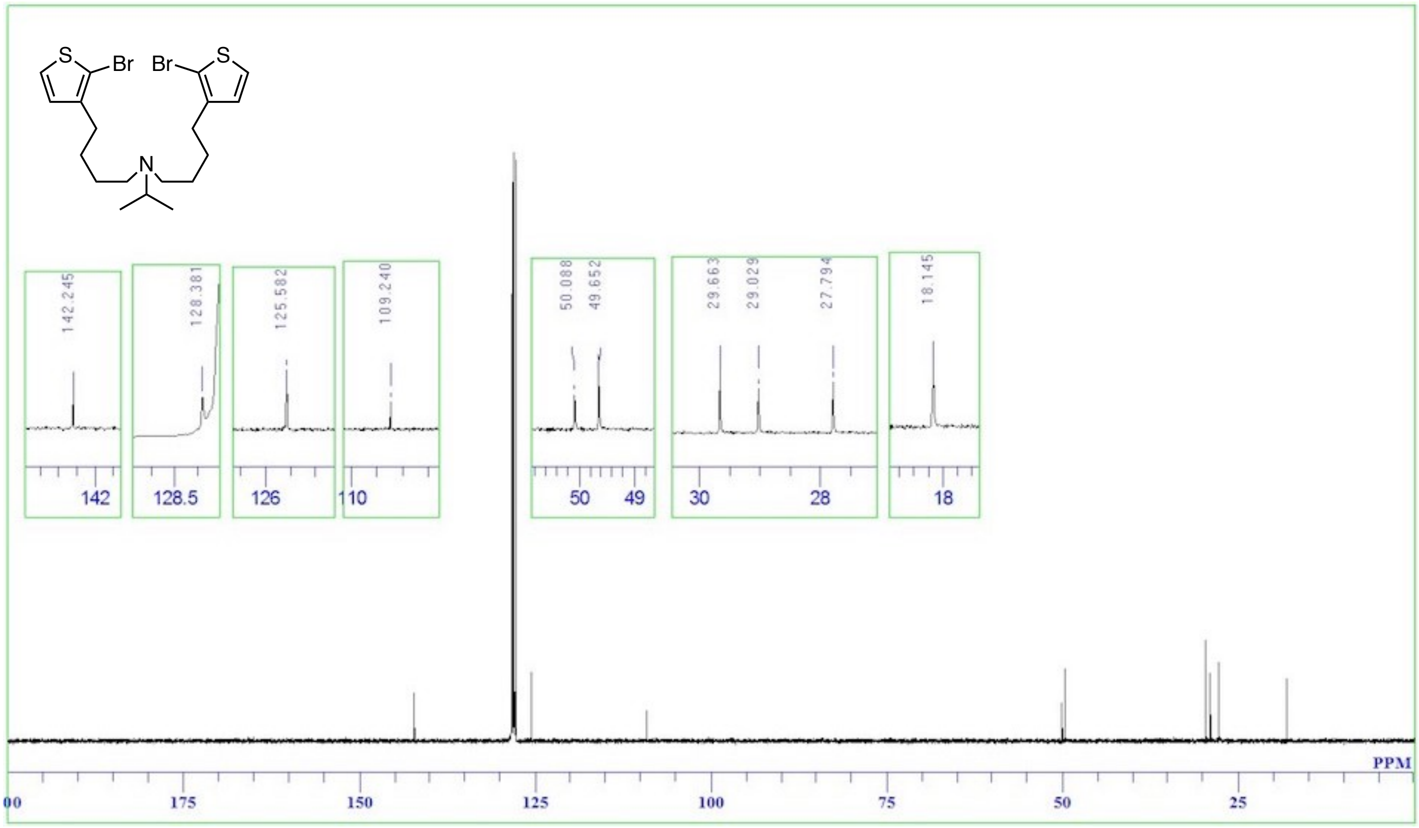

Fig. S64 ^{13}C NMR spectrum of **21** (100 MHz, C_6D_6).

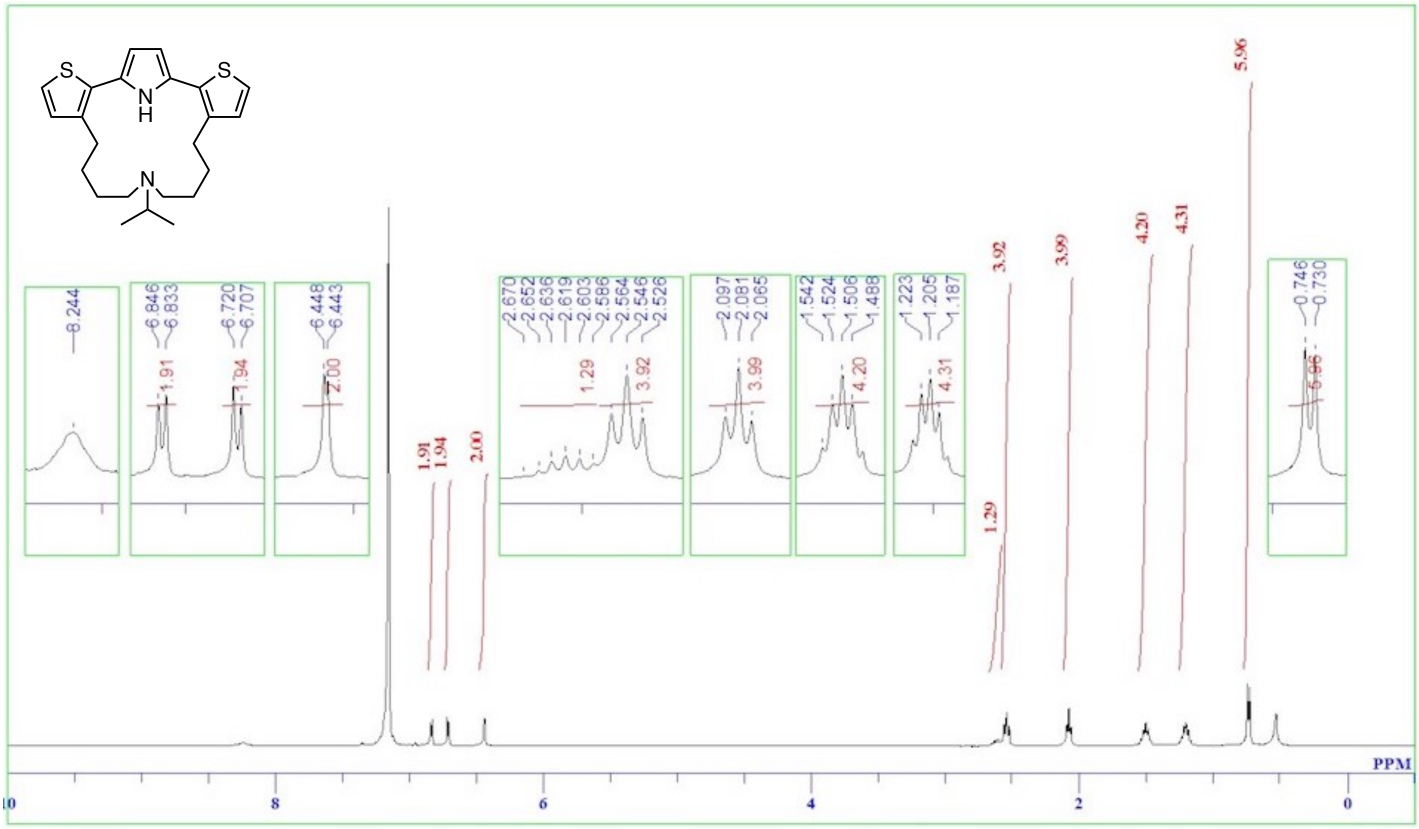

Fig. S65 ^{1}H NMR spectrum of **22** (400 MHz, C_6D_6).

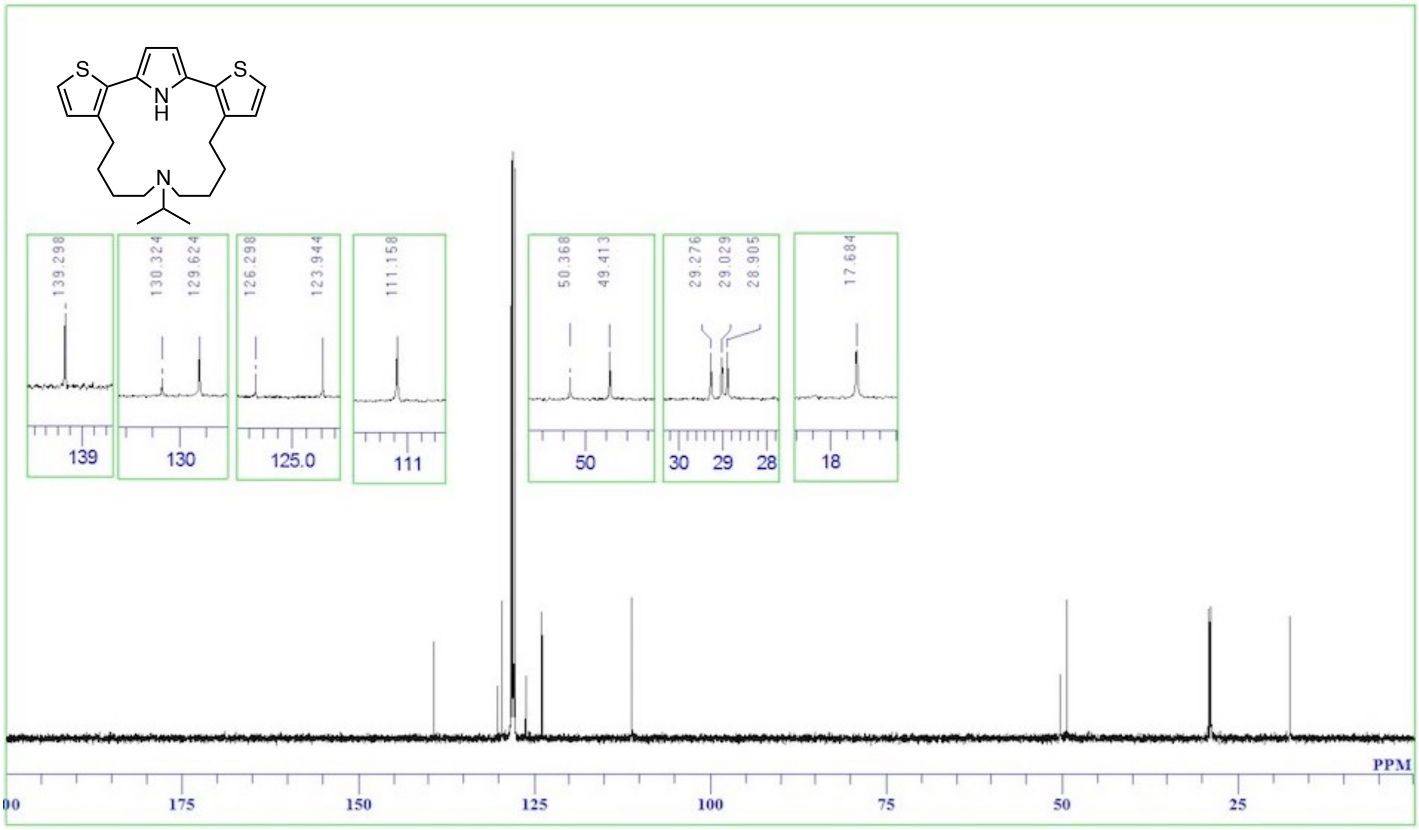

Fig. S66 ^{13}C NMR spectrum of **22** (100 MHz, C_6D_6).

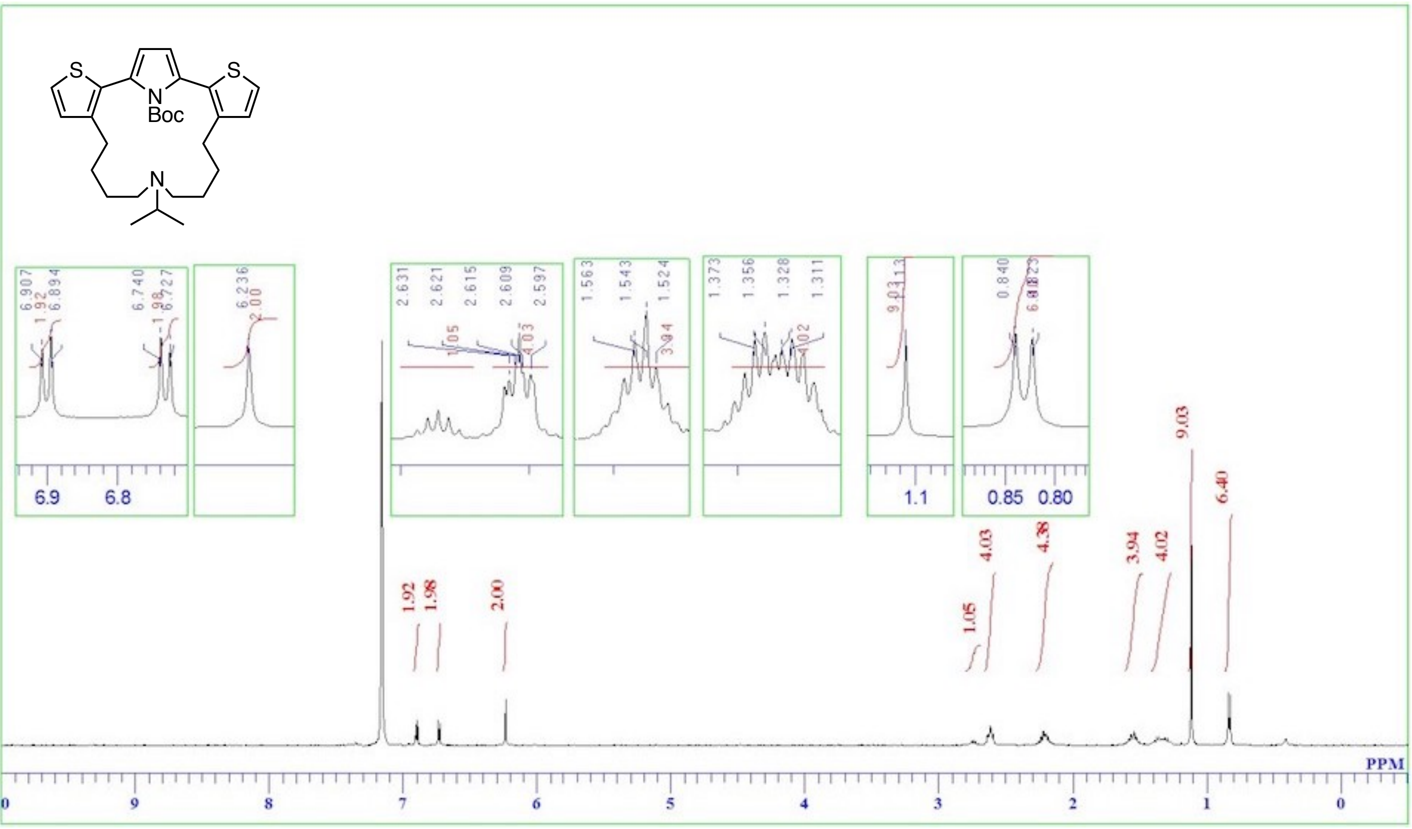

Fig. S67 ^{1}H NMR spectrum of **23** (400 MHz, C_6D_6).

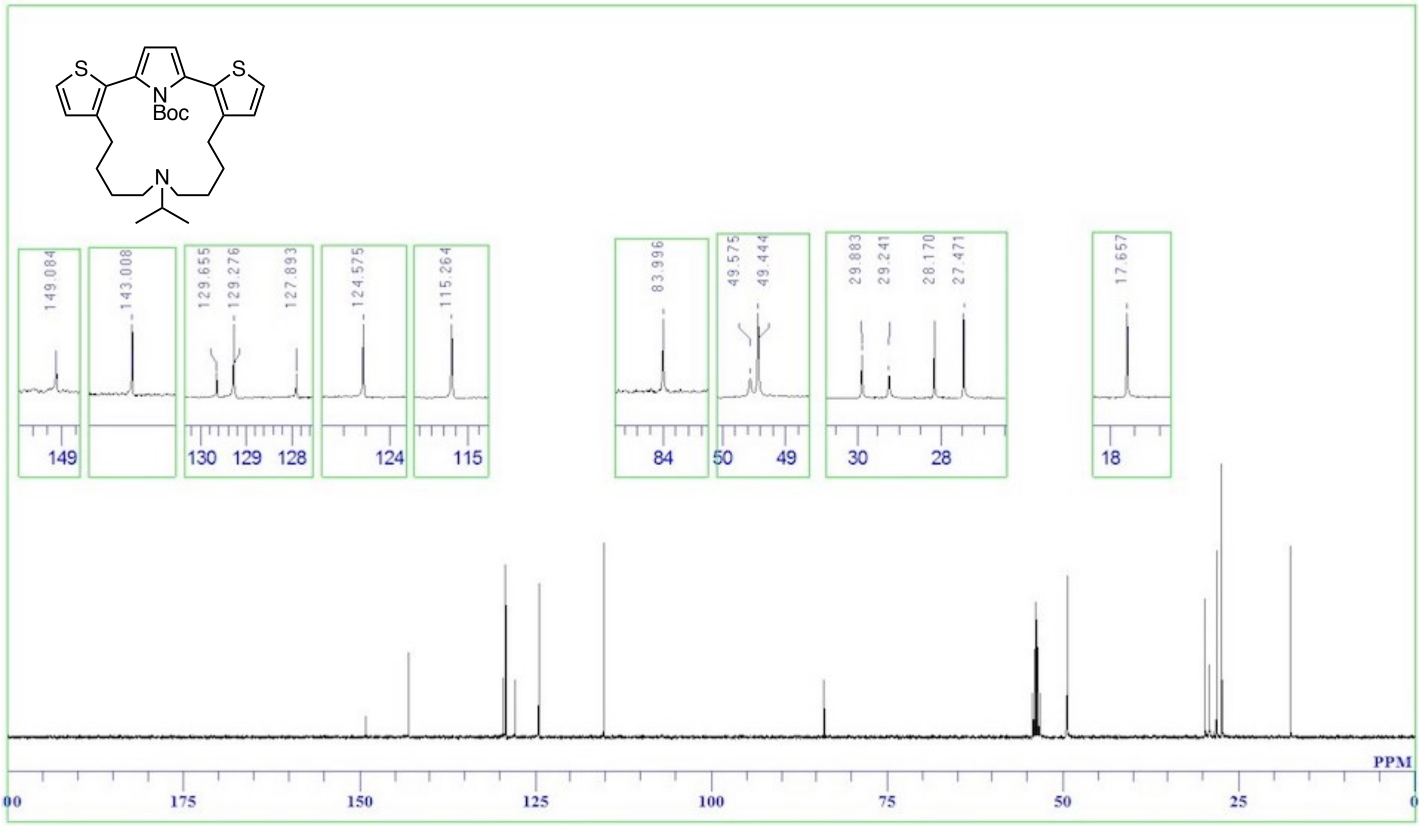

Fig. S68 ^{13}C NMR spectrum of **23** (100 MHz, CD_2Cl_2).

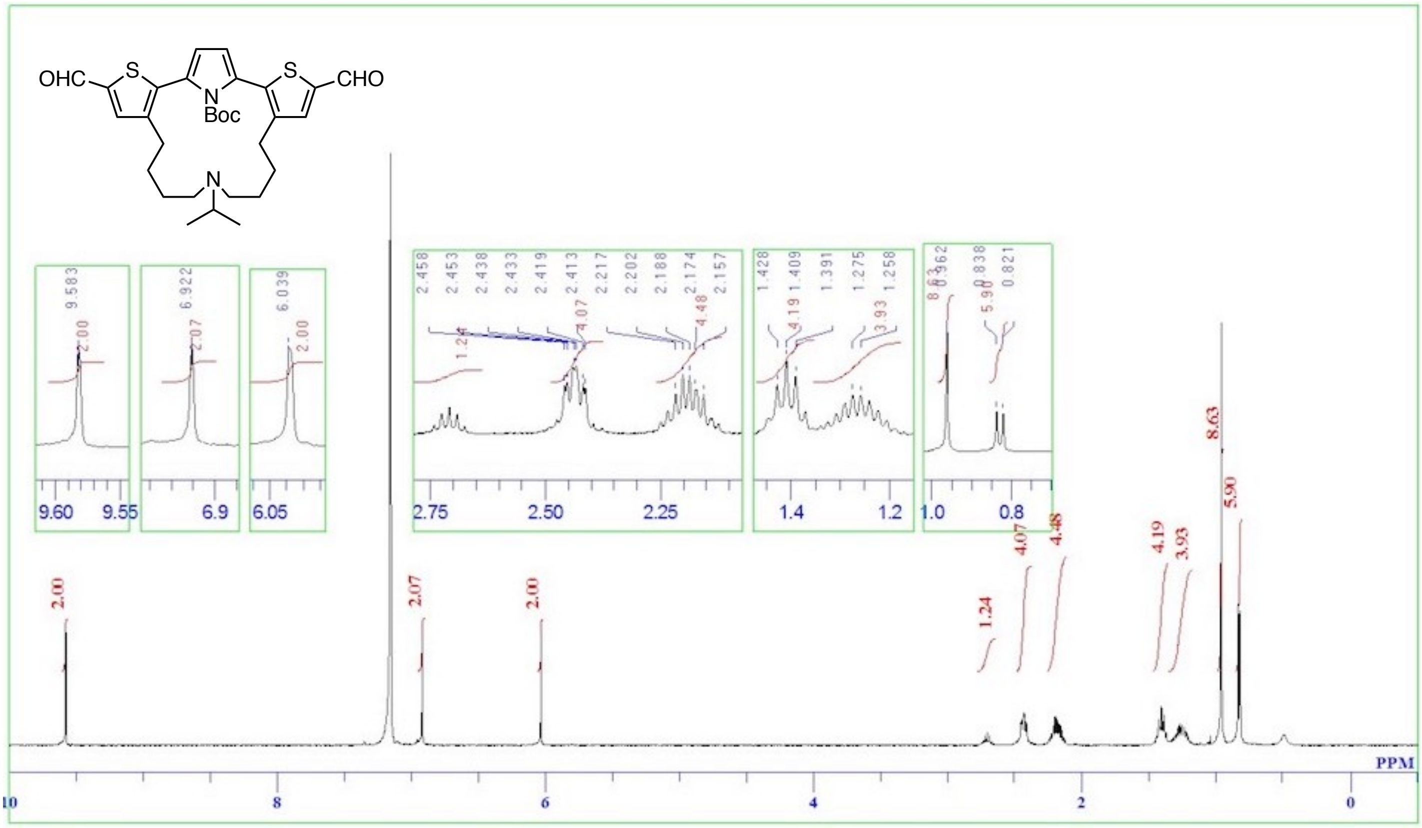

Fig. S69 ^{1}H NMR spectrum of **24** (400 MHz, C_6D_6).

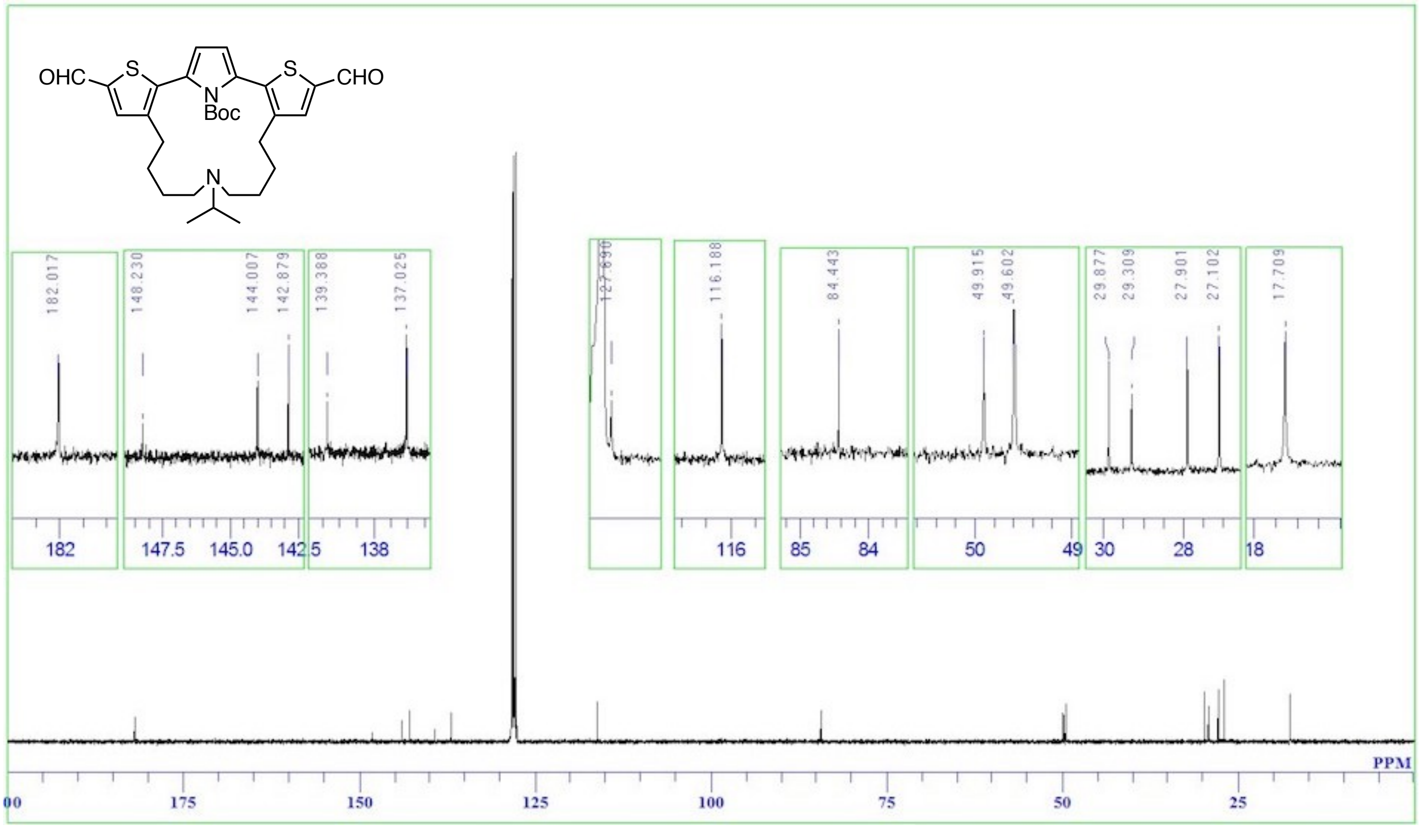

Fig. S70 ^{13}C NMR spectrum of **24** (100 MHz, C_6D_6).

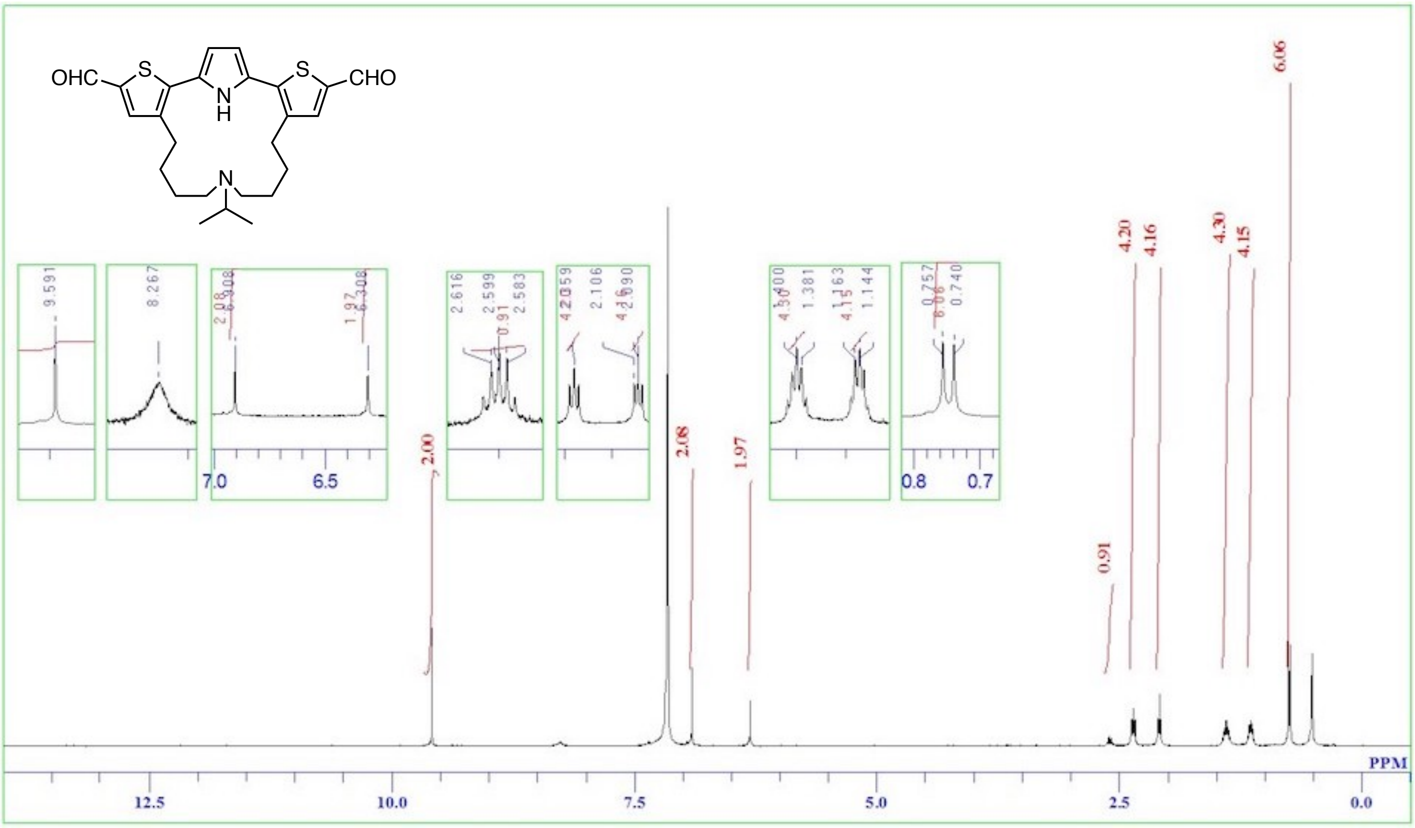

Fig. S71 ^{1}H NMR spectrum of **6** (400 MHz, C_6D_6).

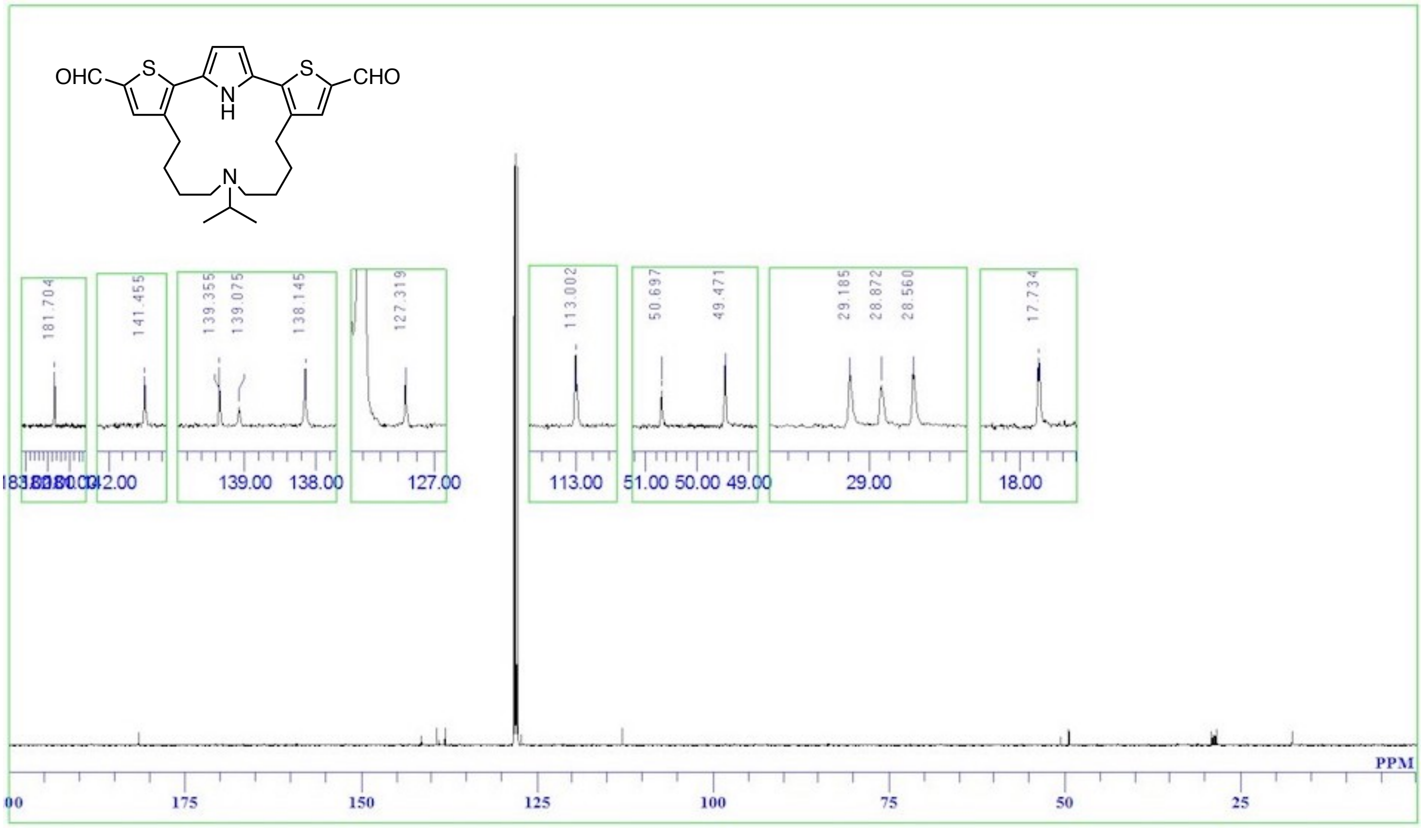

Fig. S72 ^{13}C NMR spectrum of **6** (100 MHz, C_6D_6).

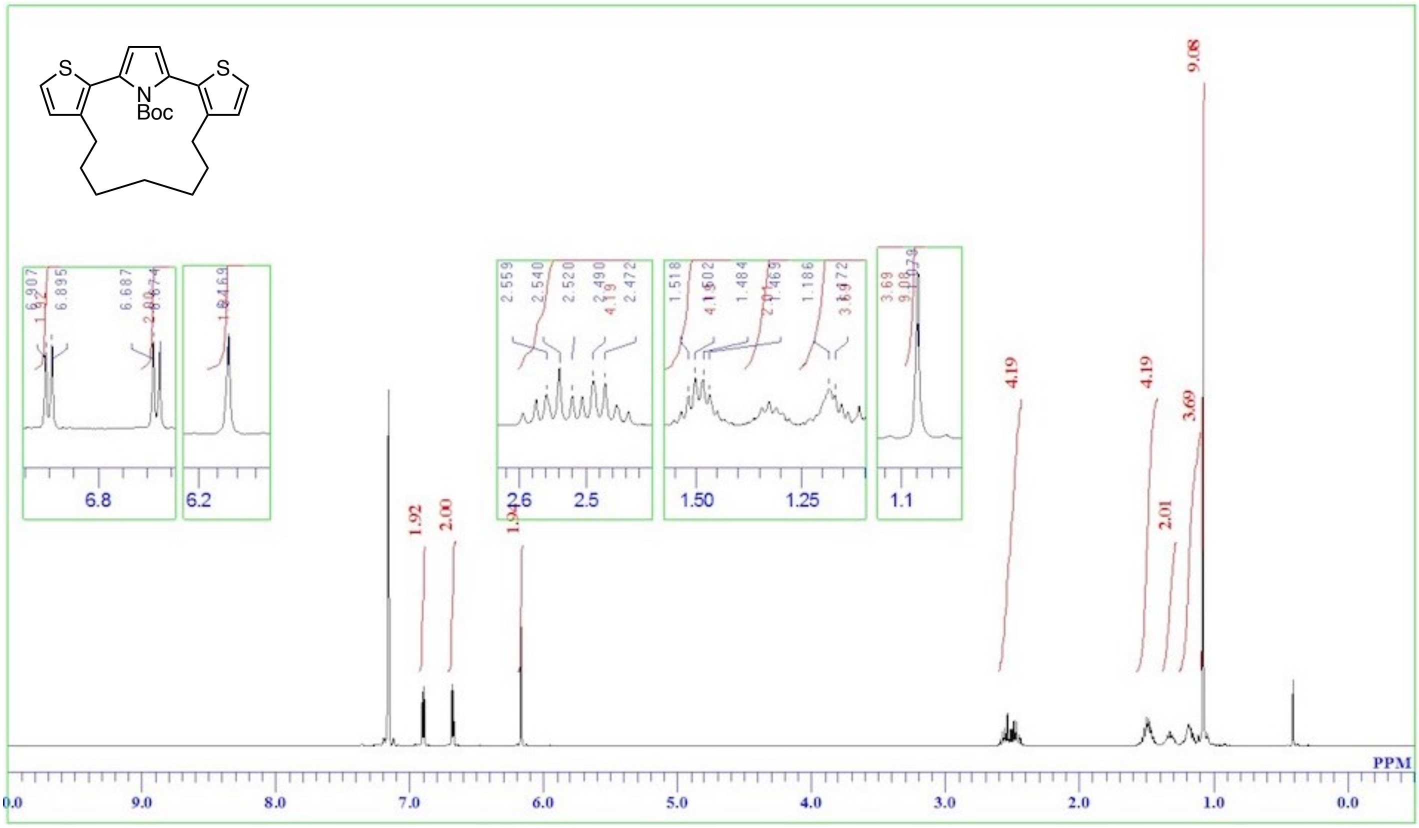

Fig. S73 ^{1}H NMR spectrum of **26** (400 MHz, C_6D_6).

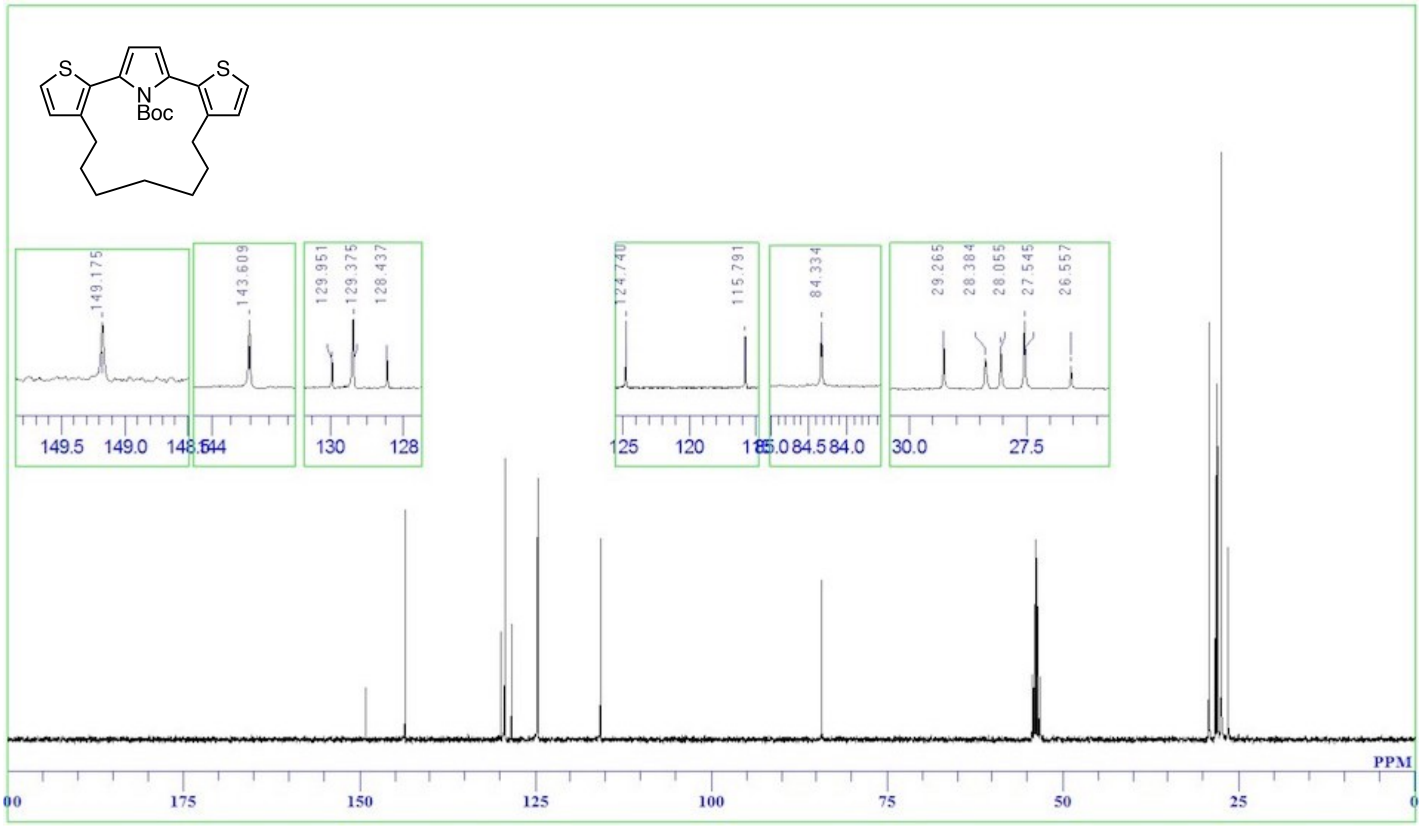

Fig. S74 ^{13}C NMR spectrum of **26** (100 MHz, CD_2Cl_2).

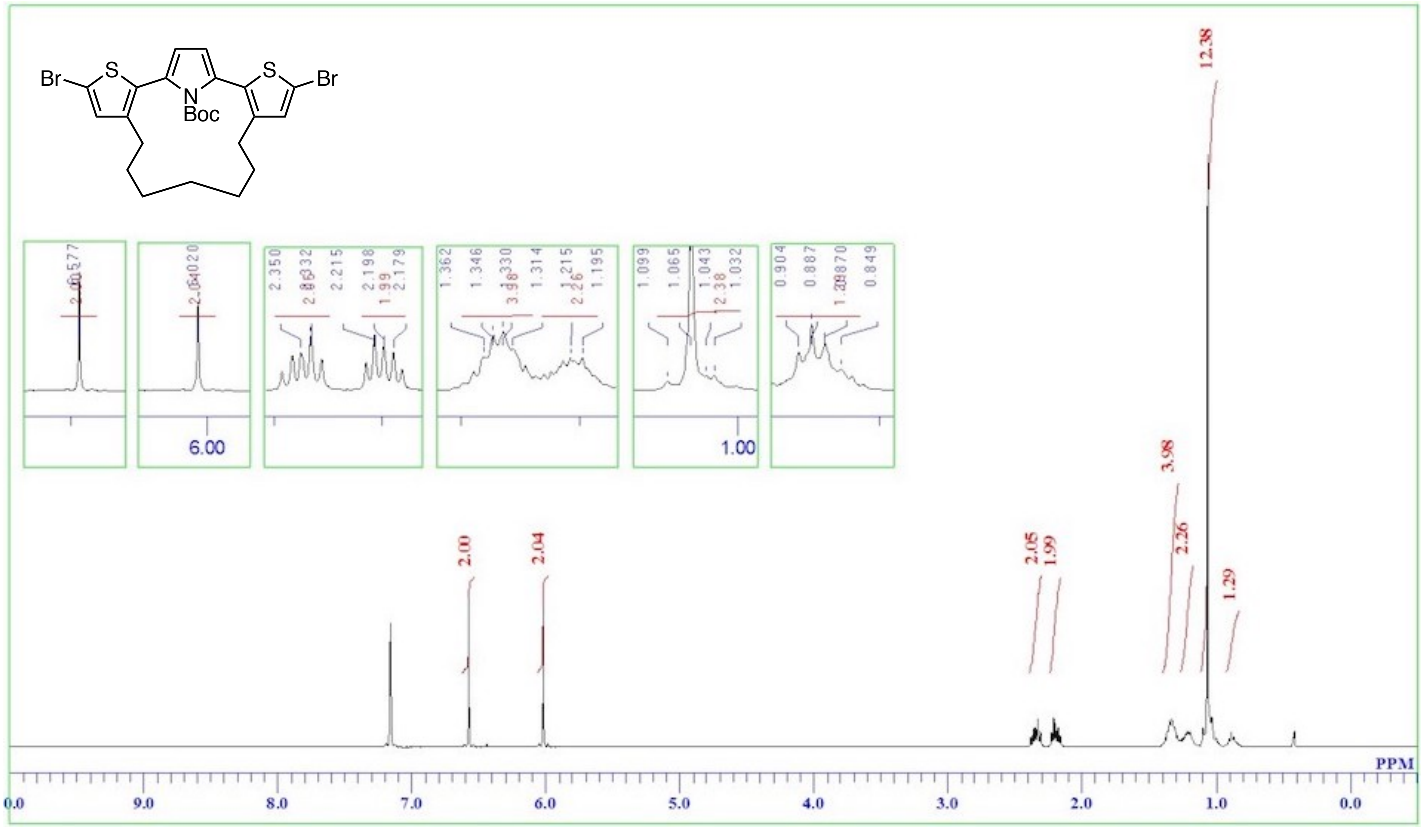

Fig. S75 ^{1}H NMR spectrum of **27** (400 MHz, C_6D_6).

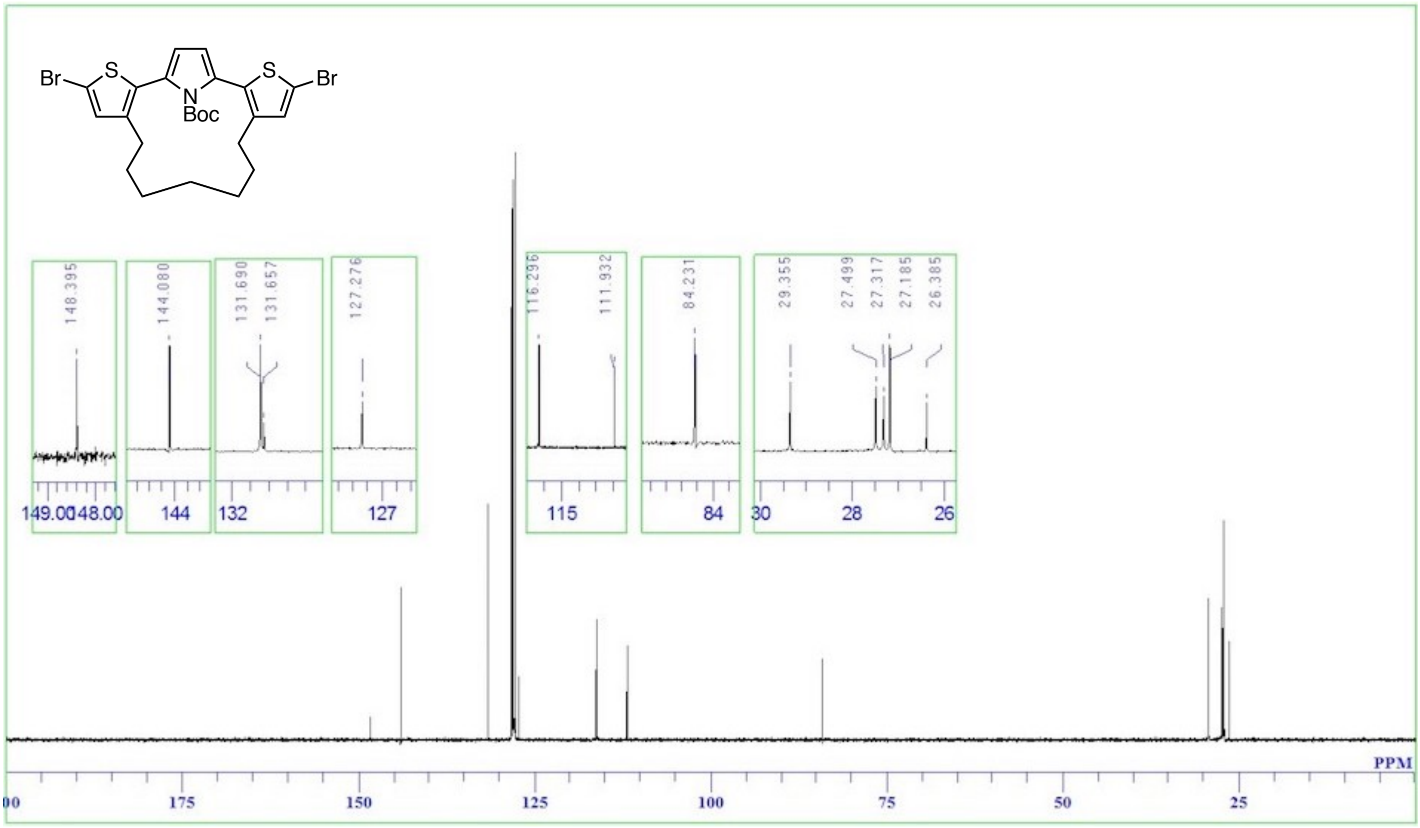

Fig. S76 ^{13}C NMR spectrum of **27** (100 MHz, C_6D_6).

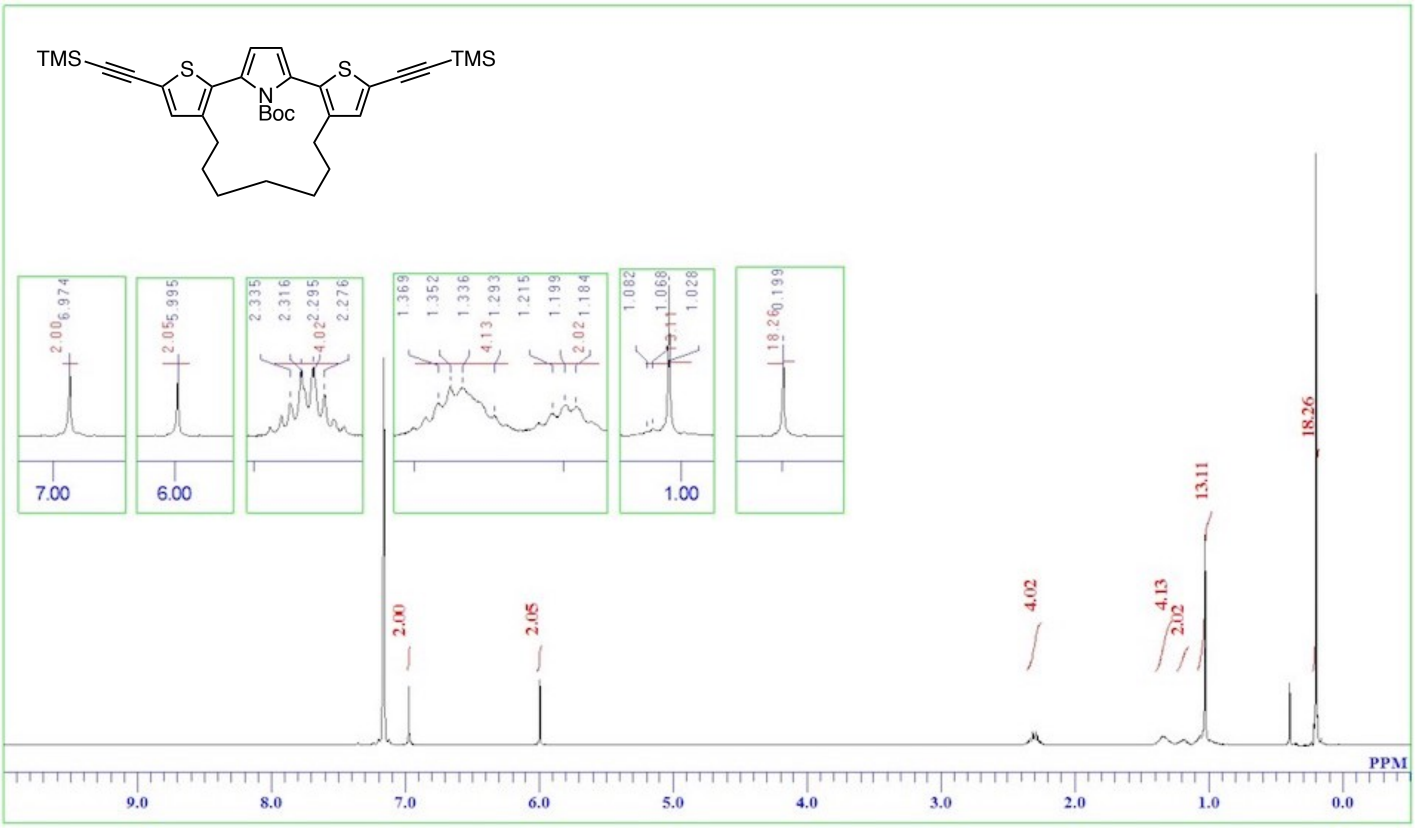

Fig. S77 ^{1}H NMR spectrum of **28** (400 MHz, C_6D_6).

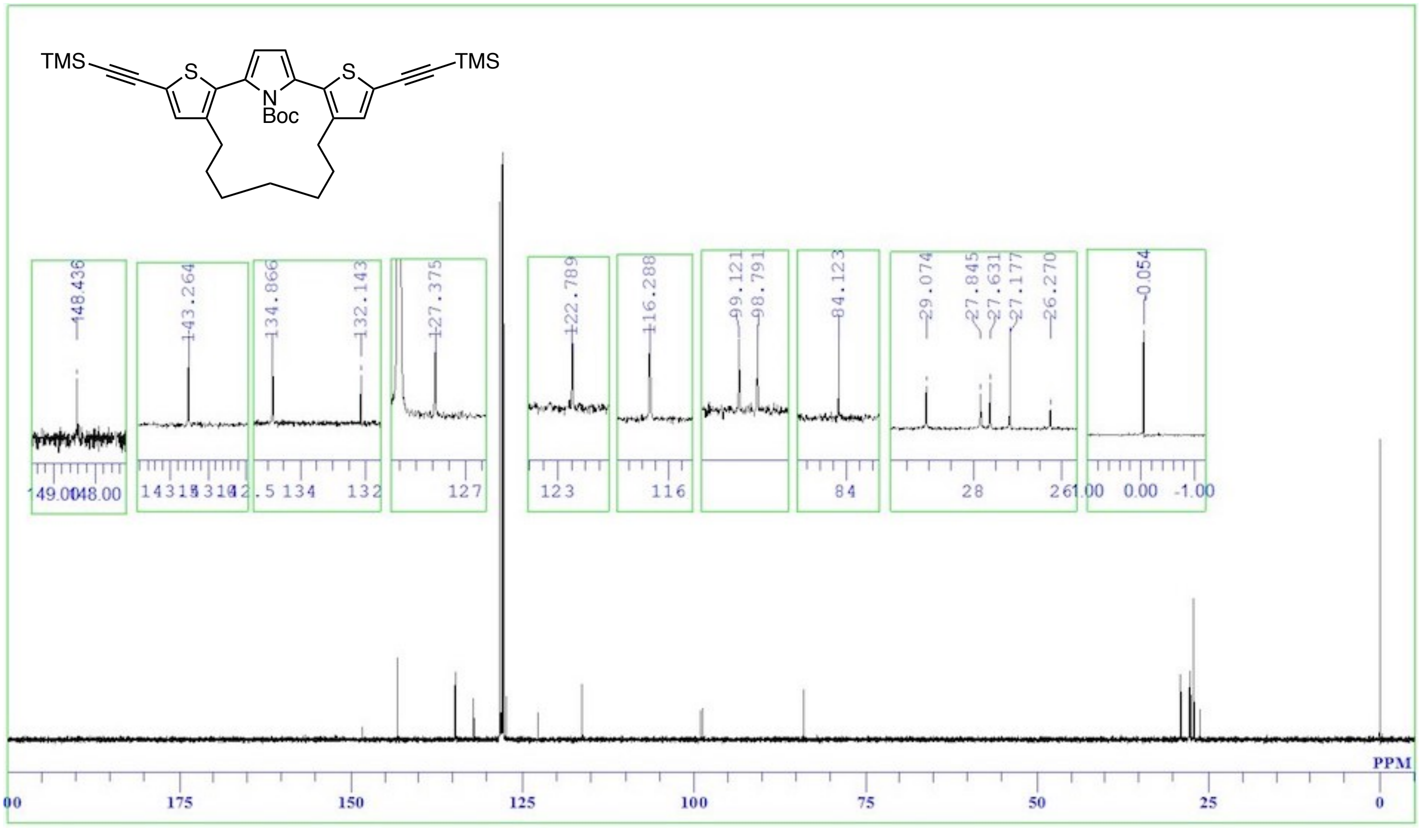

Fig. S78 ^{13}C NMR spectrum of **28** (100 MHz, C_6D_6).

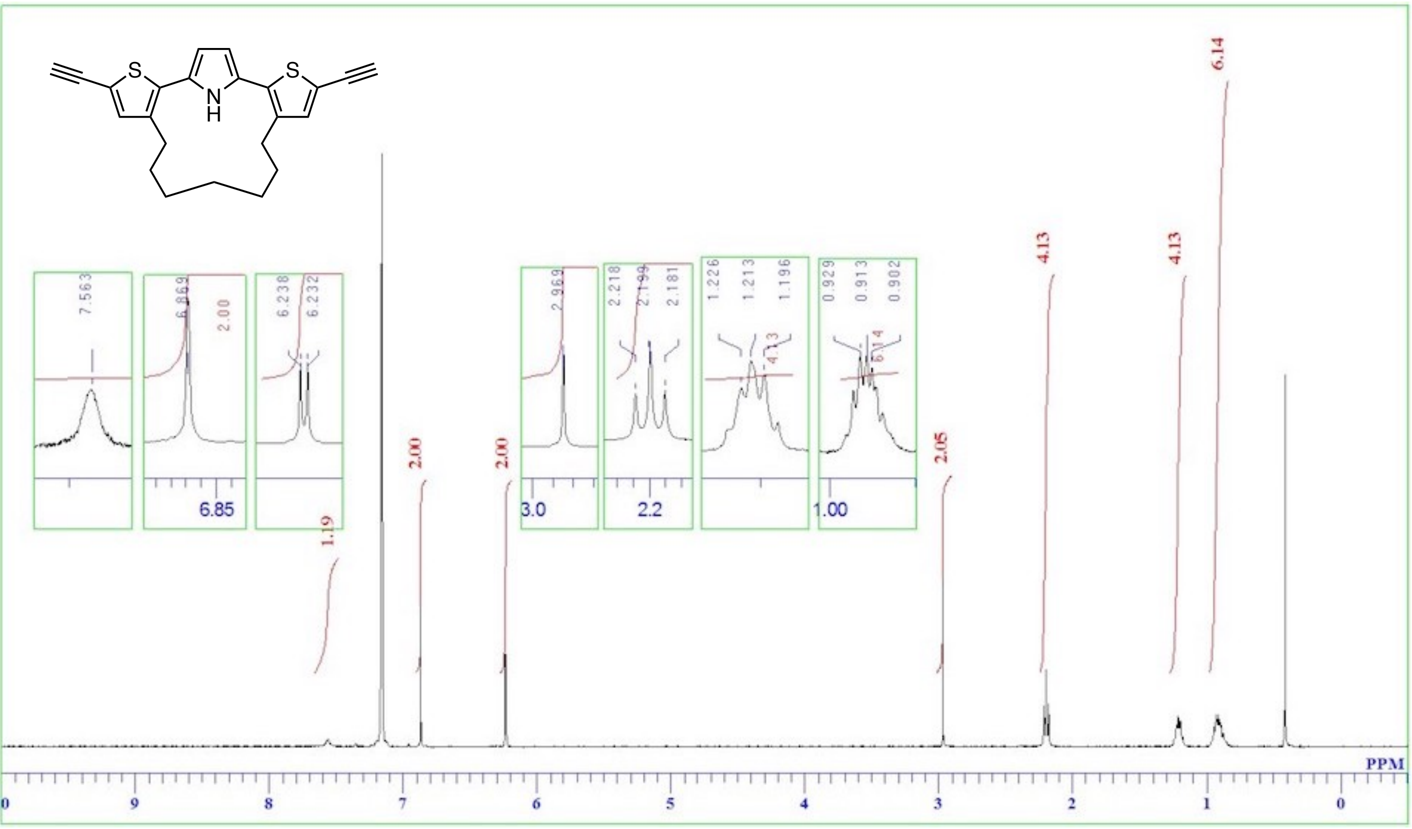

Fig. S79 ^{1}H NMR spectrum of **29** (400 MHz, C_6D_6).

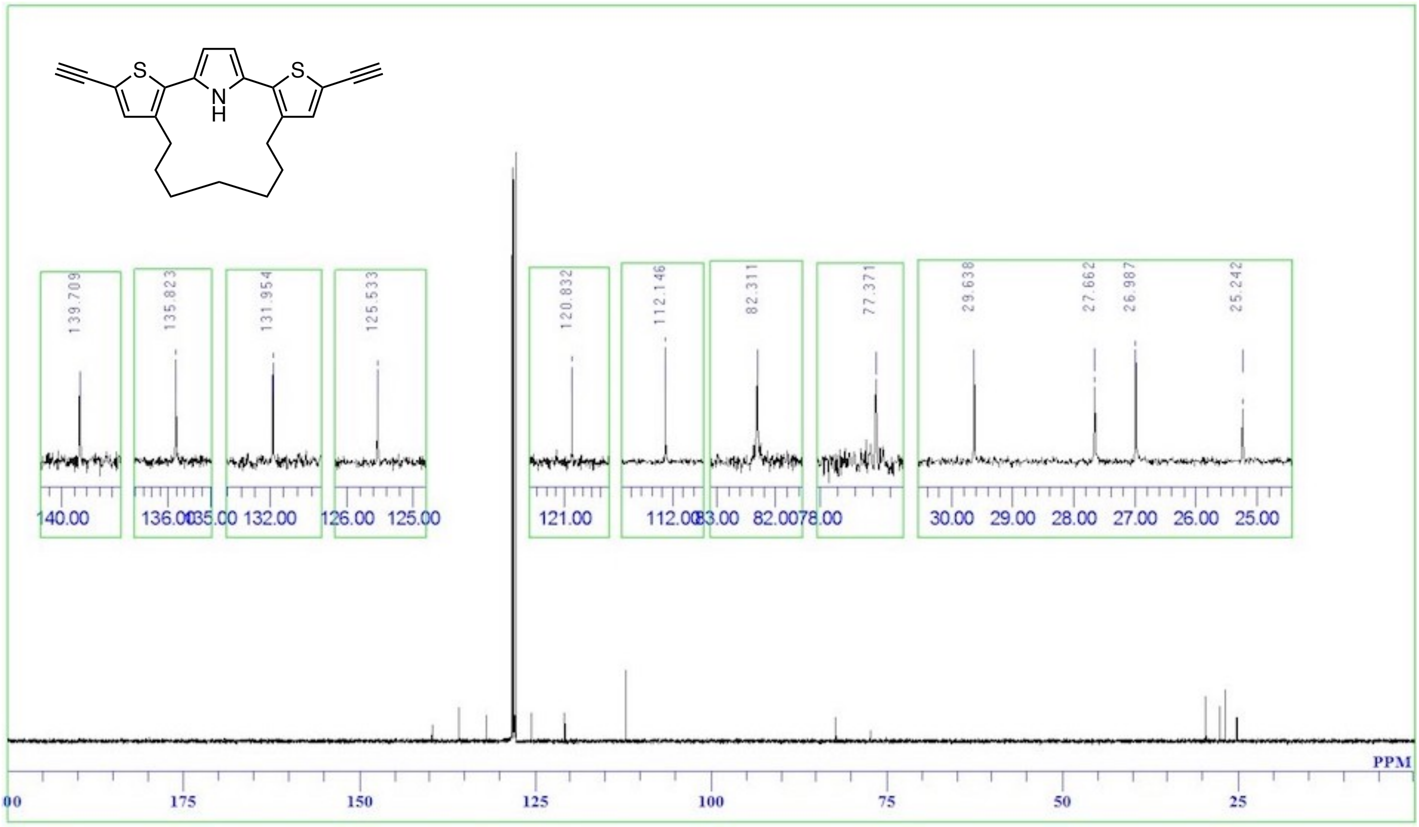

Fig. S80 ^{13}C NMR spectrum of **29** (100 MHz, C_6D_6).

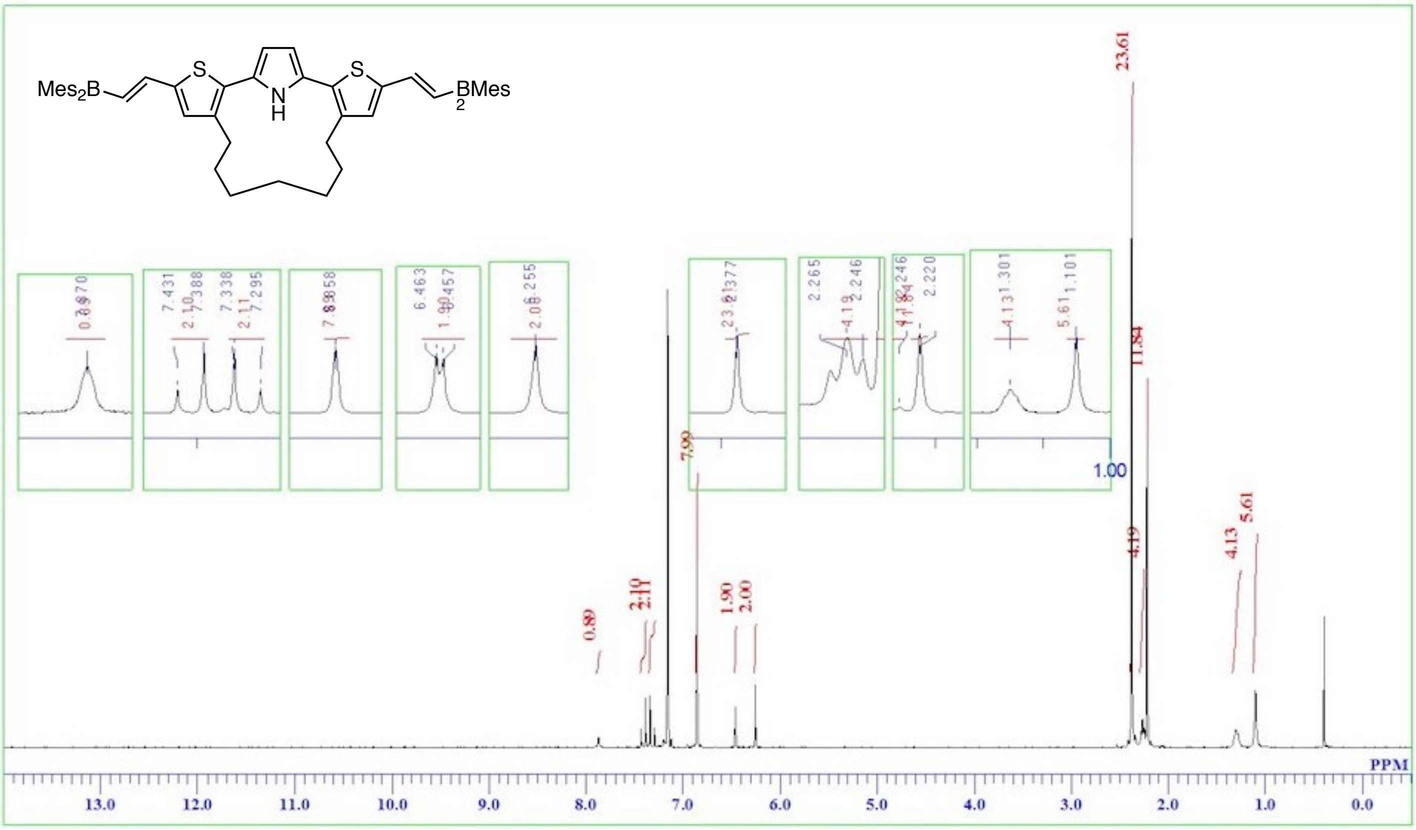

Fig. S81 ^{1}H NMR spectrum of **7** (400 MHz, C_6D_6).

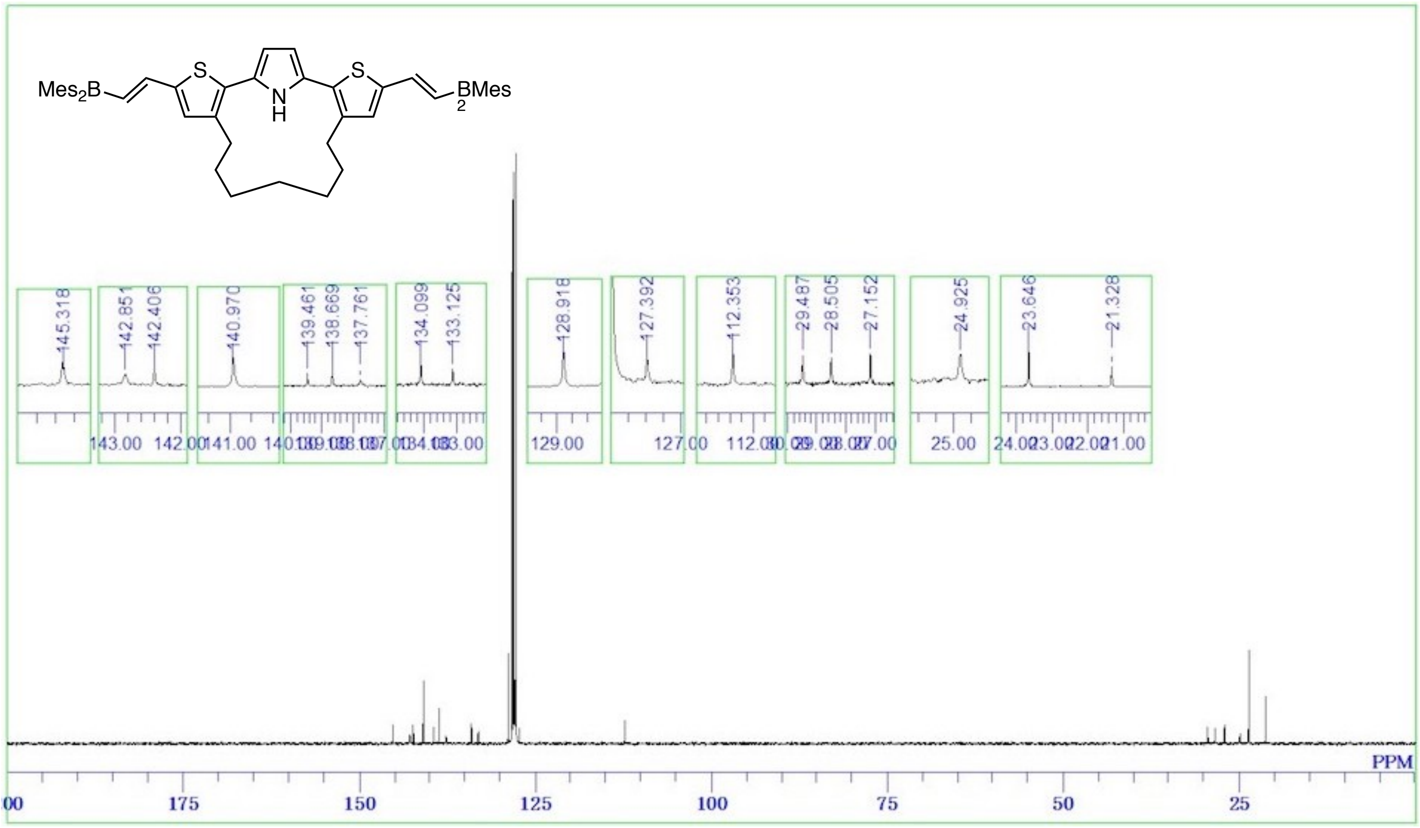

Fig. S82 ^{13}C NMR spectrum of **7** (100 MHz, C_6D_6).

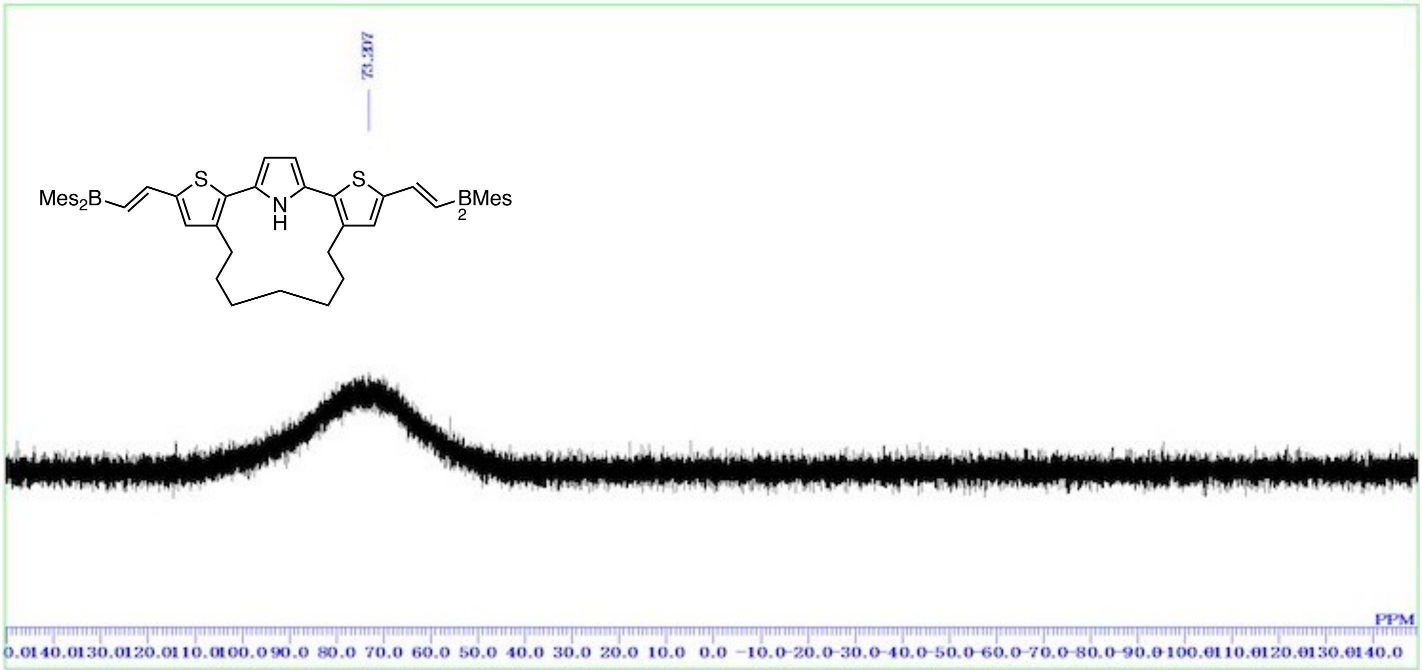

Fig. S83 ^{11}B NMR spectrum of **7** (128 MHz, THF-d_8).